ROLE OF GROUNDWATER IN RUNOFF GENERATION AT A HILLSLOPE SCALE USING ENVIRONMENTAL TRACERS

Joss Alexander Cahi

217040134

Supervisor: Professor Seifu K. Gurmessa

Submitted in partial fulfilment of the

requirements for the degree of

Master of Sciences Hydrology (MSc Hydrology)

School of Agriculture Earth and Environmental Sciences (SAEES)

University of KwaZulu-Natal

Pietermaritzburg

May 2025

PREFACE

I, Joss Alexander Cahi, declare that:

(a) The research reported in this thesis, except where otherwise indicated, is my original work.
(b) This thesis has not been submitted for any degree or examination at any other university.
(c) This thesis does not contain text, data, figures, pictures, graphs or tables from another document, unless it is specifically acknowledged as being sourced from the original document. Where other sources have been quoted, then:

   i) their words have been paraphrased/re-written, and the general information attributed to them has been referenced and
   ii) where their exact words have been used, their writing has been placed inside quotation marks and referenced.

(d) Where I have reproduced a publication of which I am an author, co-author or editor, I have indicated in detail which part of the publication was actually written by myself alone and have fully referenced such publications.
(e) This document does not contain text, graphics or tables copied and pasted from the Internet unless they are specifically acknowledged and the source is detailed, both in the document and in the References section.

Signed:  Date: 31/05/2025

Supervisor: ..... Date: 31/05/2025

AI Declaration

a) I made use of generative AI in this report/dissertation/thesis in the following areas: to write initial drafts, to draft summaries and for language editing. In all instances, the content generated by AI was fully interrogated for applicability, accuracy of content, and plagiarism. Citations were added to statements where applicable to assign credit to authors.

Signed: 

Joss Cahi - 217040134

ABSTRACT

Understanding surface water–groundwater interactions is essential for effective water resource management, particularly in the context of land use and climate change. This study investigates these interactions at two contrasting sites in KwaZulu-Natal, South Africa: the near-pristine Cathedral Peak Catchment 6 (CP Catchment 6) in the Drakensberg Mountains and the agriculturally impacted Fountainhill Estate (FHE) catchments near Wartburg. These catchments are representative of different climatic, topographic and anthropogenic conditions, offering insights into how land use and land use change influence hydrological connectivity.

At CP Catchment 6, intensive field-based monitoring was conducted over two years using a combination of hydrometric measurements, stable isotopes, electrical conductivity (EC), radon (^{222}Rn) and satellite-derived soil moisture modelling (OPTRAM). Sampling occurred across multiple temporal scales (event-based and seasonal scales) to capture both baseline and dynamic hydrological processes. The catchment exhibited stable groundwater contributions facilitated by steep topography, connected wetlands and limited disturbance. Baseflow was sustained by meteoric-origin groundwater, while significant rainfall events rapidly mobilised pre-event water stored in wetlands due to groundwater ridging. These findings validate and expand upon existing conceptual models (e.g., Harrison *et al*., 2022), highlighting the critical buffering role of wetlands and subsurface flow systems in maintaining perennial streamflow.

In contrast, at FHE, hydropedological desktop assessments, historical soil surveys, OPTRAM modelling and EC monitoring data revealed fragmented hydrological connectivity driven by agricultural land use. Practices such as irrigation, soil compaction and fertiliser application in the surrounding farms have resulted in elevated solute loads and episodic flushing during storm events. The presence of farm dams moderated downstream water quality but altered natural flow regimes. The OPTRAM model proved effective in identifying active flow paths and subsurface recharge zones, even in the absence of extensive in-situ data.

A comparative analysis underscores how natural and anthropogenically altered systems diverge in their hydrological responses. CP Catchment 6 illustrates efficient, topography-driven hydrology with strong wetland-groundwater interaction, while FHE displays disrupted, highly variable flow paths shaped by land use activities. This research refines conceptual models of runoff generation across diverse landscapes and emphasises the need to incorporate subsurface flow processes into hydrological models. These findings have practical implications for

catchment management, especially in balancing water supply, land development and ecosystem sustainability in South Africa's heterogeneous environments.

ACKNOWLEDGEMENTS

The research presented in this thesis formed a component of a Water Research Commission (WRC) Project (C2022/2023-00892) titled “Adding surface water-groundwater interaction dimension in runoff generation studies and in catchment water management practices using isotope tracers”. I wish to thank the WRC for funding this project. I would also like to acknowledge and thank the following people for their assistance with this thesis:

The South African Environmental Observation Network (SAEON) Grasslands-Forests-Wetlands Node provided portions of data for the Cathedral Peak Research Catchment 6.

Mr Ed Gevers for providing the data for the Fountainhill Estate.

My supervisor, Professor Seifu Gurmessa, for his supervision, advice and input throughout the project.

Mr Mutondi Tshikororo for conducting and providing the isotope data for Catchment 6 of the Cathedral Peak Research Catchments.

My wife, Melissa, for the continuous support, motivation, encouragement and sacrifice, without which I would not have been able to finish this thesis.

My family for the continuous support, motivation and encouragement.

My mother-in-law, May-Gene, for the countless hours spent editing and reviewing this thesis.

TABLE OF CONTENTS

LIST OF FIGURES

LIST OF TABLES

LIST OF ABBREVIATIONS

ACRU	-	Agricultural Catchments Research Unit
CGS	-	Council for Geoscience
CP	-	Cathedral Peak
DWS	-	Department of Water and Sanitation
EC	-	Electrical Conductivity
ERT	-	Electrical Resistivity Tomography
FHE	-	Fountainhill Estate
GMWL	-	Global Meteoric Water Line
ISCO	-	Teledyne Instrument Specialities Company
MAP	-	Mean Annual Precipitation
NDMI	-	Normalised Difference Moisture Index
NDVI	-	Normalised Difference Vegetation Index
OPTRAM	-	OPtical TRApezoid Model
REA	-	Representative Elementary Area
^{222}Rn	-	Radon

SAEON	-	South African Environmental Observation Network
SiO2	-	Silicon Dioxide
SM	-	Soil Moisture
SMOW	-	Standard Mean Ocean Water
SWIR	-	Short Wave Infrared
TDR	-	Time-Domain Reflectometry
TDS	-	Total Dissolved Solids
UKZN	-	University of KwaZulu-Natal
WRC	-	Water Research Commission

INTRODUCTION

Since the early 1900's, anthropogenic activities have increased the global water usage; this increase has occurred at such a rate that it has exceeded the demand from human population growth (World Bank, 2023). With this increase in water usage has come global challenges surrounding the provision of a sustainable and equitable water supply. This growing demand, paired with the increasing impacts of climate change, has exacerbated water scarcity, with approximately two-thirds of the global population now facing water stress or scarcity (Mekonnen and Hoekstra, 2016). This problem may only worsen as the weather patterns shift due to climate change, making the standard water availability patterns no longer reliable (Milly *et al*., 2005; Bischoff-Mattson *et al*., 2020). Many regions are projected to experience more extreme and intense precipitation events, worsening the current norms, e.g. the wet season becomes wetter. As a result of these trends, urban areas are facing either a present or imminent threat to their water supply, as evidenced by Cape Town's recent Day Zero crisis in 2017, 2018 and 2019 (Bischoff-Mattson *et al*., 2020).

South Africa is a semi-arid country that receives, on average, less than 500mm of annual precipitation (Terblanche *et al*., 2001; Bischoff-Mattson *et al*., 2020). In the province of KwaZulu-Natal, the number of consecutive dry days has been increasing, with the number of extreme events also increasing (Rounalt *et al*., 2013; Ndlovu *et al*., 2021). These adverse challenges threaten the livelihoods of many of the rural occupants of KwaZulu-Natal, a predominantly rural province characterised by high-density poverty (David *et al*., 2018; Ndlovu *et al*., 2021).

In response to the challenges presented, South Africa has developed complex and extensive water supply systems. These systems rely heavily on surface water sources to make up the vast majority of South Africa's supply, with networks that include trans-basin and international transfers (Bischoff-Mattson *et al*., 2020). In this context, the definitions for surface water and groundwater are as follows: surface water is defined as "any body of water found on the earth's surface, including both the saltwater in the ocean and the freshwater in rivers, streams and lakes. A body of surface water can persist all year long or for only part of the year." (National Geographic Education, 2023). Groundwater is a relatively vague term and can, therefore, be defined in a number of ways depending on the context of the study (Triska *et al*., 1989; Gibert *et al*., 1990; Vervier *et al*., 1992; Holmes, 2000).

In the past, surface water and groundwater were thought of as separate entities (Brunke and Gonser,1997; Winter *et al*., 1998; Sophocleous, 2002; Cook *et al.*, 2003). However, more recently, this has started to change as groundwater and surface water are thought of as two interlinked and closely related systems (Ezugwu and Apeh, 2017). The importance of this connection between surface and groundwater was highlighted by Winter *et al*. (1998). This is important as whilst these two systems may differ, they can interact at different spatial scales, such as a catchment and hillslope scale, as well as temporal scales. The interactions that occur between surface water and groundwater are of vital importance as these interactions can lead to changes in water quality and temperature (Brunner *et al.*, 2017; Ezugwu and Apeh, 2017). This understanding allows for better management and protection of the water system by determining ecological flows/reserves required and sustainable limits for extraction from both the surface and groundwater systems (Brunner *et al.*, 2017; Ezugwu and Apeh, 2017; Lazo *et al.*, 2019). To accurately understand the mechanisms and processes that govern these interactions, a variety of environmental tracers and physical measurements can be used; the physical methods of studying these interactions are often invasive and may potentially alter these interactions, e.g. flow gauging weirs or boreholes (Hübner *et al.*, 2015). This has led to the rise of applied chemical and naturally occurring environmental tracers such as the stable isotopes of water and radon (^{222}Rn) (Elliot, 2014). These tracers do, however, have drawbacks, but these can be overcome by using combinations of various tracers with hydrometric observations of the surface and subsurface flows and fluxes (Lorentz *et al.,* 2004).

For many years, the interactions between surface water systems and groundwater systems in river systems have been the subject of study. However, these interactions are also the focus of several fundamental issues, ranging from ensuring safe and sustainable water supply, understanding and maintaining water quality in surface water systems and preserving the ecological health of these systems (Sophocleous, 2002; Boulton *et al.*, 2010; Boano *et al.*, 2014; Brunner *et al.*, 2017; Lazo *et al*., 2019).

The role of mountains in the global hydrological cycle cannot be overstated. Mountainous areas cover 24% of Earth's land surface (Kapos *et al*., 2000) and contribute 50% of global runoff thereby playing a vital role in regulating streamflow for more than half of the global population (Viviroli *et al*., 2007). These areas receive greater amounts of precipitation and are characterised by lower rates of evapotranspiration. However, mountain ecosystems are undergoing rapid changes due to warming temperatures, with studies showing that high-elevation regions are heating faster than adjacent lowlands (Somers and McKenzie, 2020). This

is expected to increase the frequency and severity of extreme weather events such as droughts and floods (Pörtner *et al*., 2019; Vuille *et al*., 2018).

South Africa's Drakensberg Mountains, part of the Maloti-Drakensberg Transfrontier Conservation Area, are of particular hydrological importance. These mountains contribute significantly to water production and baseflow maintenance, yet they have received limited research attention due to their remote and often harsh environmental conditions (Manning and Solomon, 2005). Recent studies have begun to challenge the traditional assumption that mountain catchments act solely as rapid runoff zones. Instead, evidence shows that they also store considerable groundwater, which plays a critical role in regulating streamflow, especially during dry seasons (Liu *et al*., 2004; Soulsby *et al*., 2002; Tetzlaff *et al*., 2007).

The uThukela River catchment, located within the Drakensberg range, is one of the largest catchments in South Africa and includes key tributaries originating from mountain headwater catchments such as the Cathedral Peak (CP) region. These upper catchments, many of which are considered "hydrologically pristine", offer invaluable opportunities for investigating hydrological processes. CP Catchment 6, in particular, is a well-instrumented research site with decades of hydrometeorological data and limited anthropogenic disturbance, making it ideal for studying surface water–groundwater interactions.

However, to fully understand catchment-scale hydrology, it is essential to study not only pristine headwaters but also more impacted mid- and lower-catchment areas. This study addresses this by including Fountainhill Estate (FHE), located in the central Umgeni catchment. FHE offers a contrasting landscape, characterised by a mosaic of intensive agriculture, commercial forestry, natural grasslands and wetlands. Unlike CP Catchment 6, which is minimally impacted by human activity, FHE reflects the land-use changes and development pressures common to many parts of South Africa.

FHE is strategically situated between the catchment headwaters and the large-scale water infrastructure, such as the Midmar and Albert Falls dams (both upstream) and the Nagle Dam (further downstream). This mid-catchment location, along with its diverse land uses and proximity to growing urban centres, makes it a key site for examining how land cover and anthropogenic influences affect water movement, storage and mixing. By studying both CP Catchment 6 and the FHE catchments, the research captures a gradient of hydrological conditions, from relatively undisturbed montane systems to more developed and managed

landscapes, offering a more comprehensive understanding of water dynamics within the uThukela catchment.

This research focuses on updating the conceptual model of hillslope runoff generation at these sites by using a combination of field-based tracer techniques and remote sensing methods. It specifically incorporates:

- Stable isotopes of hydrogen and oxygen to trace sources of water and mixing processes;
- Radon (^{222}Rn) as a groundwater tracer due to its high solubility and short half-life, which makes it sensitive to recent groundwater–surface water interactions;
- Electrical conductivity (EC) and temperature measurements to characterise flow paths and mixing zones;
- The Optical Trapezoid Model (OPTRAM), a physically-based remote sensing model, to estimate surface soil moisture and identify hydrological response units across the catchment (Sadeghi *et al*., 2017; Babaeian *et al*., 2018).

Hillslopes form the fundamental hydrological units in catchments, influencing the timing, quantity and quality of runoff delivered to streams (McGlynn and McDonnell, 2003; Hallema *et al*., 2017). The mechanisms of hillslope runoff generation are complex and influenced by a range of factors, including topography, soil type, vegetation, land use and the temporal distribution of rainfall (Chahinian *et al*., 2005; McGuire and McDonnell, 2010). Human activities such as deforestation, urban development and agriculture can alter these mechanisms by decreasing infiltration, increasing overland flow, and changing subsurface connectivity (Zhang and Schilling, 2006; Hallema and Moussa, 2014).

Despite their importance, hillslopes are often oversimplified in hydrological models. This study seeks to address that gap by providing a detailed, tracer-informed understanding of how water moves through various hillslope systems. By combining field measurements with remotely sensed soil moisture data, the study investigates how hillslope processes contribute to different flow regimes, including baseflow, stormflow, and dry season flow.

1.1 Research Aims and Objectives

The aim of this research is to observe, quantify, understand and model the surface water-groundwater interactions in a near-pristine catchment and human-impacted/agricultural hillslope catchments. The scale being studied is the hillslope scale, using a variety of environmental tracers in combination. This research also aims to update the current

understanding and conceptual models of the governing mechanisms of runoff generation in small catchments.

To achieve this, certain objectives have been set. These can be seen below:

- To verify assumptions and shortfalls experienced when creating water balances in associated models;
    - These assumptions include:
        - The surface water sources for various streams studied,
        - The contribution of groundwater to streamflow.
    - The shortfalls include:
        - A lack of understanding of the runoff generation mechanisms that contribute to overland flows during events,
        - A lack of understanding of the role of groundwater in streamflow generation.
- To identify sources and pathways of the surface water, vadose zone water and groundwater and their contributions to normal, high and low flows using tracers and remote sensing imagery (OPTRAM model and other indices);
- To provide an understanding of the mechanisms governing the movement of surface, vadose zone water and groundwater in contributing hillslopes; and
- To update and improve the current conceptual models of the groundwater flows existing in the respective catchments.

These objectives aim to answer the following research questions:

- Does groundwater play a vital role in generating stormwater and low flows? If so, what is the mechanism of the flow?
- What is the role of land use changes/alterations in impacting the runoff generation mechanisms?

By addressing these questions, the study contributes to a more nuanced understanding of hydrological connectivity in mountain environments, with implications for both water security and ecosystem sustainability in the context of climate change.

1.2 Structure of Thesis

This thesis consists of nine chapters, detailed below:

Chapter 1 - This chapter provides the purpose for and the significance of this research, along with the aims and objectives this thesis addresses.

Chapter 2 - This chapter presents the literature review of the key literature pertaining to the mechanisms by which the groundwater contributes to surface water systems and the methods used to study them.

Chapter 3 - This chapter describes the two study sites' locations, climatic, physical (e.g. hydrological, pedological, etc.) characteristics, the land uses and the monitoring networks installed at these sites in detail.

Chapter 4 - This chapter details the methodology used to collect and analyse the samples and data obtained for this thesis.

Chapter 5 - This chapter presents the results of the investigation at each of the sites studied.

Chapter 6 **-** This chapter presents a detailed discussion of the results in the broader hydrological context of hillslope hydrology. It also includes the conceptual models of each of the study sites and the implications of these models.

Chapter 7 **-** This chapter presents the conclusions drawn from this research.

Chapter 8 **-** This chapter contains a comprehensive list of the references used for this thesis.

LITERATURE REVIEW

In this chapter, a review of the relevant literature is presented. This includes literature pertaining to the methods used to analyse and study the water sources of a catchment, and the resulting interconnectivity of the catchment's surface water and groundwater systems. This section also presents the major mechanisms by which the surface water and groundwater interact at a hillslope scale, as well as case studies of previous studies conducted where these methodologies were applied.

For many years, the interactions between surface water systems and groundwater systems in river systems have been the subject of study. However, these interactions are also the focus of several fundamental issues, ranging from ensuring safe and sustainable water supply, understanding and maintaining water quality in surface water systems, and preserving the ecological health of these systems (Sophocleous, 2002; Boulton *et al.*, 2010; Boano *et al.*, 2014; Brunner *et al.*, 2017; Lazo *et al*., 2019).

2.1 Quantifying Surface Water-Groundwater Interactions at Various Scales

When studying these surface water-groundwater interactions, there are several physical, chemical and modelling approaches that can be used to characterise the spatial patterns, magnitudes and timescales associated with these surface water-groundwater exchanges (Brunner *et al*., 2017). Environmental tracers are regularly used to study and quantify these interactions as they can provide information on the sources, pathways, residence times and the mixing of surface water and groundwater (Kendall and Doctor, 2003).

When trying to quantify these interactions, it is important to understand the flow path mechanisms at different spatial scales, such as a hillslope scale, for various reasons, expanded upon below (Lorentz *et al*., 2004; Bertrand *et al*., 2013). Firstly, the mechanisms governing water storage in hillslopes also govern its release. Water released from this store during dry seasons can affect both small and large catchments (Lorentz *et al*., 2004). In small catchments, the hillslope storage releases can govern the sustainability of small catchment practices, whilst in larger catchments, it can have a large degree of control over periods of low flow rates (Lorentz *et al*., 2004; Spencer *et al*., 2021). The lateral flow mechanisms from a hillslope are closely linked to the type and location of the land uses within a catchment (Lorentz *et al*., 2020; Mahlangu *et al*., 2020). The change in the land use or location of the land use results in a shift in the lateral flow mechanisms and vice versa (Lorentz *et al*., 2004; Mahlangu *et al*., 2020). Other studies conducted on South African hillslopes have shown the importance of hydraulic

mechanisms at finer scales. Riddle *et al*. (2020) demonstrated the importance of fine-scale hillslope connectivity through interflow processes resulting in preferential flows. Tanner and Hughes (2015) showed that the lateral drainage occurring in the deep unsaturated zone is an important process in flow generation. Wenninger *et al*. (2008) validated the dominance of groundwater in stormflow generation. It is for this reason that any changes to the mechanisms that govern flows at a hillslope scale due to a shift in land use need to be understood (Lorentz *et al*., 2004).

Brodie *et al*. (2007) and Kalbus *et al*. (2006) conducted comprehensive reviews of the techniques used to evaluate surface water-groundwater exchanges and their interactions. Their work also critically examines the suitability of these methods across various scales. The techniques discussed include:

- Direct measurement of water flux,
- Heat tracer methods, which rely on temperature differences between surface water and groundwater,
- Using Darcy's law to analyse groundwater flow through porous media,
- Mass balance methods, such as hydrograph separation, differential flow gauging and the use of environmental or solute tracers, and
- Numerical modelling approaches.

Barthel (2014) and Kløve *et al.* (2011b) state that the studies trying to assess these surface water-groundwater systems and the interactions that occur within them should include both multidisciplinary knowledge and interdisciplinary knowledge. Some of the disciplines mentioned are hydrogeology, geochemistry and ecology. This call for interdisciplinary collaboration allows for a more holistic understanding of the impact land and water uses will have on an ecosystem that is dependent on these interactions. Therefore, this allows for better management and mitigation of these impacts (Conant *et al.,* 2019). Tanner and Hughes (2015) showed that hydrological model approaches could not be used as a replacement for real data collected through monitoring systems, but rather as a complementary tool. This was due to numerical models being able to simulate the hydrological processes occurring in the natural environment close to the natural state (Peel *et al.,* 2022). According to Lorentz *et al.* (2004), when quantifying the sources linked to streamflow generation and recharge rates, hydrometric observations need to be supplemented with other methods. Lorentz *et al.* (2004) recommended using a combination of naturally occurring or artificially introduced chemical environmental

tracer sampling methods to supplement these hydrometric results from both the surface and subsurface.

2.2 Lateral Flow Generation in Hillslopes

Lateral flow is a critical hydrological process that involves the movement of water downslope through the subsurface, contributing significantly to streamflow and groundwater recharge. This flow typically occurs within the unsaturated and saturated zones of the soil and is governed by factors such as soil permeability, slope gradient and subsurface hydraulic connectivity (Horton, 1933; Tóth, 1963). In sloped terrains, subsurface lateral flow often dominates runoff generation processes, especially during and after precipitation events where infiltration exceeds local storage capacity. Lateral flow processes refer to the movement of water through the subsurface and include several key mechanisms, such as interflow and saturation overland flow shown below in Figure 2-1.

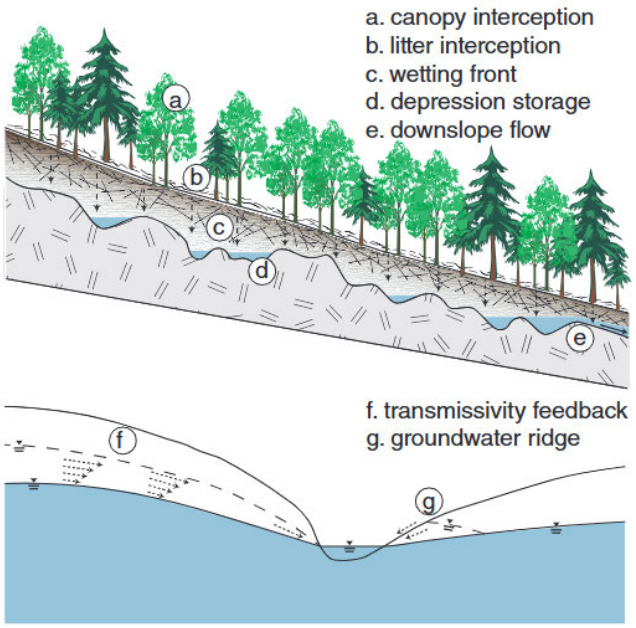

Figure 2-1: Lateral flow processes of a catchment (McGuire *et al*., 2024)

Interflow (Figure 2-2), which occurs when water moves through a permeable soil layer above an impermeable layer. These interflow processes also include mechanisms like fill and spill, transmissivity feedback, and groundwater ridging (McGuire et al., 2024). Groundwater ridging results from the local water table rising due to the convergence of water along riparian zones (Theron et al., 2022). Together, these lateral flow processes play an important role in sustaining streamflow during dry seasons (Cherry and Freeze, 1979; Dunne, 1980).

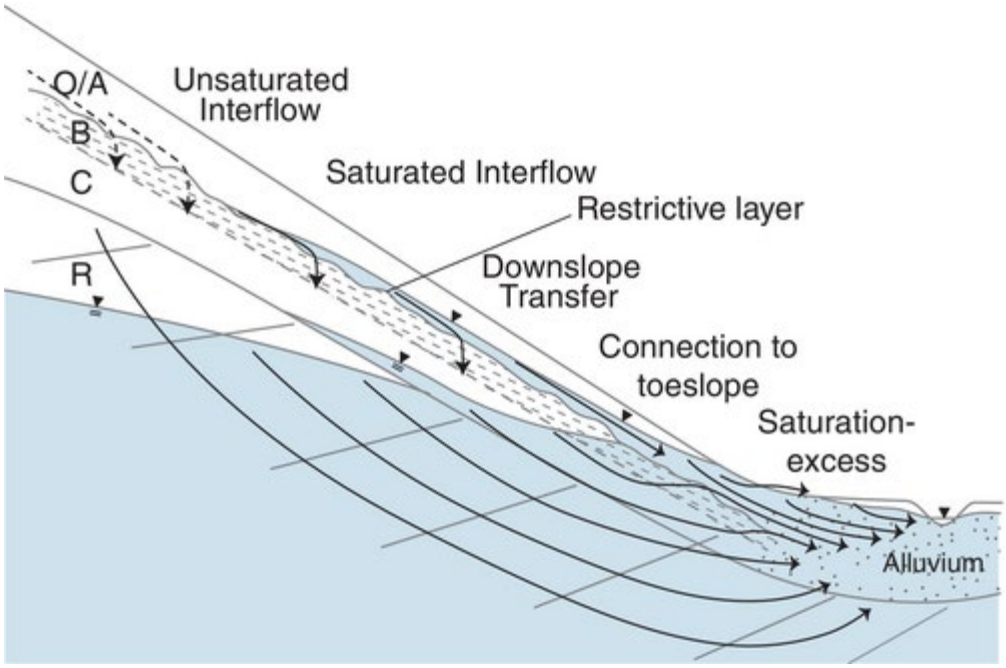

Figure 2-2: Conceptual model of interflow types and processes (McGuire *et al*., 2024)

Additionally, the fill and spill mechanism operates in landscapes with depressions or microtopography, where perched water is temporarily stored and then spills downslope as lateral flow (Spence and Woo, 2003).

2.2.1 Fill and spill mechanisms

The fill and spill mechanism is a widely observed hydrological process that governs lateral water movement and runoff generation, particularly in landscapes with variable storage capacity and threshold-dependent connectivity. This mechanism occurs when water infiltrates and accumulates in localised depressions or soil horizons until the storage capacity is exceeded, triggering lateral flow or surface runoff into adjacent downslope areas (Spence *and* Woo, 2003; Tromp-van Meerveld and McDonnell, 2006). The process is characterised by the flow pathways remaining disconnected until a critical filling threshold is reached. Once exceeded, water is rapidly transmitted through the landscape, often leading to sudden increases in streamflow. Fill and spill dynamics are especially important in catchments with spatial heterogeneity in soil depth, topography or impermeable layers (Lehmann *et al*., 2007). Recent applications of this concept in South African montane catchments, such as those in the Cathedral Peak region, have highlighted its role in facilitating episodic connectivity between hillslopes and streams (Harrison *et al*., 2022). In such contexts, fill and spill mechanisms contribute to threshold-like responses in discharge and influence the timing and magnitude of stormflow events.

The fill and spill mechanism is a threshold-driven connectivity process whereby water first accumulates in local storage (the "fill") and only when a critical depth is reached does it spill over to the next compartment or the stream. McDonnell *et al*. (2021) formalised this idea: each hillslope element (soil patch, depression, segment) has finite storage and runoff initiates only after upstream storages fill to capacity and connect (McDonnell *et al*., 2021). In other words, lateral additions (rain or inflow) fill a reservoir until a spill threshold activates an outflow pathway to downslope units (McDonnell *et al*., 2021). On forested hillslopes, it can present as perched interflow horizons that saturate and then spill into lower hollows or stream zones (Du *et al*. 2016). In the CP catchments (Drakensberg), Harrison *et al*. (2022) observed that wetlands and shallow interflow soils rapidly saturate under rainfall and then "spill" water laterally as overland or shallow subsurface flow to streams (Harrison *et al*., 2022). Kollongei and Lorentz (2014) report that small events are retained by these reservoirs, but intense events produce disproportionately large outflows once spillover occurs (Kollongei and Lorentz, 2014).

2.2.2 Groundwater ridging

Groundwater ridging is the sudden, almost instantaneous rise of the water table near streams driven by rapid infiltration of rain into a pre-wetted capillary fringe (Sklash and Farvolden, 1979; Abdul and Gillham, 1984). In this mechanism, intense rainfall pressurises the near-surface porewater, causing the phreatic surface to rise and discharge a burst of old (pre-event) water (Theron *et al*., 2022). Abdul and Gillham (1984) first demonstrated this in sandboxes and Cloke *et al*. (2006) define it as a rapid near-stream water table rise coupled with fluctuations of pre-event water, thereby increasing the saturation area at the surface. This eventually leads to overland flow dominating (Cloke *et al*., 2006).

Groundwater ridging appears only under specific conditions, with these generally being shallow slopes with nearly saturated ground and moderately high rainfall rates. For example, Cloke *et al*. (2006) summarize that ridging was observed in grass-covered gentle slopes where a capillary fringe reaches near-surface, but not in forested, macroporous soils (Cloke *et al*., 2006). Experiments (Abdul and Gillham, 1984) and models often reproduce ridging under controlled conditions (Abdul and Gillham, 1984). However, many field studies (e.g. Buttle *and* Sami 1992; Bonell *et al*. 1998) find that in humid catchments event water dominates stormflow and that capillary processes rarely generate large discharge pulses. Thus, while possible, groundwater ridging is thought to be secondary to rapid flow paths unless antecedent moisture and soil structure favour it (Cloke *et al*., 2006; Theron *et al*., 2022).

2.2.3 Groundwater Recession

Groundwater recession refers to the gradual decline in the discharge of stored groundwater to streams following precipitation events. This process plays a critical role in sustaining baseflow and maintaining lateral groundwater-to-stream connections, especially during periods of low rainfall. Lateral flow mechanisms during groundwater recession ensure that aquifers act as long-term sources of stream discharge, and these processes are particularly relevant in maintaining streamflow continuity in regions with shallow water tables or extensive alluvial systems (Kendall *et al*., 1999). Several studies have identified that during recession periods, subsurface lateral flow occurs as a result of hydraulic gradients between the aquifer and the stream (Kendall *et al*., 1999). In regions where the water table intersects the stream channel, this connection facilitates groundwater flow along shallow, lateral pathways to contribute to streamflow.

2.2.4 Interflow

Interflow can occur under saturated and unsaturated conditions and is typically driven by three primary mechanisms. The first occurs due to a percolation limitation, when the vertical water movement rate surpasses the infiltration capacity of an underlying soil layer (Weyman, 1973; Jackson *et al*., 2014; McGuire *et al*., 2024). The second mechanism is transmissivity feedback, which will be elaborated upon in the following paragraph; this mechanism occurs as a result of a rising water table intersecting more permeable surface soils Lundin, 1982; Hjerdt, 2002; McGuire *et al*., 2024). The final mechanism is downslope lateral flow, which occurs due to variations in hydraulic conductivity, particularly in soils with anisotropic properties. These mechanisms may function simultaneously across different sections of a hillslope (McGuire *et al*., 2024). The first two mechanisms often rely on a decline in hydraulic conductivity with depth, which can arise from changes in soil texture, porosity, structure or density due to soil-forming processes or contrasting geological layers (McGuire *et al*., 2024).

Transmissivity feedback is a dynamic increase in hillslope hydraulic conductivity as the water table rises into highly conductive shallow layers (McGuire *et al*., 2024). This concept was initially proposed by Lundin (1982). This mechanism explains how pre-event groundwater can surge to streams. This occurs as rainfall infiltrates the soil, resulting in a rise of the water table. As it saturates soil layers of higher permeability, the capacity of the soil to generate flow significantly increases (Lundin 1982; Kendall *et al*., 1999; Hjerdt, 2002). Field studies confirm this behaviour under wet conditions as shown by Kendall *et al*. (1999). In their analysis, the

stream chemistry showed dilution by shallow flow, indicating mobilisation of older, deeper water once rapid transmissivity begins. Conceptually, transmissivity feedback is most important on till or layered soils where conductivity increases upward. When the water table falls, the loss of saturated highly permeable layers causes flow to slow to a stop, whereas during recharge, the sudden addition of conductive layers accelerates flow beyond what head gradients alone would predict (Hjerdt, 2002; Kendall *et al*., 1999).

A suite of interacting processes controls hillslope streamflow generation. Groundwater ridging, recession, fill and spill and transmissivity feedback represent different ways subsurface water can be mobilised. Studies in South African mountains (Drakensberg) and similar humid, steep landscapes emphasise threshold connectivity (Harrison *et al*., 2022; Kollongei and Lorentz, 2014) and the strong influence of antecedent moisture. Shallow, high-permeability layers and perched water tables are common, so filling and transmissivity effects are expected to be necessary. Extensive preferential pathways (e.g. fractures) or very coarse soils may diminish classic capillary ridging. In practice, multiple pathways often coexist, e.g. an event may start with fill and spill from hollows, peak with both ridging and transmissivity feedback in saturated zones, and end with groundwater recession. Understanding their conceptual distinctions and triggers helps interpret tracer and discharge data and improve hydrologic models for mountainous catchments.

2.3 Environmental Tracers to Quantify Surface Water-Groundwater Interactions

One of the methods of studying surface water-groundwater interactions is through the use of different environmental tracers. Environmental tracers are compounds that are either naturally occurring or artificial. These compounds are usually found ubiquitously within the near surface, allowing them to be used as tracers (Elliot, 2014; Sun *et al*., 2018). These compounds can enter the hydrological system from various sources, such as the atmosphere or flow paths, as the water flows over or through different materials and substrates (Elliot, 2014; Bertrand *et al*., 2013). These environmental tracers are crucial to creating sustainable management policies to protect the state of water resources, such as the quality, quantity and environment (Elliot, 2014). Environmental tracers such as electrical conductivity (EC) (Vogt *et al*., 2010), stable isotopes of water (Yang *et al*., 2012), water temperature (Kurtz *et al*., 2014) and noble gases (Popp *et al*., 2021), have all been used and have shown to generally be good indicators of the spatial as well as the temporal patterns of surface water-groundwater interactions.

2.3.1 ^{222}Rn as an environmental tracer

The environmental isotope ^{222}Rn is a naturally occurring radioactive noble gas that is colourless, inert and odourless, with a half-life of 3.8 days (Sukanya *et al*., 2022). It is produced through the radioactive decay of radium, a daughter of uranium, found in rocks and soils (Gundersen and Wanty, 2020). ^{222}Rn is used predominantly as a tracer for groundwater; the ^{222}Rn enters groundwater through transfusion from the host porous media (Salih, 2003; Wang *et al*., 2018; Sun *et al*., 2018). The concentration of ^{222}Rn in this groundwater is a function of the surrounding rock, the soil's uranium and radium abundance, and the relative ease of the ^{222}Rn from the soil matrix (Sahu *et al*., 2016; Girault *et al*., 2018; Chen *et al*., 2022). ^{222}Rn is also an ideal tracer to study surface water-groundwater interactions as it escapes to the atmosphere by gas transfer, making its concentration in surface water negligible (Sukanya *et al*., 2022).

Before using ^{222}Rn as a tracer, investigations of surface water-groundwater interactions and other subsurface processes required expensive and invasive methods of finding these answers (Hübner *et al*., 2015). These drawbacks have resulted in ^{222}Rn's use and the research into it as an environmental tracer becoming more widespread in various hydrogeological applications (Barbieri, 2019; Strydom *et al*., 2021; Chetia *et al*., 2022). Currently, ^{222}Rn is one of the most used natural tracers for assessing groundwater discharge in hydrogeological studies (Burnett *et al*., 2003).

When measuring ^{222}Rn in water, two different sampling methods/techniques can be employed (Sukanya *et al*., 2022). The first of these methods is instantaneous or grab sampling. This is when a single-point sample is collected over a relatively short period, from seconds to minutes. The second method is continuous or active. This involves constant monitoring over a period that can range from several weeks to years; however, this depends on the research's objective (Freyer *et al*., 1997; Sukanya *et al.*, 2022). This sampling can be done by passively or actively detecting the ^{222}Rn in the water (Marques *et al*., 2004). When measuring ^{222}Rn in the subsurface or groundwater, it must be noted that it takes approximately 20 days for the water entering the subsurface or groundwater system to reach equilibrium with the production and decay of ^{222}Rn (Sukanya *et al*., 2022).

One of the limitations of using ^{222}Rn as an environmental tracer for groundwater is that, often the assumption is that the spatial production of ^{222}Rn is constant within aquifers or the sediments (Peel *et al.,* 2022). In the study conducted by Peel *et al*. (2022), the high-resolution

measurements taken showed that ^{222}Rn emanation rates were at a maximum within a range of a few meters below the surface. This finding could have significant implications when interpreting the behaviour of ^{222}Rn activities in groundwater, especially in any infiltration zones. To correct this, knowledge of the spatial distribution of ^{222}Rn production rates is required (Peel *et al*., 2022). Therefore, the assumption that the ^{222}Rn production is constant could lead to a lack of understanding of the infiltration patterns of the surface water. Another limitation of ^{222}Rn as a tracer is that the groundwater being sampled may have been infiltrated by younger groundwater with a lower level of ^{222}Rn, mixing with the water of a higher ^{222}Rn concentration, diluting it (Schubert *et al*., 2011). This limitation highlights the importance of sampling at various temporal scales, such as during the wet and dry seasons.

2.3.2 Stable Isotopes of Water

The stable isotopes of water can help improve our understanding of the natural processes occurring in our environment, whether it's atmospheric circulation processes or hydrological flow paths and sources (Kendall and Doctor, 2003; Lemma *et al*., 2020). These stable isotopes of water for oxygen are oxygen-16, oxygen-17 and oxygen-18, whilst the hydrogen isotopes are protium (hydrogen-1) and deuterium (hydrogen-2) (Kendall and Doctor, 2003). These isotopes are naturally occurring stable water isotopes that can be used with great success as environmental isotopes to trace flow paths.

When studying the isotopic composition of water, it is standardised by comparing it to the isotopic makeup of ocean water. To do this, an internationally accepted reference sample of ocean water known as Standard Mean Ocean Water (SMOW) was established (Craig, 1961a, 1961b). As determined through mass spectrometry, water's isotopic composition is quantified as deviations from the SMOW standard, expressed as parts per thousand variations. These deviations are written $\delta^{2}H$ for the deuterium and $\delta^{18}O$ for ^{18}O.

The isotopic composition of water is influenced by two primary processes: phase changes and mixing of waters from different sources. Phase changes such as evaporation and condensation alter isotopic ratios through fractionation, where lighter or heavier isotopes are preferentially retained or lost depending on the direction of the transition (Juan *et al*., 2020; Kendall and Doctor, 2003). Mixing processes, on the other hand, involve the combination of water bodies with distinct isotopic signatures, such as the blending of infiltrating rainwater with groundwater or the interaction between river and lake water (Juan *et al*., 2020; Kendall and Doctor, 2003).

A third process, often treated as a subset of mixing, involves biological enrichment and depletion. Through transpiration and photosynthesis, plants absorb water from their surroundings without isotopic fractionation occurring during root uptake (Dawson and Ehleringer, 1991). However, the isotopic composition of the water taken up can vary depending on species, environmental conditions and the characteristics of the available water sources (Dawson and Ehleringer, 1991), thereby indirectly influencing local isotopic patterns.

These processes collectively govern isotopic variation throughout the hydrological cycle. In precipitation, variation arises primarily from isotopic fractionation during evaporation and condensation (Juan *et al*., 2020; Lemma *et al*., 2020; Jung *et al*., 2020). During evaporation, lighter isotopes are preferentially removed, enriching the remaining water in heavier isotopes. Conversely, condensation results in precipitation that is isotopically lighter, as heavier isotopes condense more readily (Lemma *et al*., 2020).

In addition to these physical processes, environmental and climatic variables, including latitude, altitude, precipitation type and amount, source region, relative humidity and distance from the coast, significantly influence the isotopic composition of hydrogen and oxygen in precipitation (Stumpp *et al*., 2014; Sun *et al*., 2019). These factors contribute to the spatial and temporal variability observed in isotopic data across different regions and climatic zones.

In most surface water systems, especially river systems, two main components contribute to the stream flow (Kendall and Doctor, 2003; Mazor, 2003). These components are surface water contributions as a result of direct rainfall to the channel, runoff or recharge due to fast-moving water in the subsurface and unsaturated zone, and the second is groundwater (Kendall and Doctor, 2003; Mazor, 2003). The ratio of these contributions is highly variable in each catchment and depends upon various physical, climatic and anthropogenic factors (Liu *et al*., 2019). The physical characteristics can be the topography, soil type, land cover and geology, whilst the climatic factors are the amount and seasonal variation of precipitation, temperature, potential evapotranspiration, etc (Kendall and Doctor, 2003; Kattan, 2008). The anthropogenic factors include dams and reservoirs, irrigation and agriculture (Liu *et al*., 2019). The isotopic signature of a river reflects the ratio of these water source components, and these signatures can show how the precipitation and groundwater contribution amounts and isotopic compositions vary with time (Kendall and Doctor, 2003).

The change in the isotopic composition of rivers where the streamflow is dominated by precipitation will show more considerable variations due to the seasonal variation, whilst the

effect of this seasonal variation will be smaller in river systems dominated by groundwater discharge (Kendall and Doctor, 2003). The impact of evaporation on the isotopic composition of surface water systems also increases with the size of the catchment due to the time taken for the water to reach the river system (Gat and Tzur, 1967). In these large catchments, the precipitation events are crucial components in the headwater and upper portions of the catchments (Genereux and Hooper, 1998). Genereux and Hooper (1998) found that the contribution to streamflow from precipitation in small, forested catchments from an event is approximately 40% (this value can increase for the duration of the storm itself), whilst Friedman *et al.* (1964) and Salati *et al*. (1979) showed that in the lower portions of catchments, the contribution of the precipitation could be of little importance.

2.4 Case studies of the applications of surface water-groundwater interactions

2.4.1 International case study 1: Awash River Basin, Ethiopia

This study by Kebede *et al*. (2021) examines the regional-scale surface water-groundwater interactions. This study used both geochemical and isotopic tracers, such as ^{222}Rn and stable isotopes ($\delta^{2}H$, $\delta^{18}O$) and piezometric observations to trace flow patterns and assess connectivity. The study site was the Awash River basin in Ethiopia. The outcomes of this study were:

- Identifying areas of hydrological gains or losses and the factors affecting these gains or losses,
- Studying the effect that anthropogenic activities and structures have on these water resources.

The findings of this study were that the contribution of the regional groundwater flows to the streamflow is minimal and was found to be exiting the catchment entirely. This finding was in line with the previous conceptual models of the catchment, and the river was categorised as a losing river. This was said to challenge a common assumption of the catchment being self-contained. Salinity was identified as a key issue, particularly near Lake Beseka, where irrigation-induced seepage into fractures increases downstream salinity, posing threats to agricultural and domestic water use. Tributaries and wetlands were found to be critical in buffering salinity during dry seasons. The study concluded that anthropogenic effects on the catchment's hydrological responses were complex. It was also noted that the river could be at risk from future extreme drought events affecting the wetland and river networks' capacity to mitigate the current salinity problem. The findings of this study showed the need for a holistic

and integrated approach and strategies that combine irrigation efficiency improvements, wetland conservation and long-term hydrological monitoring to address these complex challenges effectively.

2.4.2 International case study 2: Bale Mountains, Ethiopia

In a study by Lemma *et al*. (2019), the spatial and temporal effects on isotopic composition of precipitation (δ^2H, $\delta^{18}O$) of the Bale Mountains in Ethiopia were examined. This research aimed to better understand the atmospheric circulation patterns and improve paleoclimate interpretations for the region. The study also sought to determine the effects of the isotopic compositions of the precipitation and whether it is possible to trace the precipitation sources of the Bale Mountains. To achieve this, precipitation samples were collected along an altitudinal transect ranging from 1304 m to 4375 m above sea level over a one-year period, with isotopic analysis revealing significant seasonal and altitudinal trends. The study found that precipitation during the dry season is primarily sourced from the Gulf of Aden and the Arabian Sea, while during the rainy season, moisture originated largely from the Southern Indian Ocean.

The isotopic data showed a clear amount effect where rainfall from higher altitudes was isotopically lighter than lower-altitude rainfall. This, however, was linked to changing moisture sources rather than precipitation volume alone. An altitude effect was observed, with depletion in heavy isotopes ($\delta^{18}O$) at higher elevations, attributed to orographic lifting. The authors derived local meteoric water lines (LMWLs) specific to the Bale Mountains. These were compared to both global and regional meteoric water lines (GMWL), with variations influenced by local climatic conditions and moisture sources being found.

This research provided the first analysis of isotopic precipitation patterns for the Bale Mountains, offering insights into the regional hydrological drivers occurring. It also emphasised the importance of ecosystem service management in the Bale Mountains National Park to maintain resilience against climate change-related challenges.

This study concluded that the results would help better understand factors that influence the isotopic composition of precipitation and allow for better interpretation of the paleoclimate records of East Africa. This also has significant implications for the ecosystem service management effort in the Bale Mountains National Park, especially with regard to the challenges that climate change will present.

2.4.3 International case study 3: Maimai, New Zealand

In a paper written by Brammer (1996), the aim was to provide detailed overviews of the previous studies conducted at a site and how these studies evolved and changed the conceptual models of the hillslope processes. They also looked at how the methods, scope and scale of the study affected this change. This study examined the value of working on a site that has a long history of being studied. It was found that the single-method approaches of the late 1970's showed how the use of a single tracer method could result in misinterpreted results due to a lack of understanding of the limitations of the method used. Later studies that were conducted using a variety of integrated methods were able to characterise the hillslopes studied as well as to determine the hillslope and runoff processes occurring. Other studies conducted highlighted the errors and shortfalls of the methods used by previous studies. It is for these reasons that having a rich history of studies is invaluable, as they concluded that each study reviewed in their paper showed a development of previous ideas and understanding, whilst sometimes alternative possible interpretations of the hillslope processes arose, leading to new opportunities and avenues of research.

2.4.4 International case study 4: Rocky Mountains, Canada

The study conducted by Spencer *et al.* (2021) aimed to build upon the previous work done to improve the conceptualisation of the runoff generation mechanisms. The study focused on the Star Creek catchment on the eastern slopes of the Rocky Mountains, Canada. The objectives of this study were:

- To characterise the variation of the streamflow sources at a spatial and temporal scale,
- To determine the relative contributions of the sources.

These objectives were achieved through the use and analysis of the natural environmental tracers in the stream water and source water chemistry. The source water chemistry was measured from the bedrock groundwater, the hillslope groundwater, soil water, snowmelt and the rainfall. The sample data were analysed for the major cations and anions (Na^+, Mg^{2+}, Ca^{2+}, K^+, Cl^- and SO_4^{2-}) and silica (Si as SiO_2) and using the end-member mixing models to determine the different sources and ratios of source contributions. This study found that due to the variability of the data analysed, the sources could not be quantitatively determined. However, the relative percentage contributions of these sources were qualitatively determined. This allowed for the determination of the key runoff-generating processes to be inferred. The hillslope processes observed were:

- Snowmelt resulted in a water table increase, therefore connecting the hillslope water storage (the water storage capacity of the hillslope's soils, sediments and underlying rock layers) to the river, increasing discharges.
- In some of the subcatchments studied, the hillslope water was responsible for base flows,
- In one of the catchments, the tracer signature was different to that of all the sampled sources, suggesting a contribution by deeper groundwater.
- The water stored in the till had a longer residence time than water stored in the bedrock. This water was thought to contribute to flows toward the end of the wet season.

The conclusion was that to determine streamflow sources quantitatively, more research needs to be done on the variability of the groundwater chemistry for bedrock and tills. They also concluded that multiple subsurface systems could contribute to the continued and higher baseflows than in other regional shallow soils.

2.4.5 International case study 5: Kumamoto, Japan

Iwagami *et al*. (2010) conducted a study on the role of bedrock groundwater in generating runoff. This was achieved by using tracers (SiO_2 and stable isotopes) and studying the potential of this bedrock groundwater over both a wet and dry season. The groundwater potential was studied using hydrometric observations (water level observation and monitoring). This was done to determine the role of the groundwater in the infiltration and discharge. This study took place in the headwater catchment of the Ma catchment in the Uki district of southwest Japan. This study found that:

- During the dry season, the groundwater maintained the baseflows in the river.
- During high-intensity storms, the contributions of the bedrock groundwater to the stormflow generated were significantly lower.
- From a hydrograph of the three contributing components (rainwater, soil water and bedrock groundwater) and hydrometric observations, the groundwater contribution was quantitatively measured in the streamflow.
- Increases in bedrock groundwater during mid-intensity events resulted in a secondary runoff peak.

- Contributions to the catchment discharge through lateral flows at the soil-bedrock interface were also observed.

This study concluded that the contributions of bedrock groundwater and soil water depend on the location of the water table.

2.4.6 Local case study 1: Mpumalanga, South Africa

Madlala *et al*. (2021) assessed the valley bottom wetlands' dependence on groundwater from shallow unconfined aquifers in an environment where coal mining occurs. This research was conducted on two wetlands using benthic sediment sampling, stable isotope testing (δ^2H and $\delta^{18}O$), hydrochemistry and water level monitoring. The study aimed to locate the surface water-groundwater interactions in the wetlands being studied. Therefore, the study was set up to achieve the following objectives:

- To use hydrometric and various environmental tracer approaches to assess the spatial and temporal interactions between the wetland and aquifer,
- To assess the water quality changes due to the surface water-groundwater interactions.

This study found a strong connectivity between the surface water and the groundwater, as indicated by both similarities in the hydrochemistry and the stable isotopes. The primary source of the wetlands, aquifers and piezometers was found to be the shallow aquifers of the cathcment. It was also found that the wetland piezometer fluctuations followed the expected seasonal variation, except during the mine de-watering periods. This showed that the mine had a negative impact on the wetland persistence and that mining activities could have adverse effects on wetlands, dependent upon the subsurface discharges from aquifers.

2.4.7 Local case study 2: Eastern Cape, South Africa

Uhlenbrook *et al*. (2005) investigated subsurface flow pathways and hydrological processes in the Weatherley catchment, a small semi-arid headwater in South Africa's Umzimvubu basin. The study combined traditional hydrometric measurements, tensiometers, and advanced geophysical techniques such as 2D Electrical Resistivity Tomography (ERT) to explore water movement, residence times, and the interaction between subsurface storage and streamflow generation. The key findings of this paper are:

- Rainfall triggered perched groundwater formation in shallow soil layers due to vertical flow impediments, resulting in temporary contributions to streamflow.

- Subsurface flows were shown to interact with deeper aquifers and groundwater seepage contributed to baseflow at the toe of the studied hillslopes.
- The influence of subsurface structures as a result of the bedrock profile was observed on both the water movement and storage.
- The buffering effect of wetlands was observed, these wetlands store rainfall-derived water during wet seasons and the following dry season release it as baseflow.

The study demonstrated the value of combining multiple methods to achieve a comprehensive understanding of subsurface hydrology. While tensiometers and neutron probes captured water movement at shallow depths, ERT provided detailed images of deeper aquifers and subsurface flow pathways. Together, these methods revealed both event-based and seasonal hydrological dynamics. This paper shows the importance of subsurface flow processes, lateral flow pathways and groundwater contributions for streamflow generation in semi-arid catchments. It emphasized the need for integrated, multidisciplinary approaches to study hillslope hydrology, particularly where geological and hydrological complexity governs water distribution and storage.

Below is an example ERT result from Uhlenbrook *et al*. (2005) showcasing spatial variations in subsurface resistivity along a hillslope transect (Figure 2-3).

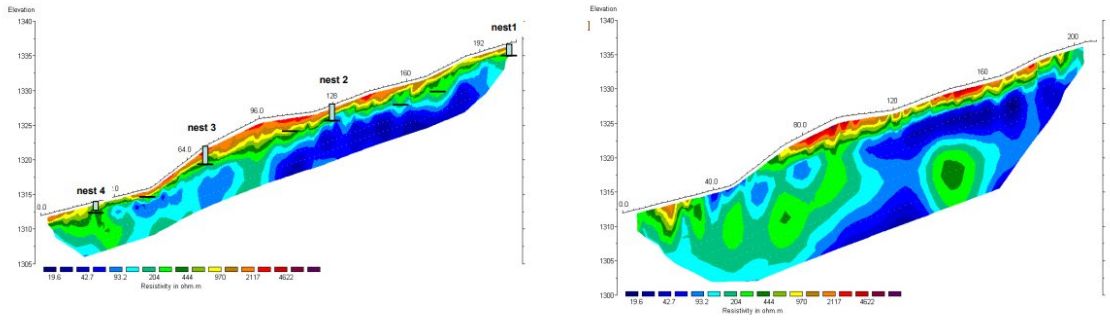

Figure 2-3:Results of the 2-D electrical imaging survey at the investigated hillslope using a Wenner 2-D configuration (Uhlenbrook *et al*., 2005)

This case study illustrates how advanced geophysical techniques, combined with conventional hydrological tools, can improve the characterisation of flow paths and inform water resource management in heterogeneous environments.

2.4.8 Local case study 3: Kruger National Park, South Africa

In a paper by Lorentz *et al*. (2020), the study aimed to characterise the surface water-groundwater interactions occurring in the low-order ephemeral catchments. To accomplish

this, the study used a combination of in-situ methods, including hydrometric observations, hydrochemistry and remote sensing. This study aims to characterise the flow path, the existing hydrological connectivity between the stream and the hillslope, and the groundwater recharge rates. This study was conducted on the Southern Granite Supersite located in the Sabie and Crocodile catchments in Kruger National Park, South Africa. From this study, it was found that the streambeds of these ephemeral catchments are important preferential recharge points. It was also noted that these streams are crucial in the recharge of groundwater, which is a significant component of the water balance in these catchments. These streambeds and their soils are important, but they are threatened due to anthropogenic activities such as sand mining. It was also found that the preferential flows connect the hillslopes through interflow processes.

2.4.9 Local case study 4: Middelburg, South Africa

Mahlangu *et al.* (2020) conducted a study with the aim of improving cemetery guidelines. This would allow for better selections of new burial sites and management of existing ones. This research was conducted at a study site located in Middelburg in Mpumalanga, South Africa. The aim of this paper was achieved through the following objectives:

- To study the surface water-groundwater interactions occurring and to determine the effects of cemeteries on these interactions,
- To determine the extent of these effects on the surface water-groundwater interactions in order to protect water resources from contamination.

This study found that the rainfall directly replenished both surface water and groundwater, and that during the dry season, subsurface water and groundwater were responsible for the baseflows. The stable isotope results further supported this, as the subsurface water was responsible for flows in dry seasons between rainfall events during the wet season, with contributions from groundwater increasing as the wet season progressed. The wetland in the catchment was also found to be a result of lateral subsurface flows and daylighting groundwater. With regards to the water quality results obtained, it was found that the wetland and longer groundwater lag times helped improve the water quality; however, the cemetery still affected the water quality. Due to the shallow water table, it was recommended that no burials be held in the northwestern portion of the cemetery. This recommendation was made to protect the groundwater. This study concluded that longer monitoring is required in order to better understand the surface water-groundwater interactions. This improved understanding would then be able to better guide the water resources management in the area.

2.5 Evaluation of Literature

The reviewed literature provides a robust foundation for understanding the methodologies, mechanisms and real-world implications of surface water-groundwater interactions. The studies presented show the importance of studying lateral flow and runoff generation mechanisms in sustaining streamflow at different spatial and temporal scales. Studying these processes at differing temporal scales, such as event-based and long-term monitoring, can highlight seasonal dynamics and long-term sources and contributions, whilst various spatial scales can highlight localised hydrological processes and broader regional contributions. Various methods, such as environmental tracers, hydrometrics and numerical modelling, can complement each other and thereby overcome the limitations of a single method approach. The findings of these studies show the need for interdisciplinary approaches (Barthel, 2014; Kløve *et al.*, 2011b) to achieve holistic catchment management.

These case studies are from different contexts: anthropogenic, hydrological and ecological. This highlights the challenges of natural variability and human impact on studying surface water-groundwater interactions. The findings from the various Ethiopian studies emphasise the regional climate drivers that influence the isotopic composition of water sources. In contrast, the local case studies focused on the fine-scale hillslope connectivity in the study area. Another focus of these studies was the anthropogenic activities, such as mining and cemeteries, affecting aquifer recharge and water quality. These cases show the interconnection between hillslope-scale hydrological patterns and localised interventions.

From the findings of these case studies, the following conclusions can be made:

- Methodologies should be applied in integrative frameworks to characterise surface water-groundwater dynamics robustly.
- Anthropogenic impacts necessitate site-specific strategies that prioritise wetland conservation, buffer zones and long-term monitoring.
- Understanding mechanisms at different physical scales, such as transmission feedback or fill and spill processes, is key to water resource management in the face of changing environmental pressures.

To address the gaps identified in the research presented, future research should focus on high-resolution interdisciplinary approaches and refine conceptual models. Furthermore, the impact of climate change and its inherent uncertainties should be a focus of future research to guide sustainable hydrological and ecological planning.

Previous South African studies, such as those by Jewitt (2002) and Tanner et al. (2022), have emphasised the critical need for continued research at the hillslope scale, particularly through the use of isotopic tracers, to deepen our understanding of runoff generation mechanisms. These works have highlighted knowledge gaps in how lateral flow processes, such as interflow, groundwater ridging, and saturation-excess overland flow, contribute to streamflow under varying climatic and land use conditions. The current study aims to build on this growing body of literature by providing additional insights from a South African mountain catchment using a multi-method approach. By focusing on event-based and long-term monitoring of tracers such as electrical conductivity, temperature, radon, and stable isotopes, this research seeks to contribute to the refinement of conceptual models for runoff generation in complex terrain.

SITE DESCRIPTION

In this chapter, an overview of the two study areas is presented. This chapter includes the site locations, relevant meteorological variables, geology, land use, etc. The surface hydrological features and their locations are also included in this chapter. Where applicable, the previously proposed conceptual models from other research papers have been included. The two study sites are the CP research Catchment 6 and the FHE catchments. The descriptions of these sites can be found in the sections below. The base imagery for the maps in this chapter was sourced from Google Satellite (2024) and used for visual reference and background mapping in QGIS.

3.1 Cathedral Peak Catchment 6

The CP research catchments (28°58'32.12" S; 29°14'8.70" E) form part of the "Little Berg plateau" in the Drakensberg, KwaZulu-Natal, South Africa (Nanni, 1956). These catchments and their location in South Africa can be seen in Figure 3-1.

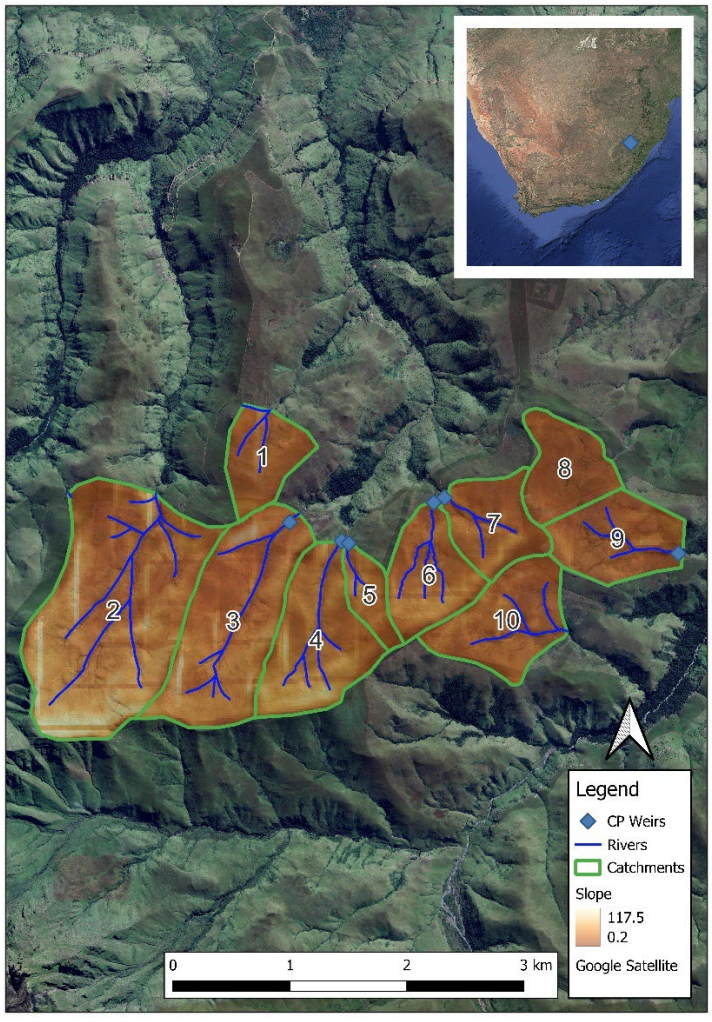

Figure 3-1: CP research catchments site map

The elevation of the research catchments ranges from 1820 m to 2463 m above sea level, with an average temperature of 13.8°C (Everson *et al*., 1998; Toucher *et al*., 2016).

3.1.1 Climate

The mean annual precipitation (MAP) is approximately 1400 mm, though only about 49% of this rainfall contributes to streamflow (Bosch, 1979). For CP Catchment 6 specifically, the MAP is slightly lower at 1340 mm. Most of the annual rainfall occurs during the summer months, which are characterized by hot and humid conditions (Bosch, 1979; Ndlovu *et al*., 2021). When analysing the data obtained from SAEON, for the period of September 2013 - October 2024, from the historical rain gauge in CP Catchment 6 (shown in Figure 3-12), the average monthly rainfall was calculated. These rainfall trends are presented below in Figure 3-2.

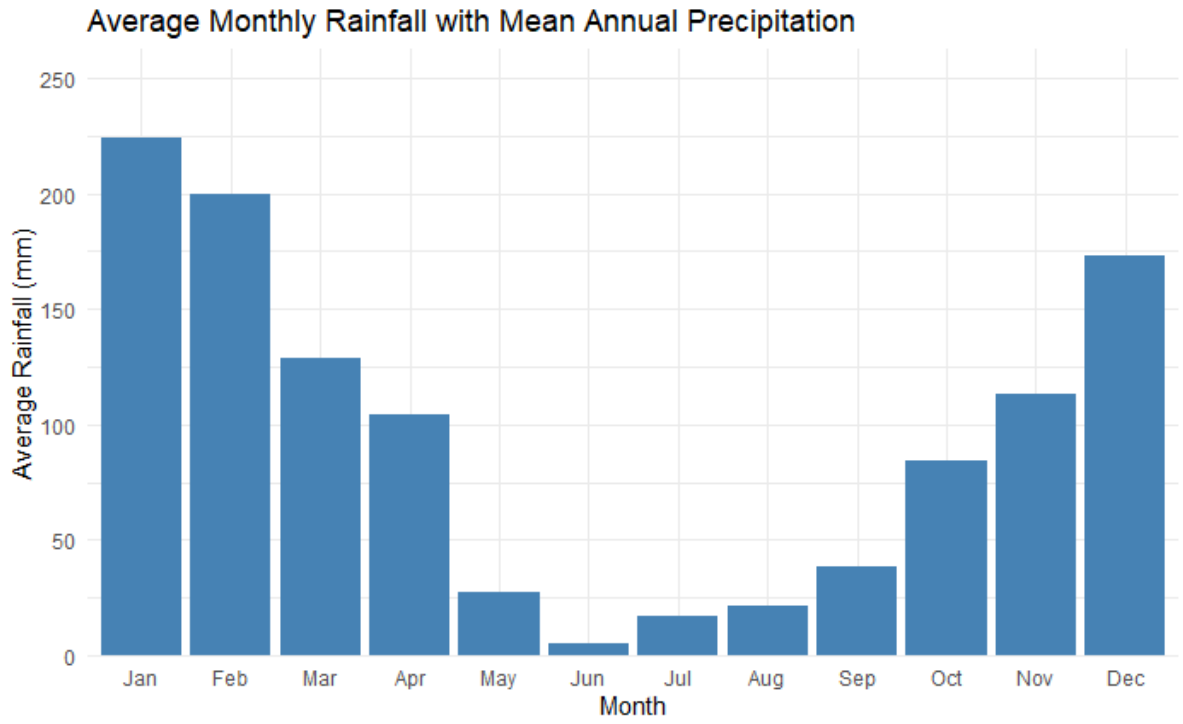

Figure 3-2: CP Catchment 6 monthly average rainfall (SAEON, 2024)

From Figure 3-2, the rainfall in the catchment primarily occurs during the summer months (December to February) and gradually declines throughout autumn, reaching its lowest point in June. The dry season, spanning May to October, is defined by these six driest months, while the wet season, running from November to April, encompasses the wettest months. Rainfall begins to increase again in spring and is largely driven by localised thunderstorms occurring between September and March. These thunderstorms originate from clouds to the west of the catchment and contribute to half of the rainfall events in the region. Orographic clouds forming

in the east of the catchment produce longer periods of softer rainfall, which can continue for several days (Nanni, 1956; Bosch, 1979; Toucher *et al*., 2016; Mucina *et al*., 2017; Harrison *et al*., 2022). The average temperature for the catchment ranges between 10.0 °C to 17.1 °C, with frost being a common occurrence during the winter months (Bosch, 1979; Everson *et al*., 1998; Toucher *et al*., 2016; Gordijn *et al*., 2018; Harrison *et al*., 2022). The Mean Annual Evaporation (MAE) for the site is 695 mm, with 54% of the rainfall received annually being evaporated (Everson *et al*., 1998).

3.1.2 Hydrology

Three tributaries join in the centre of the catchment in Wetland 1. Wetland 1 then discharges to the lower portion of the catchment, whereupon it enters Wetland 2. The discharge from Wetland 2 flows through the temporarily saturated valley bottom to the stilling pond for the catchment 6 weir. This stream network with the weir and wetlands can be seen below in Figure 3-3.

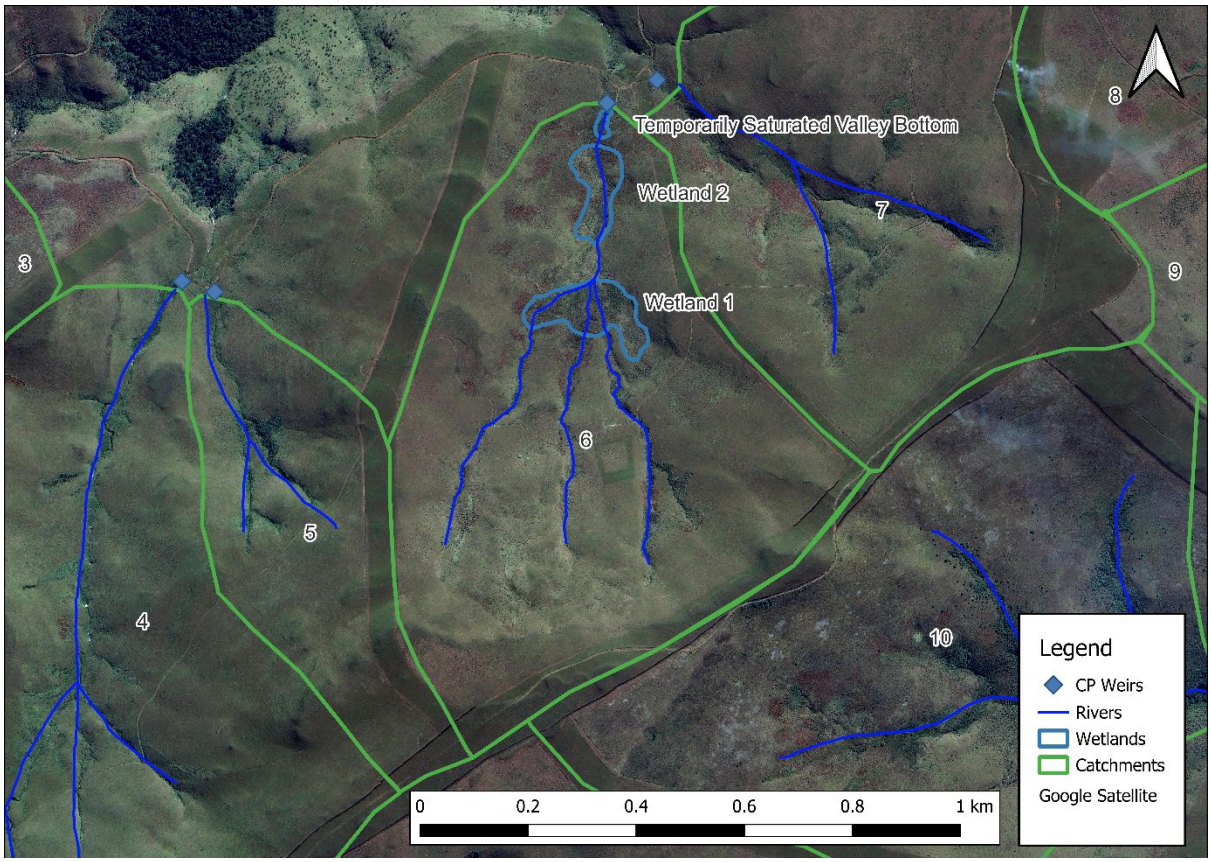

Figure 3-3: CP Catchment 6 hydrologic features

3.1.3 Terrain

The topography of catchment 6, as illustrated in Figure 3-4, exhibits distinct variations in slope across its extent. The southern boundary of the catchment is made up of a ridgeline that terminates in a small plateau. This plateau can be seen in Figure 3-4 on the catchment boundaries of catchments 5, 6 and 10. The upper portions of the catchment around the tributary headwaters, located in the southern region of the map, are characterised by steep slopes with slope angles between 1° and 31°. These steep slopes are common in high-altitude catchments and increase the potential for rapid flow processes. Moving toward the central portion of the catchment, the slopes gradually become shallower with slopes of less than of 15°, creating a transitional zone. It is in this region that the first and largest wetland of the catchment is situated (Wetland 1). In the outlet region of the wetland, the terrain rapidly transitions to steeper gradients before again transitioning to progressively gentler gradients as the lower reaches of the catchment approach a flatter topography.

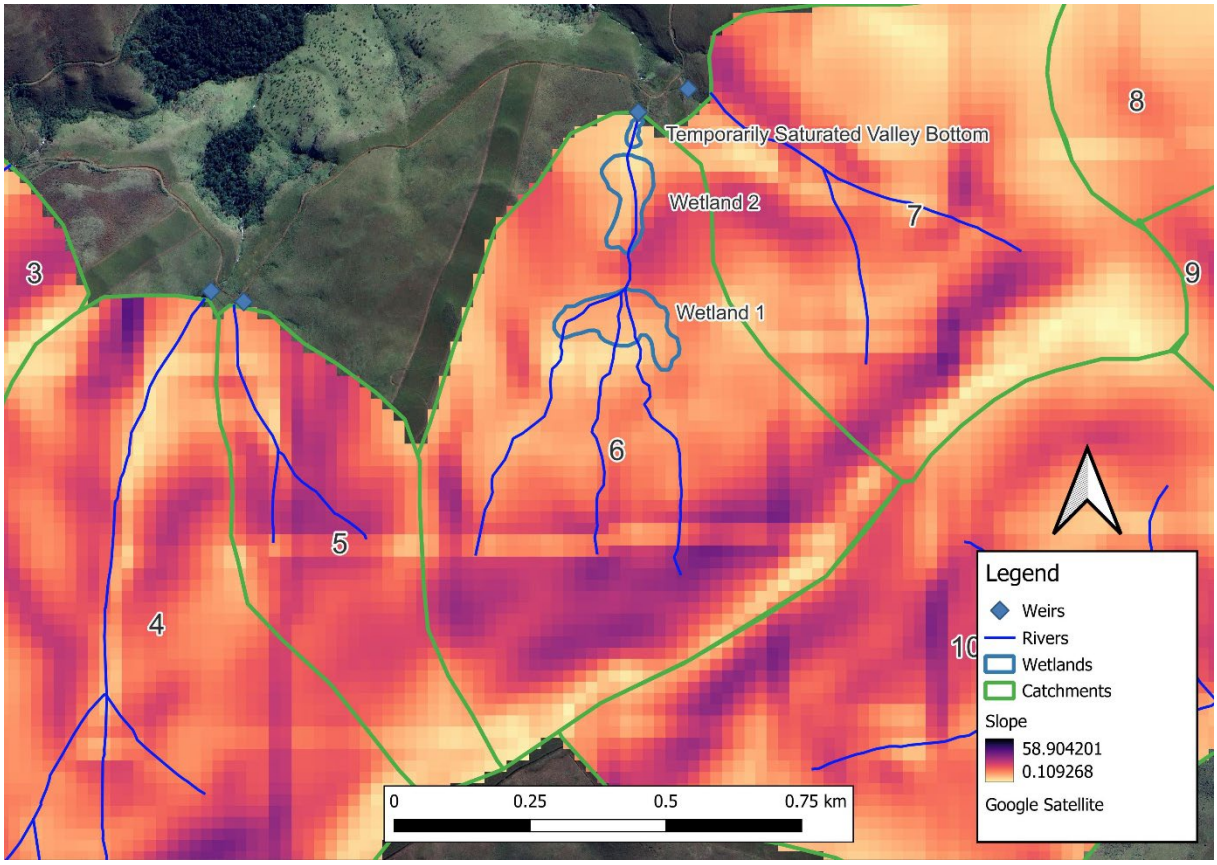

Figure 3-4: Slope map of the CP Catchment 6

The catchment is also characterized by a distinct distribution of slope aspects. On the eastern side, the slopes have a predominantly westerly to north-westerly orientation, whilst the slopes

on the western portion of the catchment are mainly oriented easterly to north-easterly. This variation in slope aspect is likely to influence factors such as solar radiation exposure, vegetation patterns and hydrological processes within the catchment. The spatial distribution of slope aspects across the catchment is presented in Figure 3-5.

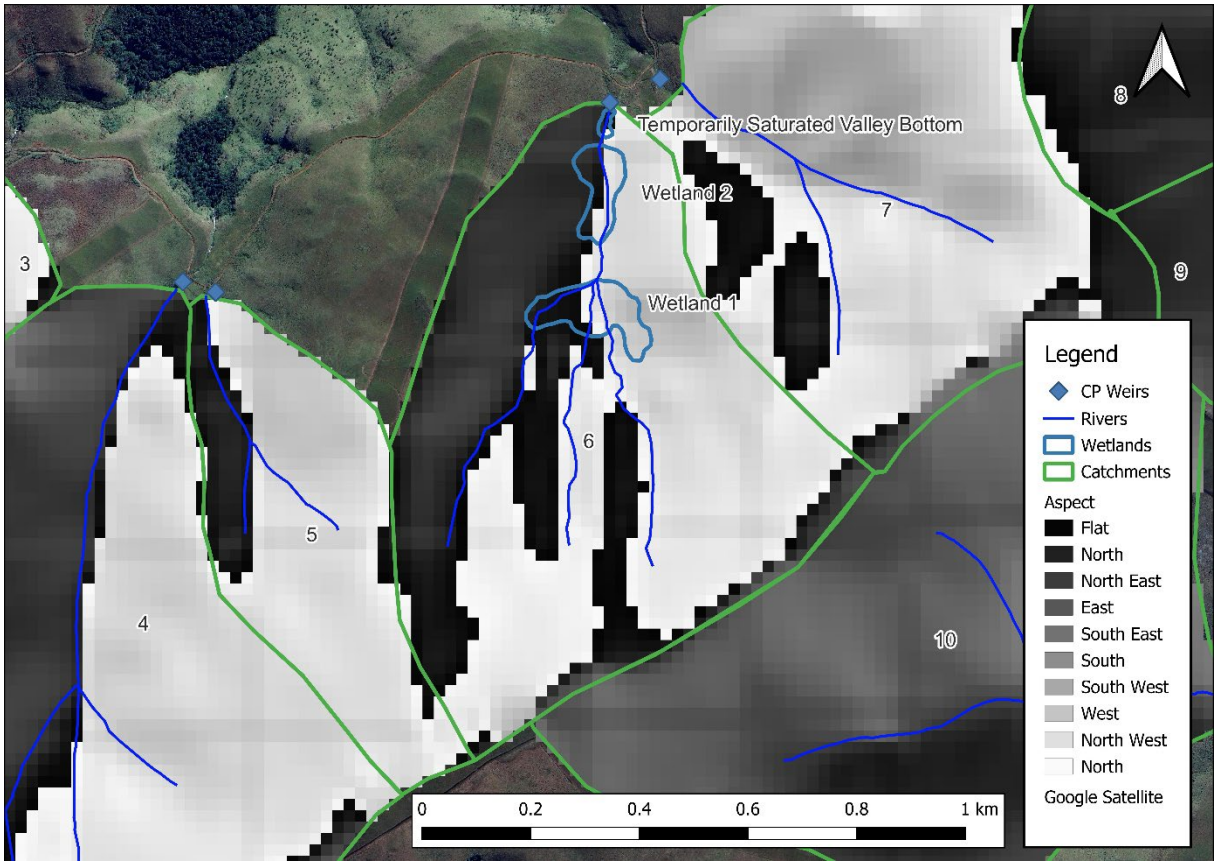

Figure 3-5: Aspect map of the CP Catchment 6

Images of the catchment boundaries taken during the site visit conducted in April 2024 are presented in Figure 3-6, Figure 3-7 and Figure 3-8 below. Figure 3-6 shows the eastern boundary of the catchment. This image was taken at the southernmost point of the boundary between catchments 6 and 7.

Figure 3-6: CP Catchment 6 – ridge on the eastern boundary

Figure 3-7 and Figure 3-8 were taken of the plateau that forms the southernmost portion of the catchment 6 boundary. Figure 3-7 shows the eastern portion of the plateau as it transitions into the ridgeline that forms the catchment boundary that runs in a north-easterly direction from the southernmost point of the catchment.

Figure 3-7: CP Catchment 6 - eastern portion of the plateau

Figure 3-8 shows the western portion of the plateau as it flattens out and extends towards the boundary of catchment 5.

Figure 3-8: CP Catchment 6 - western portion of the plateau

3.1.4 Geology

Beneath the basaltic cliffs of the KwaZulu-Natal section of the Drakensberg mountain range is a fragmented plateau (Nanni, 1956; Toucher, *et al*. 2016). This plateau is situated at elevations ranging from 1800 m to 2500 m. The terrain of this plateau is intricately carved by deep ravines and swift-flowing streams. The plateau's edge is formed by a precipitous escarpment of sandstone cliffs belonging to the Clarens Formation (Nanni, 1956; Toucher, *et al*. 2016). The experimental catchments of Cathedral Peak are located at the uppermost points of three isolated spurs (Nanni, 1956; Toucher, *et al*. 2016). The CP Catchment 6 geology consists of basaltic lavas overlying sandstones of the Clarens Formation (Nanni, 1956; Toucher, *et al*. 2016). This was confirmed by a geological survey performed in 1998 by the Council for Geoscience (CGS), which classified the region's geology at a 1:250,000 scale. The results of the survey are presented below in Figure 3-9.

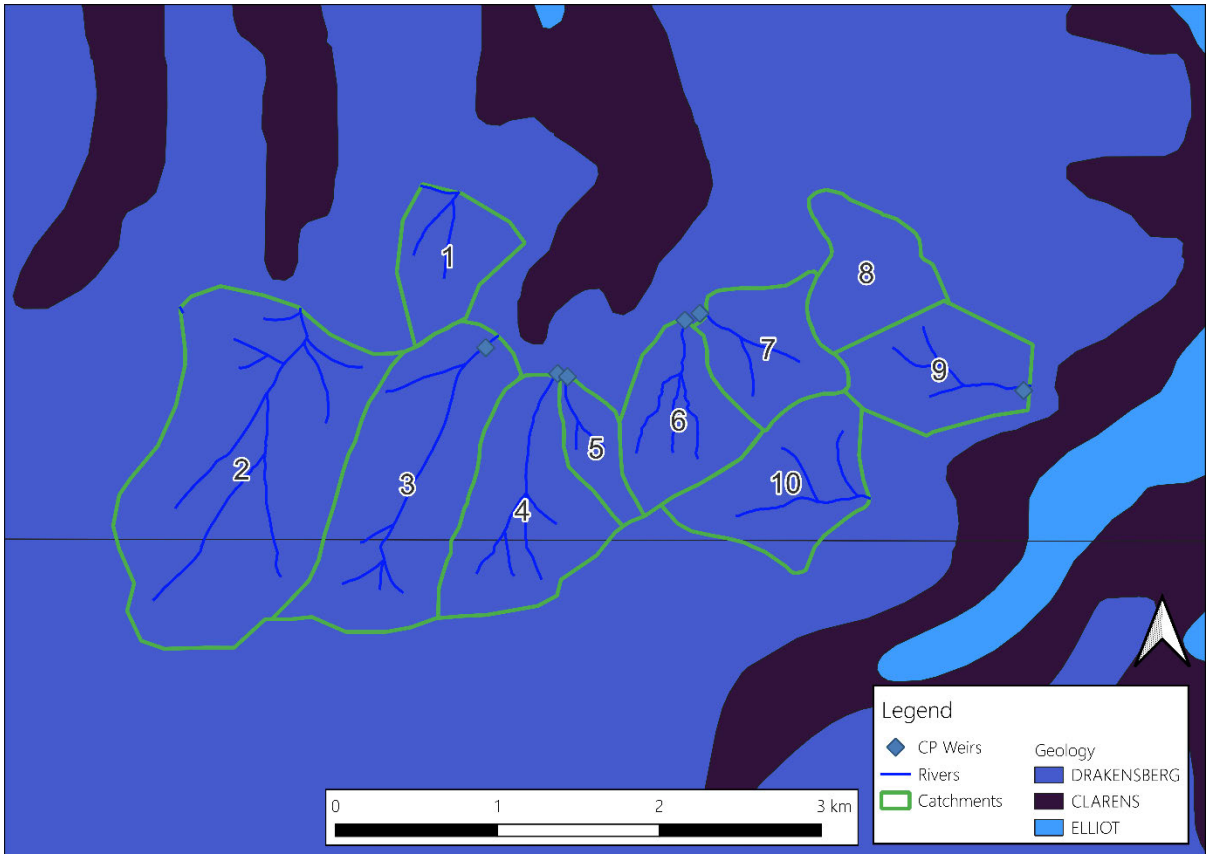

Figure 3-9: Geological map of the CP Catchment 6 (CGS, 1998)

The geology of the catchment is that it is underlain by basalt of the Drakensberg lithographic unit belonging to the Karoo supergroup stratigraphic unit (CGS 1996). Three Karoo dolerite dykes, each of an approximate width of 3 m, run through the Cathedral Peak catchments. However, they are assumed not to influence the catchment hydrology (Nänni, 1956; Toucher, *et al*. 2016). A section of the exposed basalt that makes up the small plateau and ridge line forming the southern boundary of CP Catchment 6 was taken during the April 2024 site visit. This image is presented below in Figure 3-10.

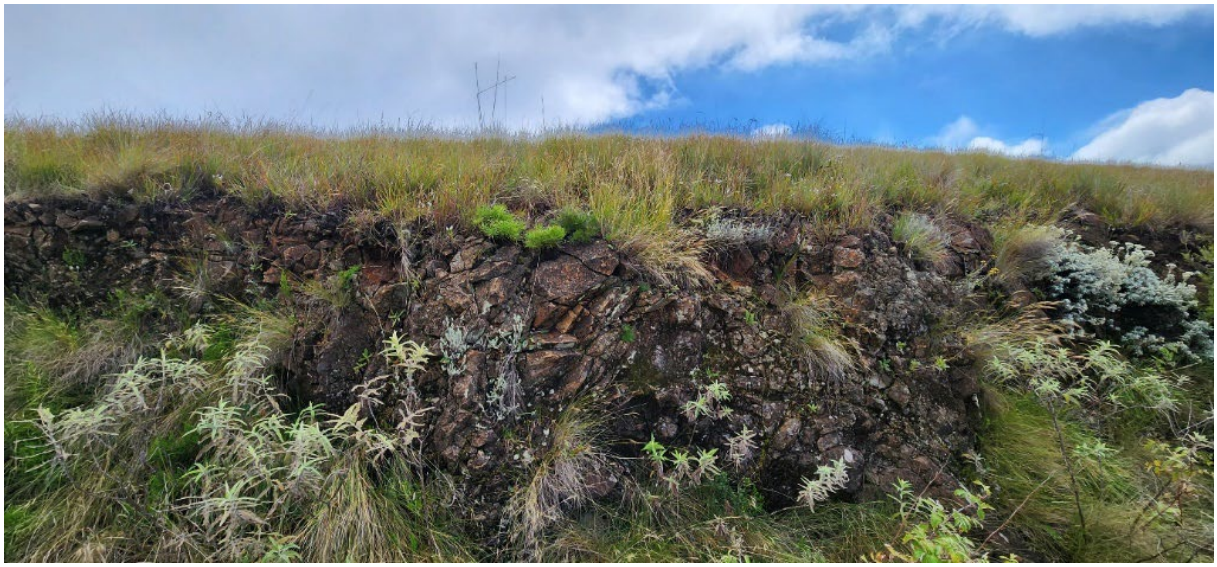

Figure 3-10: CP Catchment 6 - exposed fractured basalt on the eastern ridge and plateau

3.1.5 Pedology

The soils in the Cathedral Peak research catchments are predominantly lateritic red and yellow soils, which are heavily leached and exhibit high acidity levels (Schulze and George, 1987). In areas with frequent or prolonged saturation, such as stream banks, stream networks and wetlands, these soils gradually transition into heavy black Katspruit and Champagne soils (Granger, 1976; Toucher, *et al*., 2016). Harrison *et al.* (2022) investigated the hydropedological properties and conceptual flow dynamics of CP Catchment 6 by analysing rainfall-streamflow relationships, conducting soil mapping, and installing piezometers to monitor groundwater levels and fluctuations. The hydropedological map from Harrison *et al.* (2022) is presented in Figure 3-11.

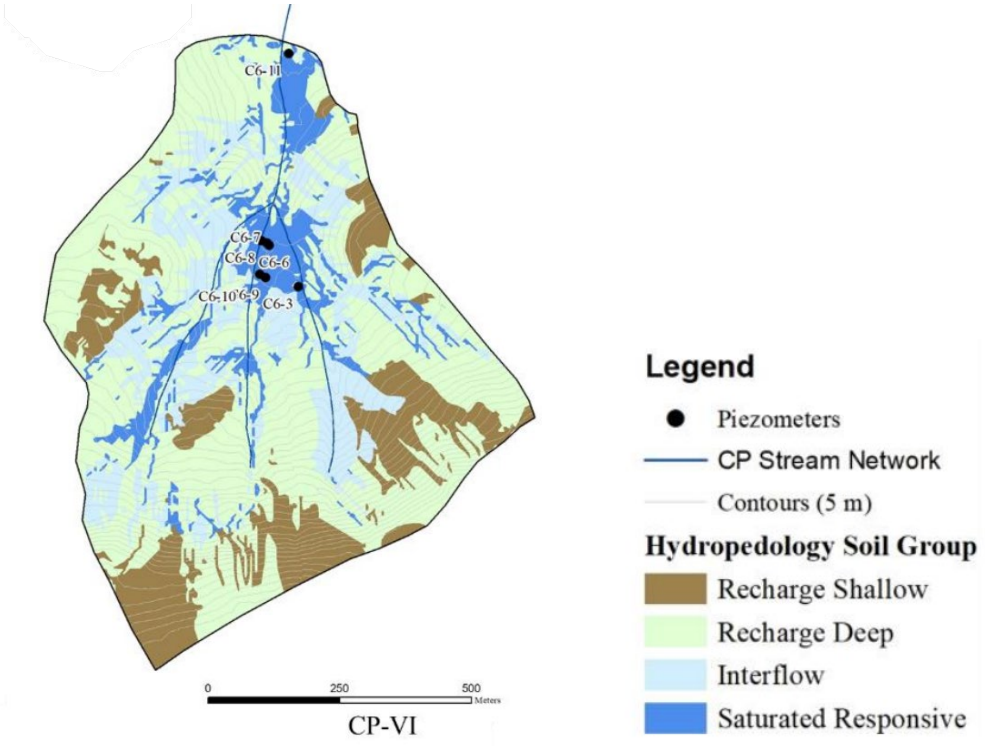

Figure 3-11: Hydropedological soil map of the CP research catchment 6 (Harrison *et al.*, 2022).

The catchment features distinct hydropedological soil groups, including recharge soils, interflow soils and saturated soils, each playing a key role in water movement through the landscape. Recharge soils, found in the upper catchment, were classified into shallow and deep recharge soils. Shallow recharge soils, less than 500 mm deep and formed along steeper slopes, facilitate vertical water flow through freely draining B horizons into fractured parent material or a lithic horizon. In contrast, deep recharge soils, exceeding 500 mm in depth and on gentler slopes, typically recharge deeper aquifers. However, lateral flow may occur along the soil-bedrock interface where low-permeability bedrock is encountered, resulting in seasonal hillslope responses and shallow aquifer recharge. Below the recharge soils lie interflow soils, where water infiltrates vertically through free-draining horizons and then moves laterally upon encountering impermeable underlying bedrock. Hydromorphic properties indicating periodic saturation develop at these interfaces due to water table fluctuations. In the middle and lower parts of the catchment, permanently saturated wetland soils store water during the wet season but generate overland flow once fully saturated due to their limited capacity to absorb additional water.

3.1.6 Land use

Over time, the CP research catchments have been subjected to various land-use activities and experimental studies. Despite these changes, the catchment is covered with a natural/semi natural mesic grassland burned biennially in spring (Dlamini *et al*., 2024). The grassland is classified as a Ukhahlamba Basalt Grassland in which the dominant vegetation includes *Themeda triandra*, a native grass species (Toucher *et al*., 2016; Harrison *et al*., 2022).

3.1.7 Current Equipment

Various climate variables are monitored at two meteorological stations and one eddy covariance tower in the research catchments. The meteorological stations are located at the top of Mike's Pass and catchment 9, and the eddy covariance tower station is located in the middle portion of catchment 6. The eddy covariance tower in the near-pristine catchment 6 measures fluxes and the energy balance. The soil moisture is monitored with a cosmic ray probe to capture spatial variations. In contrast, Time Domain Reflectometry (TDR) soil moisture probes are installed up to a depth of 1.4 m at the eddy covariance tower. Additionally, distributed soil moisture monitoring is conducted with diviner tubes and piezometers. Over and above the meteorological monitoring stations, rainfall is monitored at a further 30 sites scattered throughout the catchments. This network can be seen in Figure 3-12. This monitoring network is maintained by the South African Environmental Observation Network (SAEON): Grassland Node.

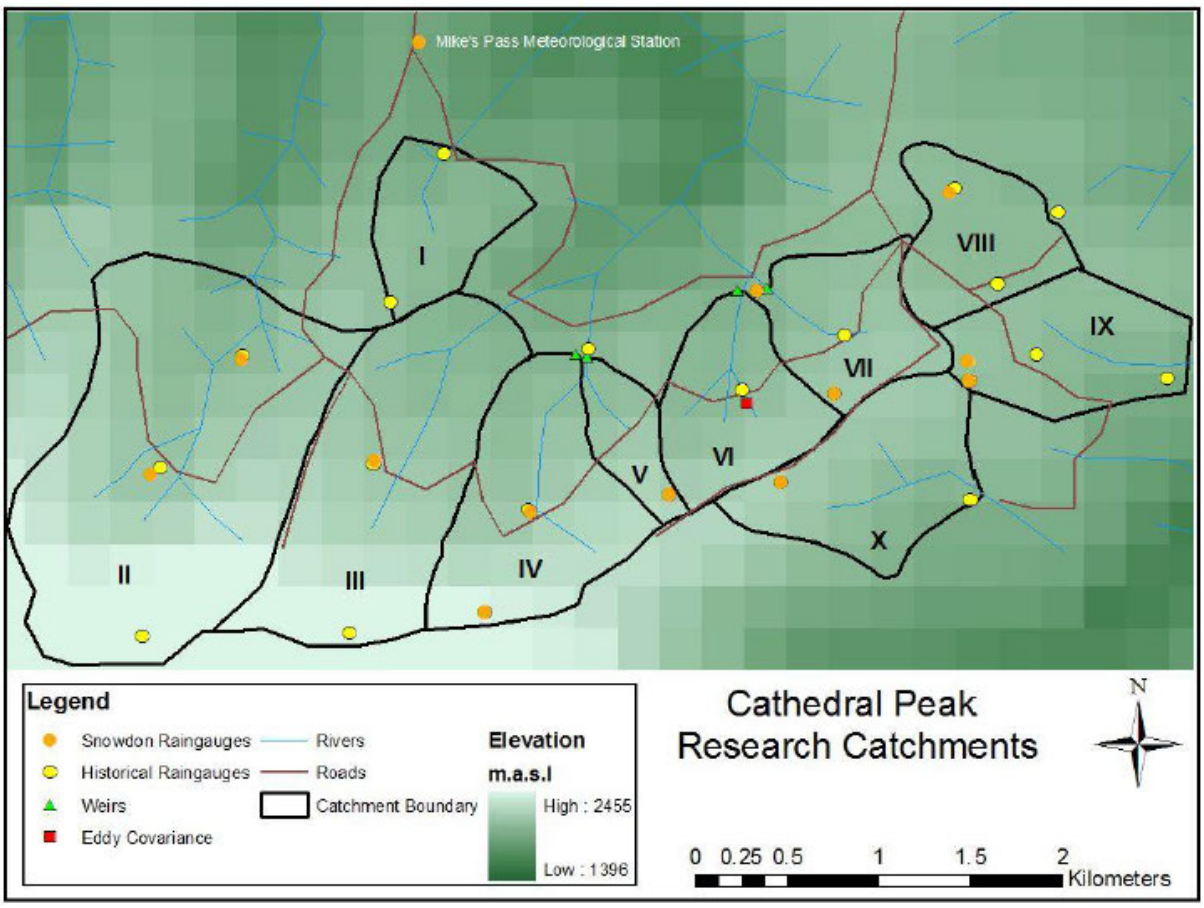

Figure 3-12: Map of the CP research catchments, the weirs and atmospheric monitoring network (Gray, 2017)

Streamflow is monitored at the outlets of catchments 3, 4, 5, 6, 7 and 9 (shown as III, IV, V, VI, VII, IX in Figure 3-12 respectively). Monthly water quality data, including EC, TDS, pH and temperature, are collected at the monitored weirs. Additionally, Teledyne ISCO samplers were deployed within CP Catchment 6.

The equipment that was added to the existing monitoring network in the catchment was two rainfall sample collectors and a piezometer. The rainfall sample collectors were placed in separate locations, with the first location being the Mike's Pass weather station and the second being the eddy covariance tower in CP Catchment 6. The rainfall sample collectors installed were the Palmex Rain Samplers RS-1D; these collectors were designed to prevent evaporation from the collected sample. The Palmex Rain Samplers RS-1D can be seen below in Figure 3-13.

Figure 3-13: Palmex Rainfall Sampler RS-1D (Gröning *et al*., 2012)

3.1.8 Latest Conceptual Model Proposed

The latest conceptual models for the research Catchment 6 were proposed by Harrison *et al.* (2022). These conceptual models were based on the hydropedological processes presented in Section 3.1.5. The model hypothesises that precipitation infiltrates the recharge soils in the upper catchment, with shallow recharge soils contributing to shallow aquifers and deep recharge soils recharging deeper aquifers or generating lateral flow when restricted by impermeable bedrock. Interflow soils facilitate lateral flow as water moves down the catchment, while wetlands in the middle and lower reaches act as critical buffers, storing water during the wet season and attenuating flow. These wetlands also maintain baseflows during the dry season but generate surface runoff when saturated. Notably, the wetland in Catchment 6 replenished more rapidly following extended dry seasons compared to wetlands in catchments 3 and 10. The conceptual models proposed by Harrison *et al.* (2022) are presented below in Figure 3-14.

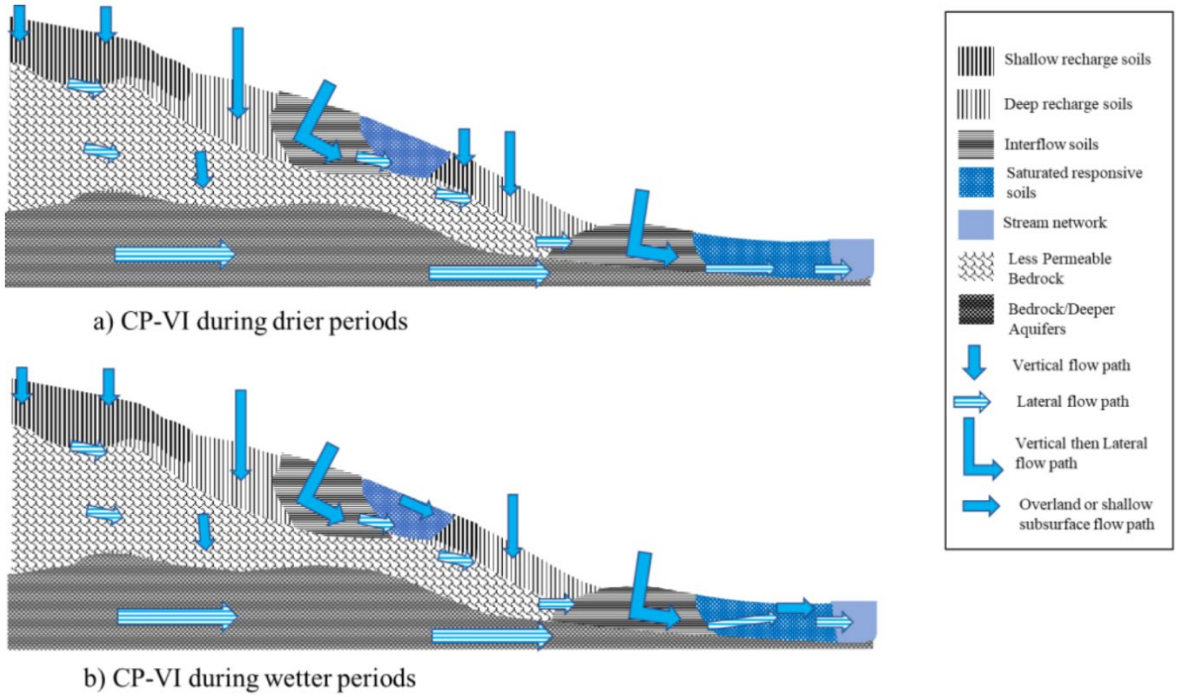

Figure 3-14: Current conceptual model of the dominant flow paths of CP Catchment 6 (Harrison *et al*., 2022).

From this study, the understanding of the flow paths in this system is that the flows move from the upper reaches of the catchment to the lower portions predominantly through shallow and deep recharge soils and are attenuated by the wetland in the middle of the catchment. This recharge was determined to be responsible for the baseflows during the dry season. It was noted that the wetland in this catchment filled faster after an extended dry season than the other wetlands studied in the Cathedral Peak Catchments 3 and 10.

3.2 Fountainhill Estate Catchments

The Fountainhill Estate (29.450677°S, 30.545511°E) is approximately 3.5 km west of Wartburg. It borders on the R614 roadway and the Umgeni River, forming part of its southwestern boundary. The property and catchment boundaries can be seen in Figure 3-15.

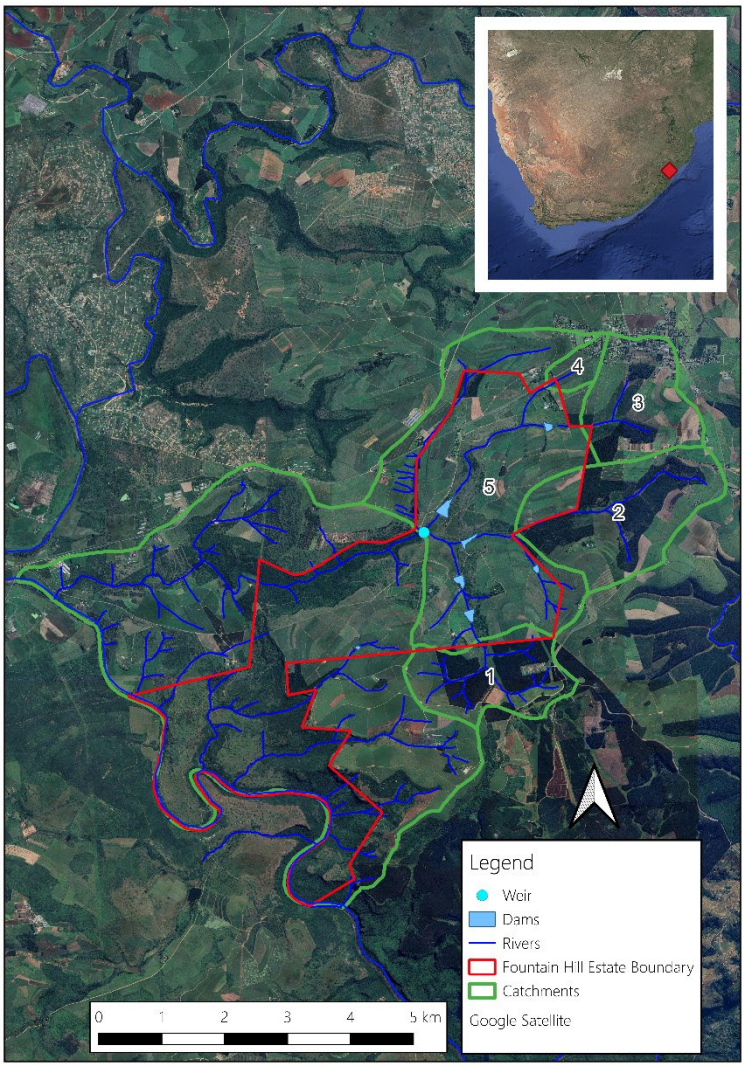

Figure 3-15: Fountainhill Estate Site Map (FHE, 2023)

3.2.1 Climate

FHE is located in the Department of Water and Sanitation (DWS) Quaternary catchment, U20G. This quaternary catchment has a MAP of 895 mm and a mean annual evaporation (MAE) (Symons Pan) of 1,200 mm (Water Resources of SA, 2012). When analysing the data obtained from SASRI, from August 2015 to October 2024, from the Fountainhill meteorological stations (shown in Figure 3-22), the average monthly rainfall was calculated. These rainfall trends are presented below in Figure 3-16. Using this data, the maximum temperature recorded was 40 °C and the minimum temperature was -4.7 °C.

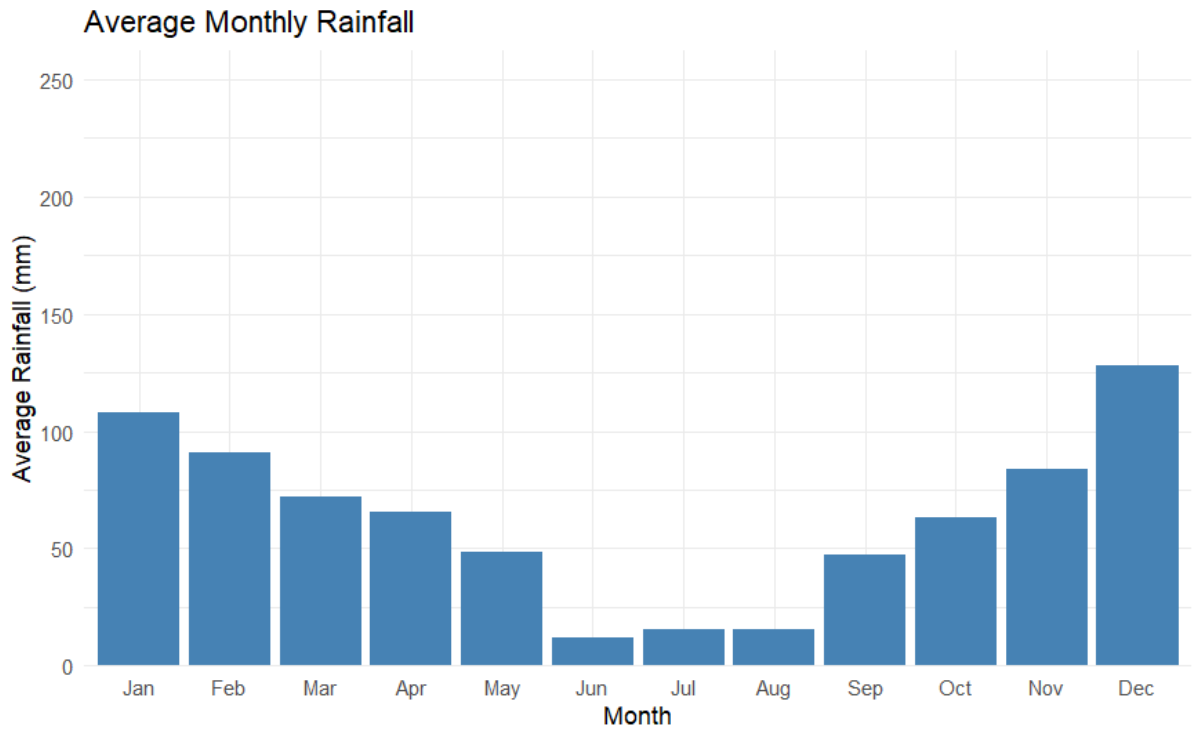

Figure 3-16: FHE average monthly rainfall (SASRI, 2025)

From Figure 3-16, the rainfall across the estate primarily occurs during the summer months (December to February) and declines throughout autumn. The winter months are categorised by dramatically lower rainfall values. As winter transitions through spring to summer, the rainfall increases substantially. The dry season, spanning June to august, is defined by these three driest months, while the wet season, September to May, encompasses the higher rainfall months.

3.2.2 Hydrology

On FHE six farm dams are used for various purposes, such as irrigation. These six dams range in volume from 18 500 m^3 to 256 000 m^3. FHE also has the following infrastructure: storage reservoirs with a total capacity of approximately 546,000 litres, an abstraction weir on the Nhlambamasoka River and five boreholes. The location of each of these dams (provided by FHE) is presented in Figure 3-17.

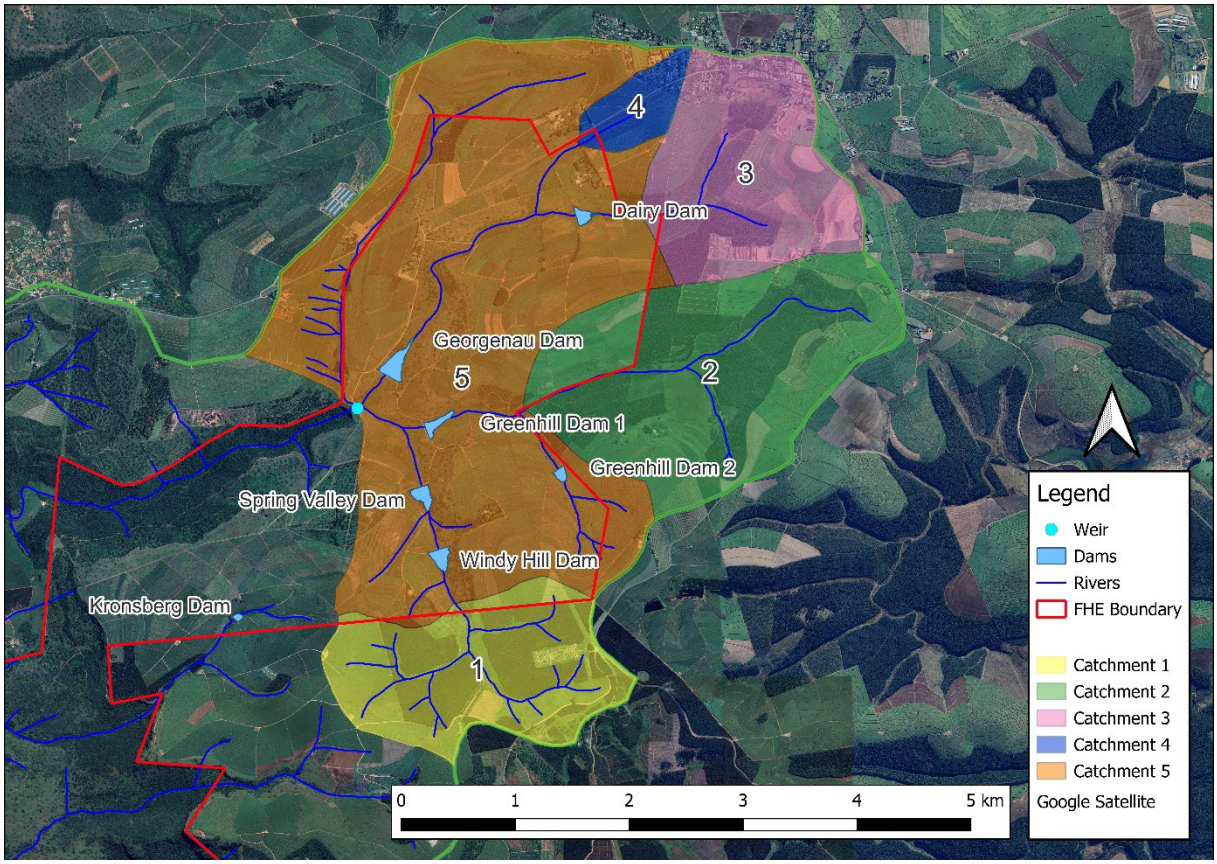

Figure 3-17: FHE dam locations

A portion of FHE is drained by the Nhlambamasoka River, which flows southwest from FHE and discharges downstream into the Umgeni River, whilst the southern portion drains directly into the Umgeni River.

3.2.3 Geology

The geology of this was determined by the geological study performed in 1998 by the CGS. The local geology of the FHE catchments has been presented below in Figure 3-18, showing the lithostratigraphic classifications of the underlying rock.

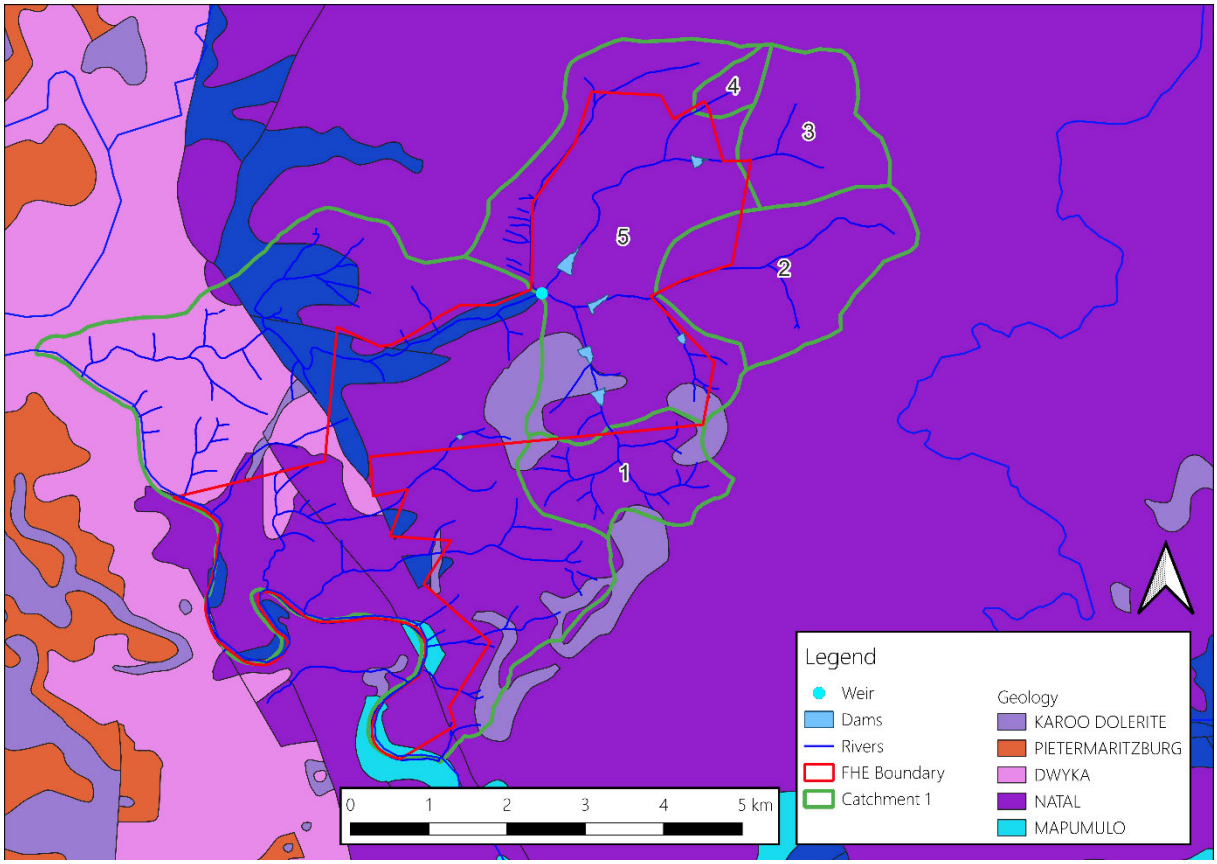

Figure 3-18: Geological map of the FHE subcatchments (CGS, 1998)

The dominant geology across the estate is of the Natal Group, with localised areas of Karoo dolerites and Dwyka Group. The Karoo dolerites are characterized by networks of sills, sheets and dykes that intrude into the surrounding overlying geological formations (CGS 1996), as observed at this site. The Natal Group is primarily associated with reddish, feldspathic and micaceous sandstone, along with subordinate quartz arenite, mudrock, granulestone and conglomerates (CGS 1996). In the lower portion of the catchment, the geology of the river channels reflects segments of the Mapumulo Group and an unclassified group. The unclassified material is identified as part of the Namibian chronostratigraphic unit, comprising pink leucocratic gneiss, subordinate quartzite and sillimanite quartzite (CGS 1996). In contrast, the Mapumulo Group is characterised by heterogeneous, layered paragneisses and migmatites with a wide compositional variation (CGS 1996).

3.2.4 Pedology

The pedology of FHE is based on a pedological study performed by KR Barichievy in 2020. The results of the study were that the FHE catchments are dominated by soils of the following forms:

- In-situ rock (lower catchments)
- Glenrosa (upper and lower catchments)
- Clovelly (upper and lower catchments)
- Hutton (upper catchments)
- Westleigh (upper catchments)
- Longlands (upper and lower catchments)

The Glenrosa soil form is identified by an Orthic A horizon that overlies a lithocutanic B horizon. This soil is associated with the shallow responsive hydropedological soil class. The Clovelly and Hutton soil forms are differentiated by the B horizon, with the former being identified by an Orthic A horizon overlying a yellow-brown apedal B horizon over unspecified material, and the latter being identified by an Orthic A horizon overlying a red apedal B horizon over unspecified material. These soil forms are associated with the deep recharge hydropedological class. The Longlands and Westleigh soil forms are differentiated by the presence of an E horizon, with the former being identified by an Orthic A horizon overlying an E horizon over a soft plinthic B horizon, and the latter being identified by an Orthic A horizon overlying a soft plinthic B horizon. These soil forms are associated with the A/B horizon interflow and soil/bedrock interflow hydropedological class respectively.

A map of the distribution of these soils across FHE is presented in Figure 3-19 and a map of the soil depth across the estate is presented in Figure 3-20.

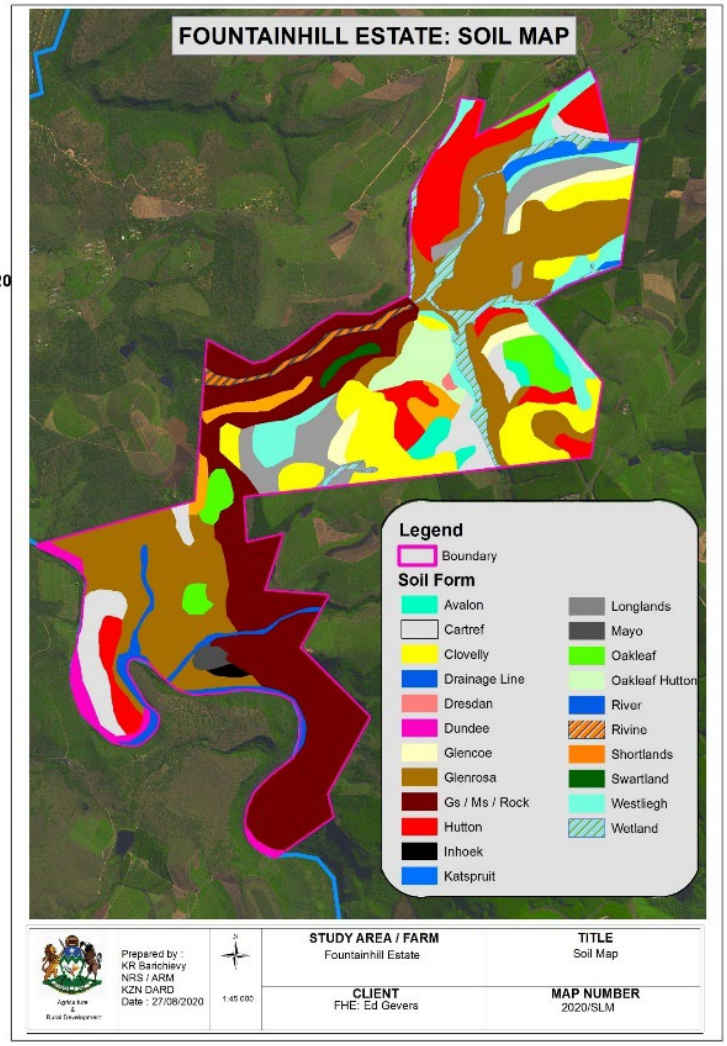

Figure 3-19: Map of the soil forms across FHE (Barichievy, 2020)

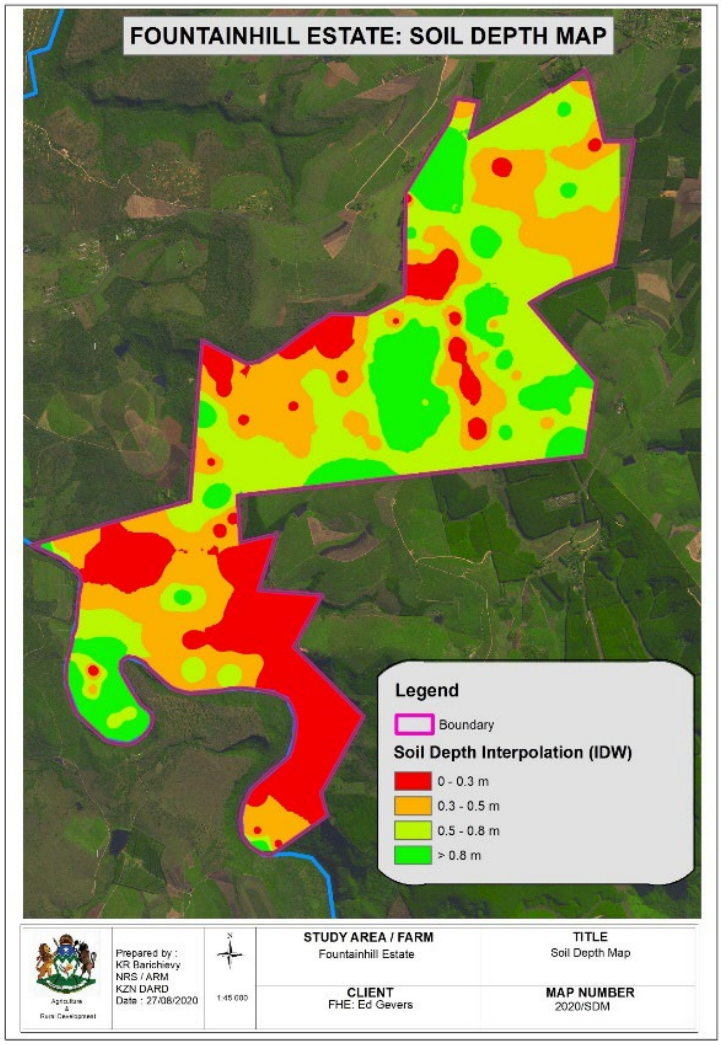

Figure 3-20: Map of the soil forms across FHE (Barichievy, 2020)

3.2.5 Land use

FHE is approximately 5587 ha, with the subcatchments (1 - 6) being studied, making up approximately 2,260 ha of the estate; it is the areas of these subcatchments that are reported below. FHE is made up of both cultivated and non-cultivated areas. The land uses include the farming of cattle (88 ha of pasture), sugarcane (630 ha) and avocado pears (48 ha) with the associated farm infrastructure. FHE also includes a large area of natural bushlands and grasslands (approximately 1,500 ha) maintained as a private game reserve with various wild animals e.g. bush pigs, giraffes, assorted buck, etc. This private game reserve includes a South African Heritage Site along with the accommodation and hospitality infrastructure associated with the reserve. This data was supplied by FHE and is presented in Figure 3-21 below.

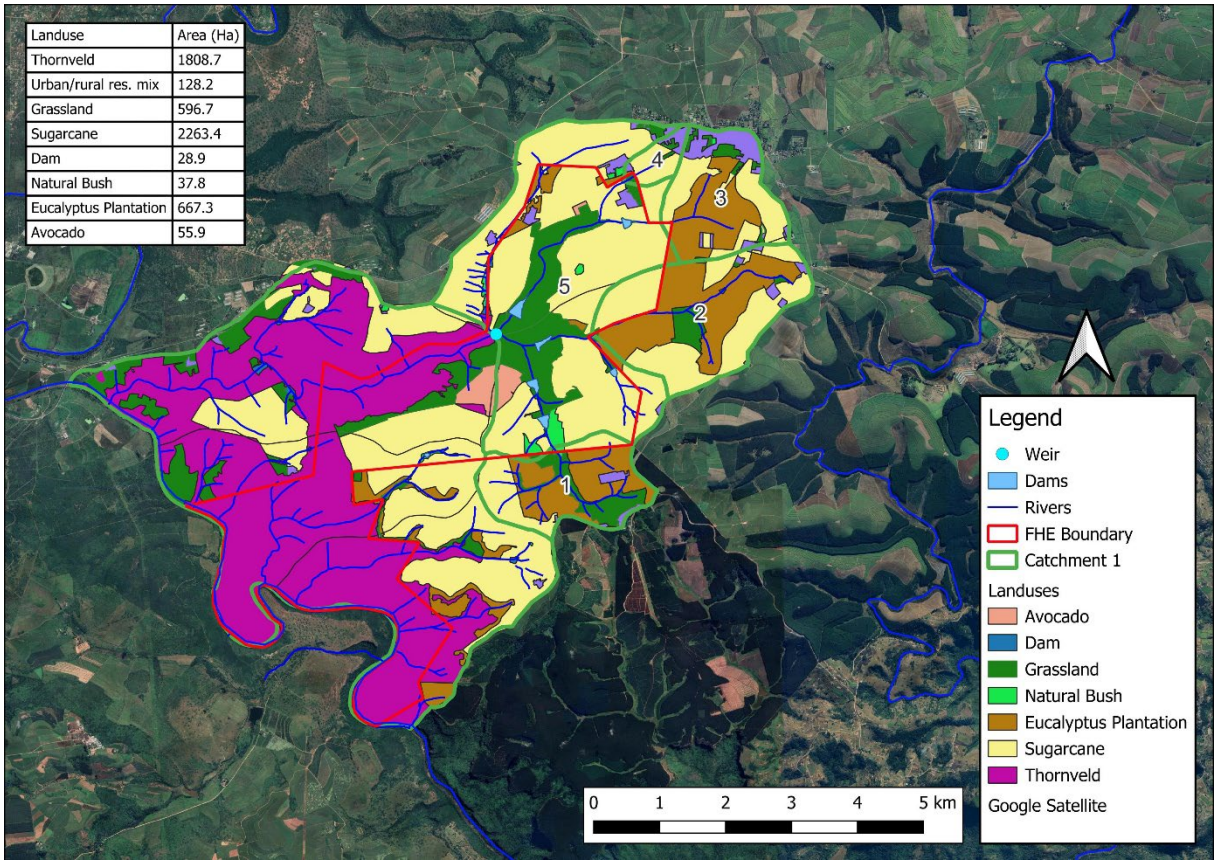

Figure 3-21: Land use map of the FHE subcatchments (FHE, 2023)

3.2.6 Equipment

The probe network installed by SRK Consulting consists of five EC and pressure probes strategically placed around the farm in the upper catchments of the farm. These probes were placed at critical points throughout the catchments. These points were determined by where water generated in the upper catchments entered the estate boundaries and where the streams discharge into the lower portion of the estate. This allowed for the calibration of the water balance (developed by SRK Consulting) against observed flows entering the FHE grounds and exiting from the weir.

The EC and pressure probes were installed in late 2020. These probes were installed as the previous method of monitoring streamflow levels and discharge (flumes) had been damaged/ destroyed during an intense period of rainfall. To gain accurate data from the probes installed in the streams, slotted tubes were sunk into the channel bed at the FHE boundary inflow points, and at the weir, the probe was fixed on a large boulder in the stilling pond. The locations of these monitoring probes and the catchments that contribute to the FHE on-site water resources are presented below in Figure 3-22

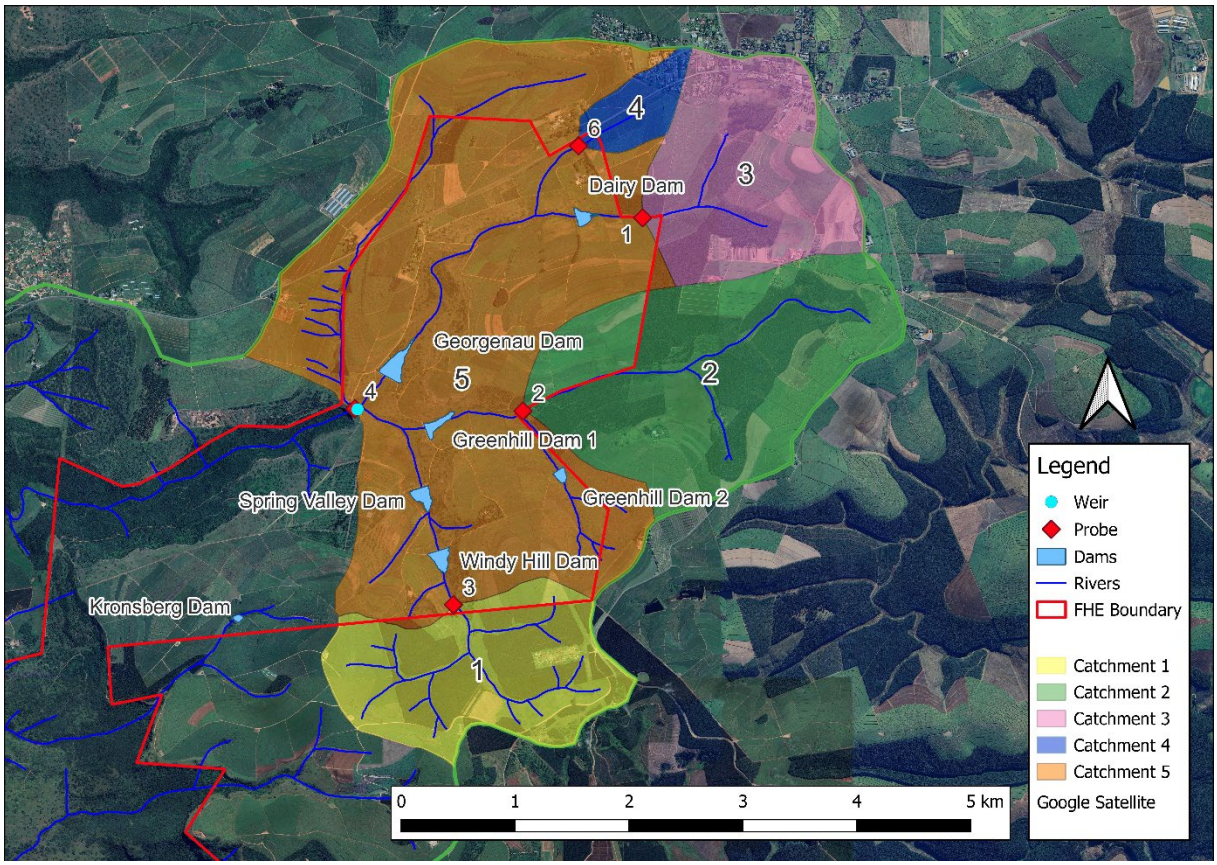

Figure 3-22: FHE monitoring network location map (FHE, 2023)

METHODOLOGY

In this chapter, the methodology used to analyse and interpret the raw data, as well as to conceptualise and understand the surface water–groundwater interactions occurring at the research sites have been detailed. The methods used for this research include a desktop hydropedological study for the FHE site, a remote sensing analysis using the OPTRAM model, and the field sampling and lab analysis procedures.

To achieve this, the methodology supplemented existing instrumentation and monitoring networks, such as the installation of new piezometers and conducting remote sensing surveys (OPTRAM). The study merges the hydropedology/pedological surveys previously conducted in the areas, remote sensing, hydrometry and tracer hydrology results to provide a holistic understanding of the surface water-groundwater interactions occurring at the site. For this study, isotope hydrology was the predominant method for studying the surface water-groundwater interactions at the CP Catchment 6 site and EC was used at the FHE site. The other tools used assist in understanding the movement of the subsurface water and the preferential pathways that exist. The isotope data collected (from rain gauges, streams and soil moisture) at nested time steps (events, hourly, daily and monthly) at hillslope scale were analysed by applying concepts such as end-member mixing models, time series analysis and transfer functions to determine water movement and its residence time.

Table 4-1: Spatial scale descriptions

Name	Scale	Description
Hillslope	10s of meters	From the catchment boundary or the nearest highest elevation point to the riparian zone and river
Catchment	100s of meters	From the greatest elevation in a catchment to the outlet

4.1 Data Analysis and Sampling

4.1.1 Cathedral Peak Catchment 6

The rainfall data from Cathedral Peak was collected by the South African Environmental Observation Network (SAEON): Grassland Node. The data was provided for the period from

February 2015 to October 2024. To understand the relationship between rainfall, streamflow and groundwater, rainfall events were identified and the relationships between the data were then studied. The water chemistry, ^{222}Rn and stable isotopes data were collected by an MSc student at the University of KwaZulu-Natal (UKZN) for the period January 2023 to July 2024.

Stable isotope data ($\delta^{18}O$ and $\delta^{2}H$) were collected from various points throughout CP Catchment 6 (Figure 4-1) across a variety of altitudes and each of the tributaries. This sampling of rainfall, streamflow and groundwater was done at a daily and monthly time scale. A three-member end-member mixing analysis (EMMA) was used to determine the proportions of the contributions of groundwater and rainfall to the streamflow for the event-based sampling. Figure 4-1 below shows the distribution of the isotope sampling locations of all sources in the catchment.

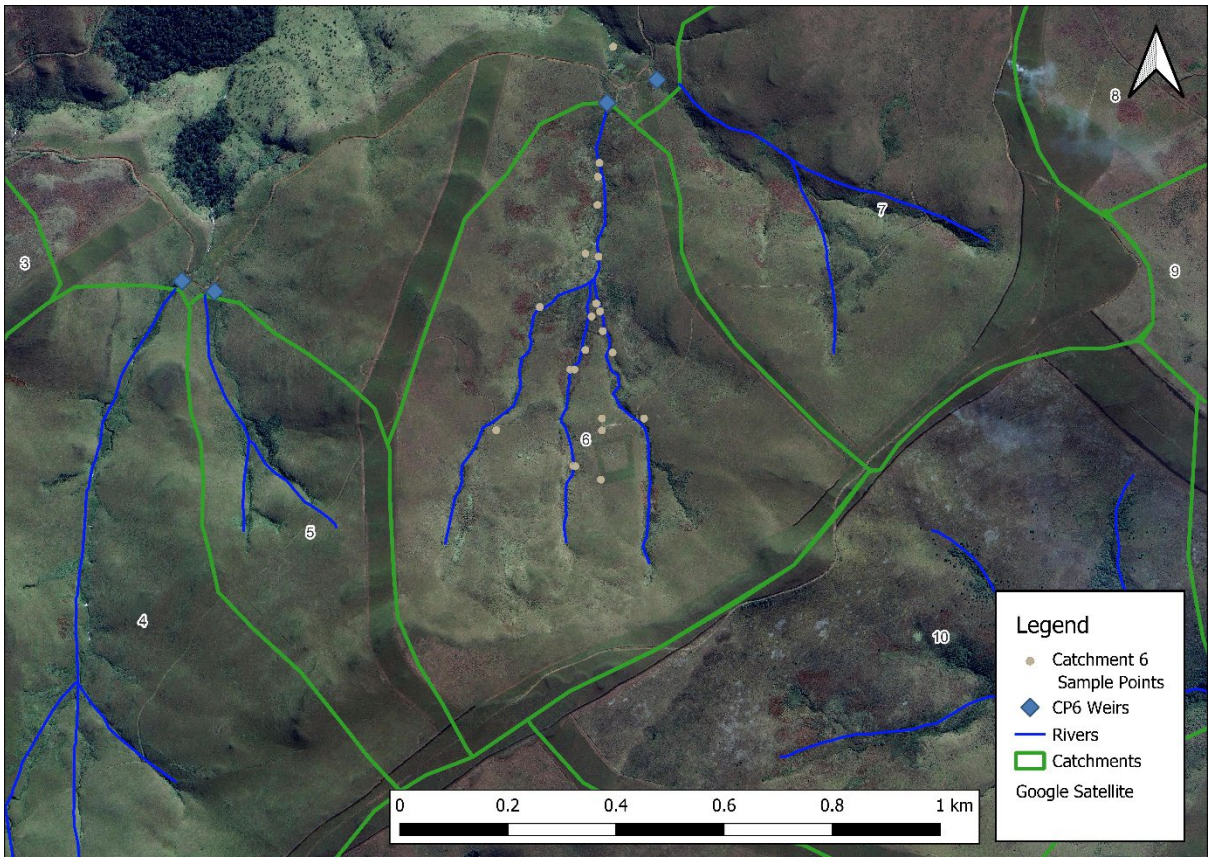

Figure 4-1: CP Catchment 6 isotope sampling locations

Electrical conductivity was measured at the weir (Figure 3-3) and at each of the isotope sampling locations (Figure 4-1). This was done at a monthly and event-based time scale. The event-based sampling was conducted for two events; the first event was from 12 – 14 December 2023 and the second was from 11 – 13 April 2024. The sampling for these events was done by sampling the streamflow using a Teledyne ISCO automatic sampler at the outlet of the lower

wetland just upstream of the weir and another automatic sampler in the upper reaches of the catchment to sample the rainfall. The sampling interval for the first event was set at an hourly sampling rate, whilst the second event was set to half-hourly. This was due to the weather forecasts showing a potentially short event at the time of setting up the sampling equipment. The Teledyne ISCO automatic sampler for the streamflow can be seen below in Figure 4-2.

Figure 4-2: Event-based streamflow sampling setup below Wetland 2

4.1.1.1 Stable isotope sampling

Isotope samples were collected and stored in high-density polyethylene bottles with a capacity of 20-60 ml (depending on the size of the sample). These bottles were filled to the brim with no pocket of trapped air, to prevent evaporation of the sample. The bottles were then sealed with conical Polyseal caps and stored in a temperature-controlled laboratory until the sample could undergo analysis.

Stable isotope analysis of the samples was conducted at the UKZN Isotope Hydrology Laboratory using the LGR-ICOSTM GLA431 Series Analyser. The precision of the analysis was determined as a long-term analytical standard deviation of ±1‰ for $\delta^{2}H$ (n=500) and ±0.15‰ for $\delta^{18}O$ (n=500). Additionally, Evian bottled water and the Pietermaritzburg tap water were used to normalise the isotopic results of all collected samples to the Vienna Standard Mean Ocean Water 2 (VSMOW2) - Standard Light Antarctic Precipitation 2 (SLAP2) scale. A mixture of the Evian bottled water and the Pietermaritzburg tap water was also prepared as a control standard. The Canadian GeoTop laboratory was used to analyse these three standards and determine their actual isotopic composition. The Vienna Standard Mean Ocean Water

(VSMOW) standards were used as a quality control and assurance for the data's integrity. The results for the isotopic sample and control results were expressed as δ-values (‰) for $\delta^{18}O$ and $\delta^{2}H$.

4.1.1.2 ^{222}Rn sampling

^{222}Rn concentrations in the surface waters were measured using a RAD7 Radon Detector produced by the Durridge Company. These measurements were taken in the surface water and the surrounding atmosphere to detect groundwater ingress into the surface water system. This testing was done at various important locations throughout the catchment. For increased sensitivity (a detection limit of 40 $Bq.m^{-3}$ of the measurements taken) the detector was fitted with a "Big Bottle System". The radon detector removes the ^{222}Rn from a water sample and passes it into a closed air loop. This process is done using an extraction module made up of hollow vinyl fibres. To determine the ^{222}Rn concentration, measurements were carried out over a one-hour duration in four separate cycles. Capture software produced by the Durridge company was used to perform the conversion of ^{222}Rn in air to ^{222}Rn in water, with the measured water temperature as an input. The standard deviation across these measurements carried out fluctuates between 10% and 20%, with greater deviation occurring at lower ^{222}Rn levels. Therefore, to reduce this fluctuation, the first measurement was omitted and the mean ^{222}Rn concentration for the water source was derived by averaging the final three measurements.

4.1.2 Fountainhill Estate

The existing monitoring network present at FHE comprises water level monitoring, stream discharge monitoring and a meteorological station located off-site at Windy Hill. The probes installed in the stream network for continuous monitoring (at 15-minute intervals) measure electrical conductivity for each site along with the water pressure. The probes installed are the WW5000-TDCS sensors and these probes measure EC and water pressure that is then converted to water depth and temperature. The data from the probes are collected using a portable base station. Figure 4-3 shows an example of the raw data received from the probes.

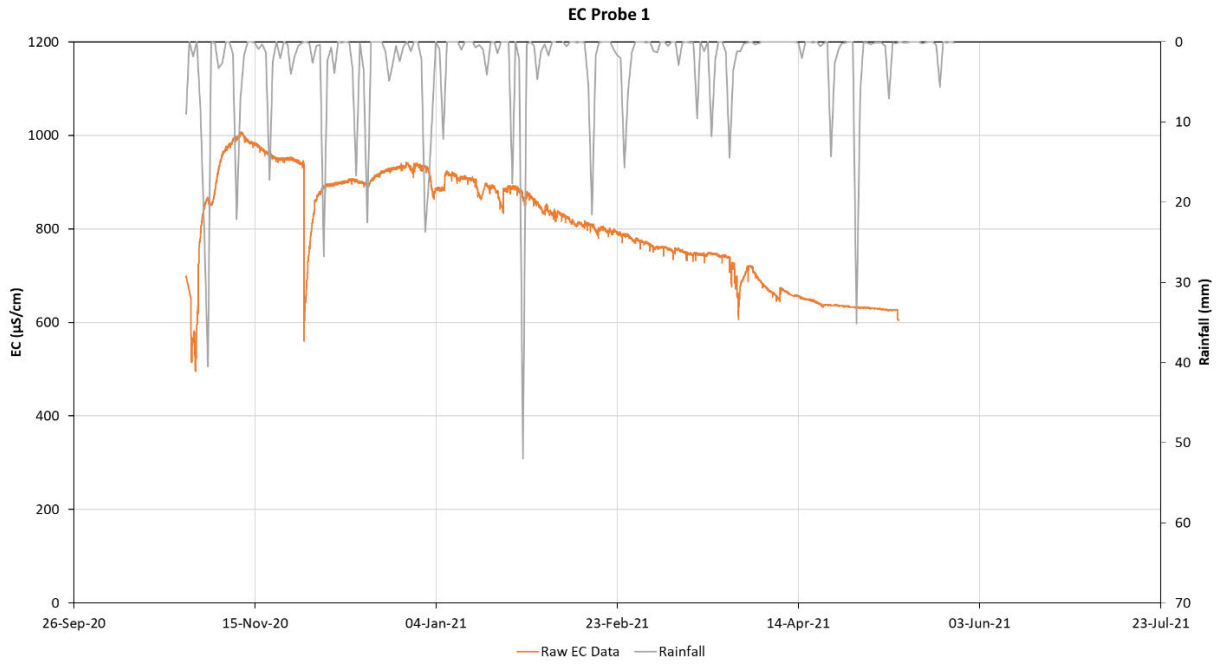

Figure 4-3: Example of the raw EC and Water pressure data downloaded from the FHE probes

4.2 OPTRAM Model

The OPTRAM model was used to estimate soil moisture (SM) distribution and to identify potential flow paths in the near surface, as well as to compare the dry and wet seasons and the changes that occur to the flow paths as a result. This model uses remote sensing spectral data from the Sentinel-2 satellite, along with vegetation indices to infer soil moisture dynamics (Sadeghi *et al*., 2017). The model relies on satellite-derived vegetation indices (VI), such as the Normalised Difference Vegetation Index (NDVI) and transformed reflectance values from shortwave infrared (SWIR) (Sadeghi *et al*., 2017). These inputs are used to analyse the relationship between "wet" and "dry" bounds on scatterplots of VI versus SWIR transformed reflectance (STR) (Sadeghi *et al*., 2017; Silver *et al*, 2024). The Sentinel-2 data is acquired from the Copernicus Data Space (CDS) platform. This data is then processed to generate VI and STR indices and clipped to the study area and time range (Silver *et al*, 2024). Scatterplots of VI and STR are then programmatically delineated by dividing the VI axis into small intervals. For each interval, STR values are extracted, outliers removed using the 1.5x Interquartile Range (IQR) method, and the top and bottom 2% quartiles are identified to define the "wet" and "dry" trapezoid edges (Silver *et al*, 2024). The analysis focuses on understanding

how soil moisture patterns influence surface water-groundwater interactions. A diagram of the methodology used by the OPTRAM model is presented in Figure 4-4.

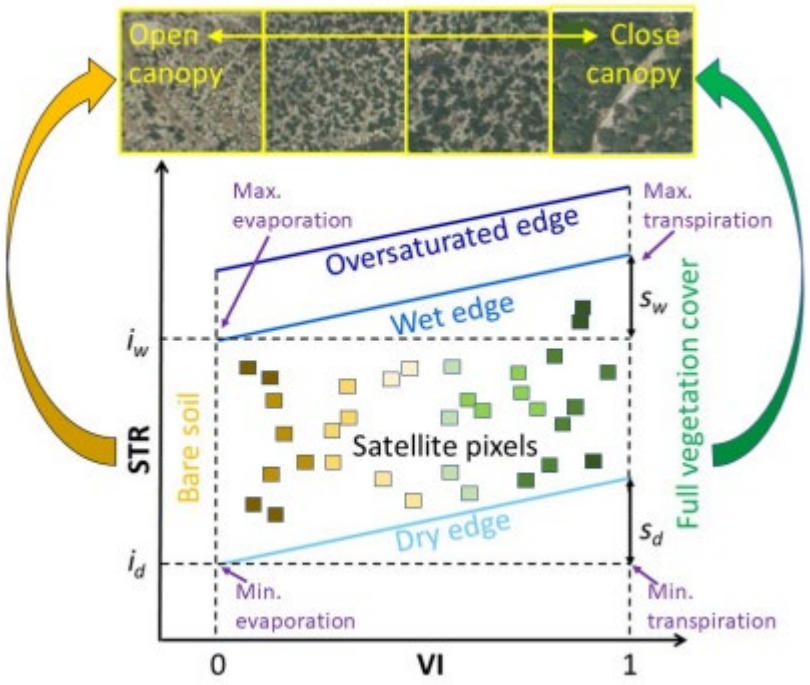

Figure 4-4: Schematic diagram of the OPTRAM model (Silver *et al*, 2024)

The equations presented by Silver *et al.* (2024) provide an approach to analysing soil moisture dynamics using various trapezoidal models. This is done by using regression lines that are fitted to the edges of the calculated trapezoid using one of three methods. The use of one of these methods is dependent upon the fit of the regression line to the data. The three methods are the linear, exponential or second-order polynomial regression methods. Each method generates coefficients required for deriving spatially explicit soil moisture maps (Silver *et al.*, 2024). The first set of equations employs linear regression to define these trapezoid edges. Equation 1 uses a linear regression fit to determine the dry edge, while Equation 2 determines the wet edge. These edges serve as the boundaries of the trapezoid when estimating the soil moisture. Equation 3 derives the soil moisture as m^3 of water per m^3 soil ($m^3.m^{-3}$), using the relationship calculated using the dry and wet edges.

In the event the linear equations do not provide a suitable fit, the exponential method can then be used, this is shown in the second set of equations. Equation 4 defines the exponential curve used to determine the dry edges, while Equation 5 determines the wet edges. Finally, Equation

6 determines the soil moisture based on the trapezoid model constructed using the exponential curve fits.

$$STR_{dry} = i_{dry} + s_{dry} \times VI \quad (1)$$

$$STR_{wet} = i_{wet} + s_{wet} \times VI \quad (2)$$

$$W = \frac{STR - STR_{dry}}{STR_{wet} - STR_{dry}} \quad (3)$$

$$STR_{dry} = i_{dry} \times \exp(s_{dry} \times VI) \quad (4)$$

$$STR_{wet} = i_{wet} \times \exp(s_{wet} \times VI) \quad (5)$$

$$W = \frac{STR - (i_{dry} \times \exp(s_{dry} \times VI))}{(i_{wet} \times \exp(s_{wet} \times VI)) - (i_{dry} \times \exp(s_{dry} \times VI))} \quad (6)$$

The exponential and polynomial regression approaches employ more complex equations involving exponential and second-order terms respectively. The delineation process and regression methods ensure that soil moisture estimates are robust and mathematically repeatable across large spatial scales. This methodology significantly enhances the capacity to estimate soil moisture over extensive areas, overcoming the limitations of point-based methods like TDR sensors and enabling scalable, regional analysis of soil moisture dynamics (Silver *et al*, 2024).

4.3 Normalised Difference Moisture Index

The Normalized Difference Moisture Index (NDMI) was used to assess the moisture content of vegetation with the study areas. The NDMI uses remote sensing spectral data from the Sentinel-2 satellite to determine the water content of the vegetation (Sinergise, 2025). It is calculated using a combination of the near-infrared (NIR) and SWIR spectral bands, as shown in Equation (7) below (EOS Data Analytics, 2022).

$$NDMI = \frac{NIR - SWIR}{NIR + SWIR} \quad (7)$$

When this equation is applied to the Sentinel2 satellite imagery the spectral bands used are B08 for the NIR and B11 for the SWIR resulting in Equation (8) obtained from Sinergise, 2025.

$$NDMI = \frac{B08 - B11}{B08 + B11} \quad (8)$$

This combination of spectral bands is used due to their ability to reduce the influence of atmospheric and illumination variability (Gao, 1996). The NIR band reflects strongly from the internal structure of leaves and dry plant material, while the SWIR band is particularly sensitive to the amount of water held within plant canopies (EOS Data Analytics, 2022). When used together, they offer a more accurate estimation of vegetation water content (Gao, 1996, EOS Data Analytics, 2022).

NDMI values range between -1 and +1 and can be interpreted in terms of vegetation density and water status. Values below 0 typically indicate bare soil or sparse, water-stressed vegetation, whereas values greater than 0.4 are generally associated with dense, well-watered canopies. Extremely high values may indicate saturated or waterlogged conditions.

Table 4-2: NDMI ranges and interpretations (EOS Data Analytics, 2022).

Range	Interpretation
-1.0 – -0.8	Bare soil
-0.8 – -0.6	Very sparse or absent vegetation cover
-0.6 – -0.4	Low vegetation density
-0.4 – -0.2	Dry sparse vegetation or wet bare ground
-0.2 – 0.0	Moderate-low vegetation, possible water stress
0.0 – 0.2	Moderate vegetation cover, moderate to high water stress
0.2 – 0.4	Moderate to high vegetation, generally healthy
0.4 – 0.6	High canopy cover, low or no water stress
0.6 – 0.8	Very dense vegetation, no water stress

0.8 – 1.0	Fully developed canopy, potentially saturated or waterlogged

The NDMI was therefore used to confirm and validate the results from the OPTRAM model applied.

4.4 FHE Hydropedological Classification

The methodology for this desktop study involved analysing soil information within the catchment area using existing hydropedological classifications. This classification process relies on using predefined hydropedological soil groups, presented in prior research, to determine flow path characteristics from existing soil classification data. Van Tol and le Roux (2019) categorised the existing soil forms into three hydropedological classes to understand the water movement across the landscape. As no paper was found for a previously conducted soil study performed by Barichievy (2020) prior to this investigation, the general hydropedological classes for the soil forms from van Tol and le Roux (2019), as outlined in Table 4-3 were used.

Table 4-3: General hydropedological class descriptions (van Tol and le Roux, 2019)

Hydropedological Class	Flow path	Description
Recharge	Deep	Found on gentler slopes and exceeding 500 mm in depth, these soils share similar traits with shallow recharge soils. However, their greater depth often supports recharge of deeper aquifers. In cases of low-permeability underlying bedrock, lateral flow emerges along the soil-bedrock interface, contributing to seasonal hillslope responses.
	Shallow	These soils are less than 500 mm deep and typically occur along steeper slopes. They feature a freely draining B horizon that transitions into fractured parent material or a lithic horizon, allowing water to infiltrate vertically into deeper geological layers

Interflow	A/B horizon	Interflow soils are defined by dual movement pathways: vertical infiltration through their free-draining upper horizons and lateral flow upon encountering impermeable bedrock. These soils are typically located downslope from recharge soils, where hydromorphic properties develop due to periodic saturation caused by fluctuating water tables.
	Soil/bedrock	Interflow soils are defined by dual movement pathways: vertical infiltration through their free-draining upper horizons and lateral flow upon encountering impermeable bedrock. These soils are typically located downslope from recharge soils, where hydromorphic properties develop due to periodic saturation caused by fluctuating water tables.
Responsive	Shallow	These soils are soils that have a short lag in runoff generation and therefore respond quickly to rainfall events. This class of responsive soils consists of a shallow soil overlaying a relatively impermeable bedrock and therefore has a limited storage capacity.
	Saturated	These soils are very responsive to rainfall events and they exhibit morphological indications of extended periods of saturation. As these soils are often at or close to saturation during the rainy season, any additional precipitation generates runoff as a result of the saturation excess.
Stagnating		These soils are typically characterised by restricted outflow and often have permeable A and B horizons. The morphological properties of these soils often

		indicate that the recharge or interflow processes are not dominant, but rather that the movement of water is upward, driven primarily by evapotranspiration.

4.5 End-Member Mixing Analysis

End-Member Mixing Analysis (EMMA) was employed to determine the relative contributions of different sources or end-members such as subsurface flows, precipitation and wetland storage, to streamflow. EMMA is a widely used technique for quantifying water source contributions by comparing the chemical or isotopic signatures of source waters to those of the streamflow mixture (Hooper, 2003; Christophersen and Hooper, 1992).

Three tracers per end-member were used to perform the analysis; these were the isotopic tracers (δ^2H and $\delta^{18}O$) and electrical conductivity (EC), which are commonly applied due to their conservative behaviour in hydrological systems and their ability to distinguish between hydrological pathways (Klaus and McDonnell, 2013; Kendall and McDonnell, 2012). The data for the different end-members was prepared along with the data from the mixture. This involved getting the data into the same format and, where necessary, filtering out missing values. The subsurface contributions were obtained from the recorded isotopic and EC values of the headwaters of the middle tributary during the dry season, when the subsurface contributions to streamflow dominate (Kendall and McDonnell, 2012; Tetzlaff *et al*., 2009). The equation used to calculate the relative fractional contributions for the EMMA can be found below in Equation 9. This equation was then used to generate an equation for each end-member and tracer used. These equations express the fractions as relative differences between streamflow and the end-member's isotopic or EC values.

$$f_{source_1}^{T} = \frac{T_{mixture} - T_{source_2}}{T_{source_1} - T_{source_2}} \tag{9}$$

Where:

$f_{source_1}^{T}$: Fractional contribution of source 1 for the given tracer T.

$T_{mixture}$: Value of the tracer T in the mixture

T_{source_1}: Value of the tracer T in source 1

T_{source_2}: Value of the tracer T in source 2

An example of Equation 9 can be seen been in Equation 10, there the contribution of rainfall to the streaflow is calculated.

$$f_{rainfall}^{\delta^2 H} = \frac{\delta_{streamflow}^{2H} - \delta_{wetland}^{2H}}{\delta_{rainfall}^{2H} - \delta_{wetland}^{2H}} \tag{10}$$

Contributions from the three tracers are then averaged and converted to a percentage contribution to calculate the overall contributions from each end-member. This was done to ensure robustness and account for variations inherent in individual tracers (Barthold *et al*., 2011; Klaus *et al*., 2015). This methodology enables a robust quantification of the hydrological contributions under both wet and dry conditions and supports interpretation of dominant flow paths and storage processes in surface water–groundwater interactions (Tetzlaff and Soulsby, 2008; McGuire and McDonnell, 2006).

RESULTS

In this chapter, the results and analysis of the data collected during this research is presented. Original data collected during this research are complemented with the secondary data. These datasets are collated and presented in the forthcoming sections.

5.1 Cathedral Peak Catchment 6

5.1.1 Event-based sampling

The event-based sampling was conducted over two different events. The first event was during the wet season and occurred from 12 - 14 December 2023, and the second event sampled was toward the end of the wet season during the transition into the dry season from 11 - 13 April 2024. Data was collected at 20-minute intervals over two days for each event. The streamflow samples were taken from the main channel between Wetland 2 and the temporarily saturated valley bottom, whilst the rainfall samples were collected at the rain gauge in the upper reaches of the catchment at the Teledyne ISCO sampler set up just below the eddy covariance tower.

5.1.1.1 EC

The rainfall from the Catchment 6 rain gauge is presented below with the EC data for each of the sampled rainfall events, in Figure 5-1 and Figure 5-2.

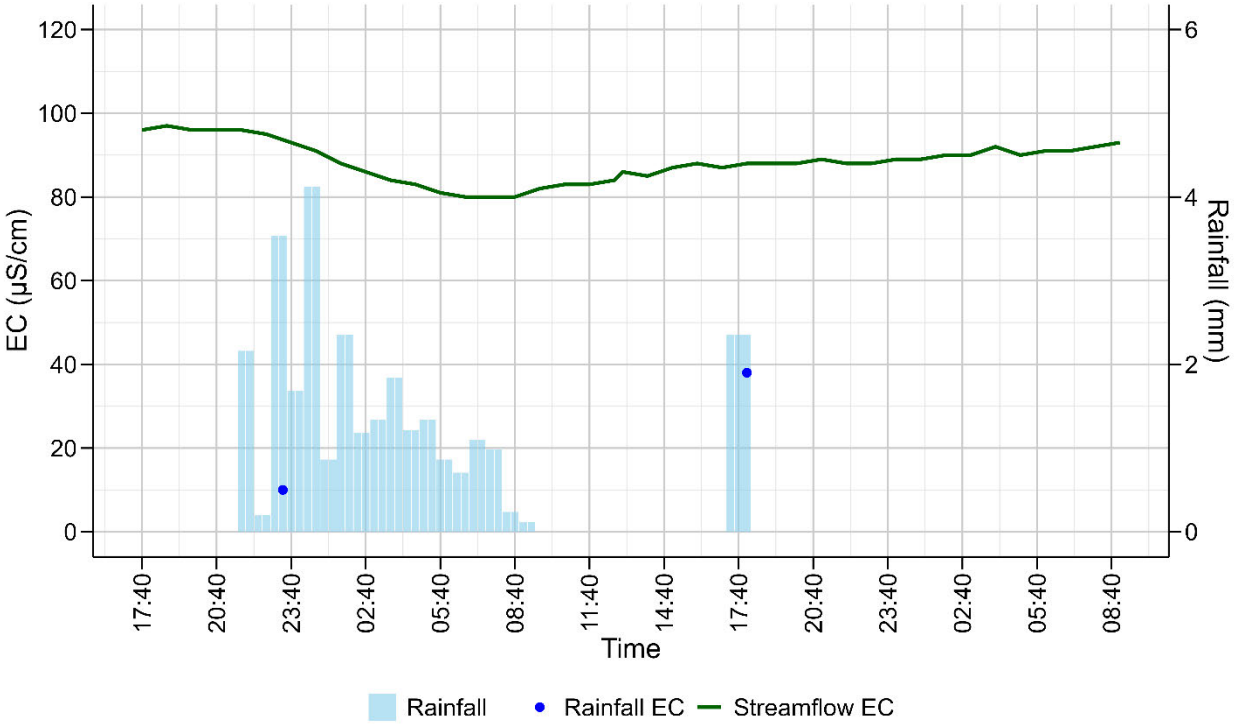

Figure 5-1: Streamflow EC and rainfall amount for the 12 – 14 December 2023 event

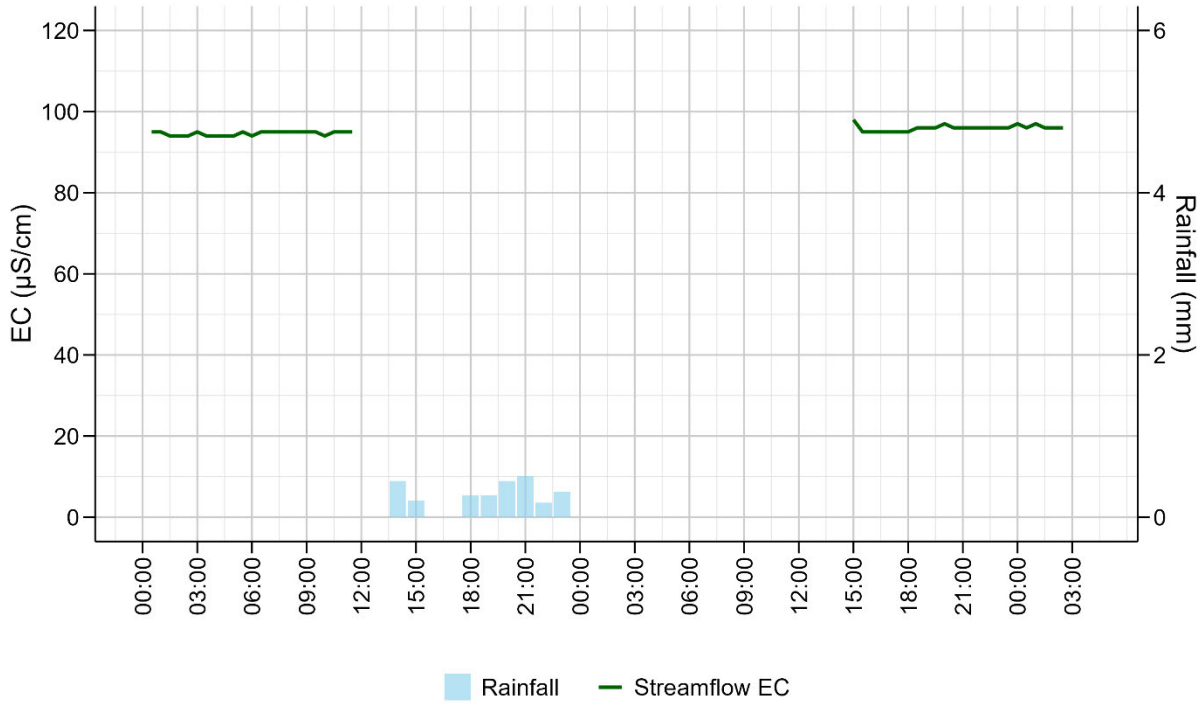

Figure 5-2: Streamflow EC and rainfall for the 11 – 13 April 2024 event

Figure 5-1 and Figure 5-2 show the EC values for the streamflow and the rainfall for the December 2023 and April 2024 events respectively. From the CP Catchment 6 rain gauge record, a total of 28.2 mm and 2.8 mm of rainfall was received (sampled at an hourly and half hourly timestep) for the December and April monitoring periods respectively. The sampling interval for the ISCO automatic sampler was determined based on rainfall events that were predicted over the proposed sampling period. However, accurately predicting these rainfall events in high-altitude catchments proved challenging. This was especially evident during the rainfall event of April 2024, when the streamflow sampler reached its sampling capacity prior to the onset of any rainfall. This removed any possibility of collecting a continuous sample record during the most hydrologically active period of the event.

From Figure 5-1, a strong inverse relationship between the rainfall and EC is observed. The relationship is shown by the steep decline in the EC values from 95 µS/cm to 80 µS/cm from the onset of rainfall. The rainfall contribution reached a maximum approximately 4 hours after the onset of rainfall and continued to be the dominant contributor for two hours. This response to the rainfall shows the clear dilution of the streamflow EC as a direct result of the stormwater runoff (typically characterised by lower EC values) entering the streamflow and temporarily reducing the EC of this water. As the intensity of the rainfall event diminishes and the event comes to a close, the EC values gradually begin to recover to pre-event levels (approximately

95 µS/cm). This recovery is likely a result of the influence of baseflow contributions from groundwater increasing. These contributions tend to have higher EC values due to longer residence times and interaction with subsurface materials. The slow recovery (approximately two days) of the EC values to pre-event levels indicates either sustained groundwater inputs or delayed subsurface flow pathways becoming dominant after the rainfall event.

During the April event monitoring period shown in Figure 5-2, low rainfall quantities were recorded, peaking at 15 ml received in an hour. Whilst there is no overlap in the samples collected for the streamflow and the rainfall, there is no recovery in the EC record shown, as the pre-event levels are the same as those of the post-event (95 µS/cm). This suggests that the precipitation received was not great enough to generate surface runoff or was effectively intercepted and infiltrated into the soil profile before reaching the stream. Another possibility is that the precipitation generated runoff; however, due to the low amount of rainfall received, it diluted the streamflow to a lesser degree than the December 2023 event (two-day recovery) and therefore, the recovery was not sampled. However, due to the low amounts of precipitation received and the lack of a dilution response, the hypothesis that the threshold for runoff generation was not met during this event is supported. This could be due to dry antecedent soil conditions, high infiltration capacity of the soil or interception by vegetation. This would result in the streamflow having remained predominantly fed by the groundwater and therefore, the EC values remained stable.

A notable pattern observed in Figure 5-1 was the increase in the EC of the rainfall with time. The rainfall can be seen to increase from 10 µS/cm near the beginning of the event to 38 µS/cm toward the end of the event. This trend is consistent with the washout or scavenging effect. This effect is due to the rainfall occurring at the beginning of the event consisting of relatively clean rainfall (with low EC values) formed at higher altitudes. As the event progresses, the ionic concentration of the rainfall increases. This is due to it collecting and dissolving increasing quantities of atmospheric aerosols, gases and particulate matter as it travels through the lower atmosphere (Likens and Bormann, 1974; Seinfeld and Pandis, 2016). Orographic uplift and long-range atmospheric transport can introduce dust, anthropogenic emissions and pollutants that contribute ions such as ammonium, sulphate and chloride to later-stage rainfall (Lundquist *et al*., 2008; Gioda *et al*., 2013). These processes likely explain the progressive increase in rainfall EC observed during this storm event, despite the overall low background levels expected in a high-altitude catchment.

5.1.1.2 Stable isotopes

Figure 5-3 and Figure 5-4 show the stable isotope plots for the December 2023 and April 2024 events respectively. The plots show the streamflow isotope data (denoted by Day 1, Day 2 and Day 3) and the rainfall captured for each day sampled. The colouring of the markers shows the time, with observation 1 being the earliest and darkest blue. The trendlines and their respective equations have been included on the plots. The equation used to generate the Global Meteoric Water Line (GMWL) can be seen below in Equation 11 (Craig, 1961; Rozanski *et al.*, 1993; Kendall and McDonnell, 2012).

$$\delta^2 H = 8\delta^{18}O + 10 \quad (11)$$

Figure 5-3 depicts the isotopic compositions of the samples taken during the event-based sampling for the period of 12 – 14 December 2023.

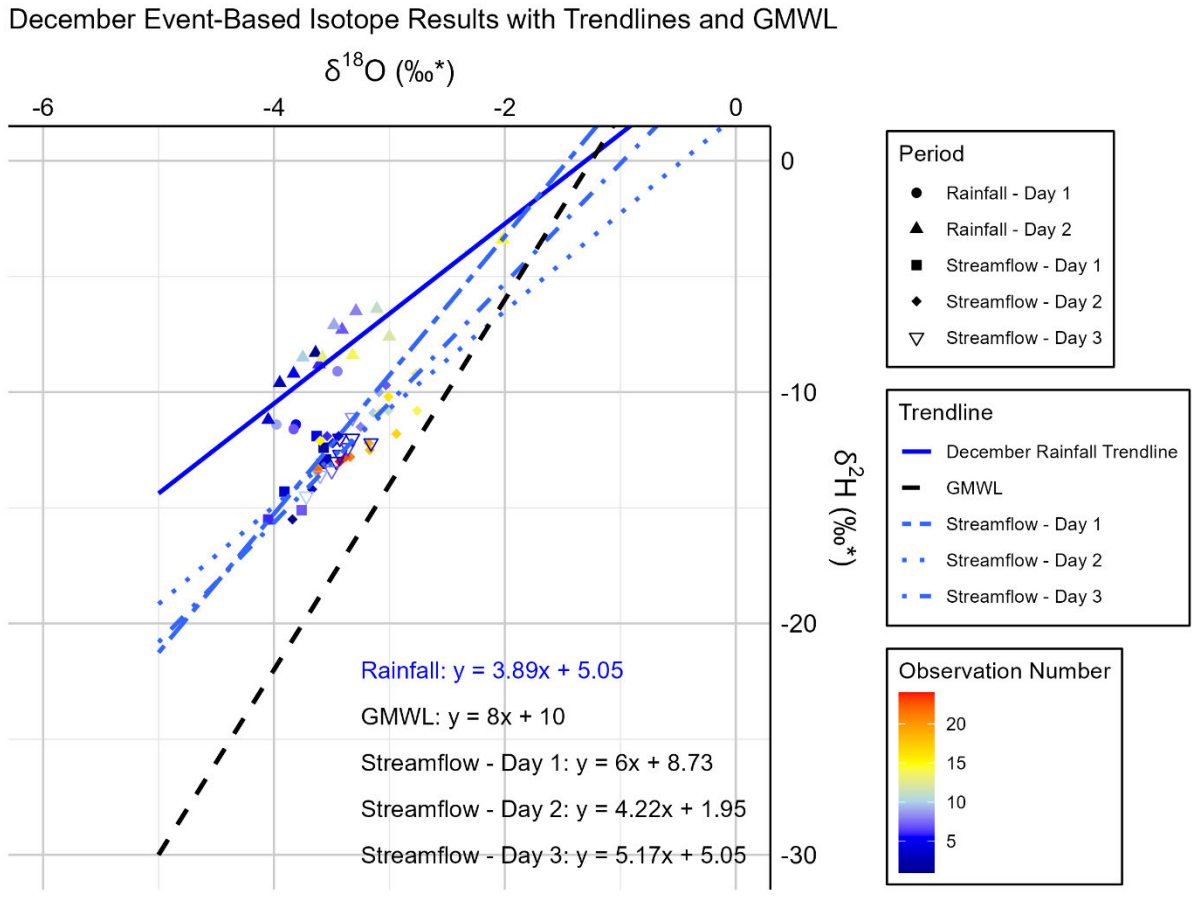

Figure 5-3: Plot of December 2023 event isotopic composition

The trendline for the rainfall received during this event can be seen below in Equation 12.

$$\delta^2H = 3.89\delta^{18}O + 5.05 \quad (12)$$

From Figure 5-3 the rainfall samples can be seen to have a slope and intercept smaller than that of the GMWL. This reduced slope highlights that the rainfall has undergone isotopic fractionation as a result of atmospheric processes e.g. the rainout effect or moisture sourced from cooler/high-altitude regions (Dansgaard, 1964; Rozanski *et al*., 1993; Kendall and McDonnell, 2012). The intercept of the rainfall trendline (5.85) is notably lower than that of the GMWL intercept (10). This would suggest that the December rainfall has undergone greater isotopic depletion than typical meteoric water, potentially due to seasonal factors such as lower temperatures or different storm characteristics (Feng *et al*., 2009).

The equations for the trendlines of the December event are depicted in Figure 5-4 for each day and are presented below in the Equations 13, 14 and 15.

$$\delta^2H = 6\delta^{18}O + 8.73 \quad (13)$$

$$\delta^2H = 4.22\delta^{18}O + 1.95 \quad (14)$$

$$\delta^2H = 5.17\delta^{18}O - 5.05 \quad (15)$$

The relatively steep slope of the first day's streamflow (6), coupled with a high positive intercept (8.73), suggests that the streamflow during the beginning of the rainfall event closely mirrors meteoric water characteristics, with minimal enrichment in heavier isotopes. There is a strong degree of connectivity between the runoff generated by the rainfall and the streamflow, with the early stormflow reaching the channel soon after rainfall commences. The similarity between Day 1 and the GMWL intercepts indicates that rainfall with minimal isotopic alteration is a direct influence on the streamflow. Due to the sampling taking place well into the wet season, this similarity could be due to a high degree of soil moisture in the catchment conditions that quickly generates runoff, thereby transporting event water downstream (Birkel *et al*., 2016).

The Day 2 slope is significantly reduced (2.63) from the Day 1 slope and is coupled with a reduced intercept (1.95). This suggests that by Day 2, there is an increasing contribution from older water sources, likely from the wetlands or shallow groundwater. However, the decreased slope indicates that the water retained within Wetland 1 and Wetland 2 is contributing more

strongly to the streamflow, with evaporative processes concentrating heavier isotopes during residence time (Craig and Gordon, 1965). These observations point to a gradual transition from rainfall-dominated streamflow of the first day to buffered wetland-sourced water contributions (Benettin *et al*., 2022).

The trendline of Day 3's streamflow shows an increase in the slope again (5.17) compared to Day 2. The intercept is also seen to increase (5.05), returning to closely match the rainfall intercept (5.05). This change suggests there may be a larger influence of stormflow contributions mixed with residual wetland-modified water on the streamflow. Although the slope remains steeper than that of Day 2, it is still lower than that of Day 1, indicating the presence of intermediate hydrological processes. These processes potentially include a combination of delayed runoff generated towards the end of the storm and contributions from the wetlands, which continue to release stored water. The buffering capacity of the wetland appears less pronounced on Day 3, potentially due to a reduction in evaporative enrichment or the reactivation of fresher subsurface and surface flow paths as a result of sustained rainfall inputs (van der Velde *et al*., 2012).

Figure 5-4 depicts the isotopic compositions of the samples taken during the event-based sampling for the period of 10 – 13 April 2024.

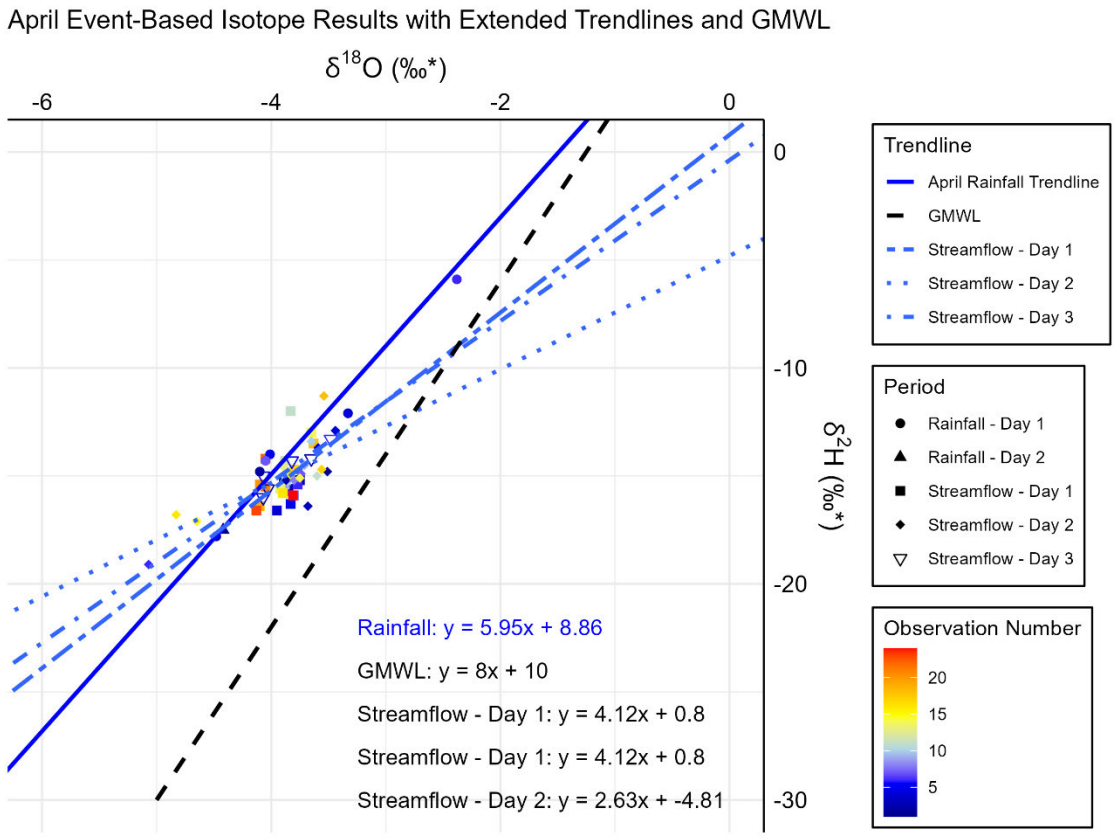

Figure 5-4: Plot of April 2024 event isotopic composition

The trendline for the rainfall received during this event can be seen below in the Equation 16.

$$\delta^2H = 5.95\delta^{18}O + 8.86 \quad (16)$$

From Figure 5-4 the rainfall samples are less enriched than the December event and more closely aligned with the GMWL. The lower slope of the rainfall trend line compared to the GMWL could suggest that the rainfall has undergone partial evaporation or slight atmospheric fractionation. This could occur as a result of moisture moving through varying atmospheric conditions and temperature gradients during the formation of the storm clouds (Dansgaard, 1964). However, due to the intercepts of the two lines being relatively close, the rainfall experienced remains consistent with meteoric water characteristics (Rozanski *et al*., 1993).

The equations for the trendlines of the April event are depicted in Figure 5-4 for each day, and are presented below in the Equations 17, 18 and 19.

$$\delta^2H = 4.12\delta^{18}O + 0.8 \quad (17)$$

$$\delta^2H = 2.63\delta^{18}O - 4.81 \quad (18)$$

$$\delta^2H = 3.73\delta^{18}O - 0.38 \quad (19)$$

The relatively steep slope of the first day's streamflow (4.12) (Equation 17), with the slight positive intercept, suggests that the streamflow during the beginning of the rainfall event closely reflects the recent rainfall contributions. This relationship shows the connectivity between the runoff generated by the rainfall and the streamflow, with the early stormflow. Despite this connection, the streamflow slope remains lower than the slope of the rainfall trendline (5.95), indicating that contributions from older water sources persist. This is potentially due to the wetland storage upstream of the sampling site (Craig and Gordon, 1965).

The significantly reduced slope (2.63) and negative intercept (-4.81) of the Day 2 trend line (Equation 18) suggest that by Day 2, streamflow is increasingly enriched in heavier isotopes derived from evaporative processes. This likely reflects water that was stored in the wetlands and subjected to fractionation through evaporation before being displaced downstream. The results indicate a transition from rainfall-derived contributions on Day 1 to a greater influence of wetland-sourced water on Day 2, consistent with buffering effects within Wetland 1 and

Wetland 2. These wetlands delay direct rainfall signatures, allowing water to mix with stored, enriched water before discharge (Benettin *et al*., 2022).

The trendline of Day 3's streamflow (Equation 19) shows an increase in the slope again (3.73) compared to Day 2 but remains below that of Day 1's slope (4.12). This shift reflects reduced evaporative enrichment and greater mixing of wetter antecedent flow or contributions due to rainfall into the streamflow. The small negative intercept (-0.38) suggests that the streamflow isotopic composition is transitioning between the wetland-modified signature and fresher contributions from stormflow, indicating hydrological recovery toward pre-event conditions.

Streamflow samples across the monitoring period display enrichment in heavier isotopes when compared to rainfall, as evidenced by persistent offsets (shift to the right of the rainfall trendline). This enrichment is primarily driven by evaporative processes within the wetlands. Early in the event, streamflow isotopic compositions exhibit depletion, closely following rainfall trends. Over time, however, enrichment increases, likely due to stormflow mobilizing evaporated water downstream (Craig and Gordon, 1965). Wetland storage plays a critical role in buffering and modulating streamflow composition, delaying rainfall signatures and leading to mixing processes that result in isotopic shifts (Kendall and McDonnell, 2012).

The figures below (Figure 5-5 - Figure 5-8) present time series plots of the $\delta^{18}O$ an $\delta^{2}H$ for the streamflow and the rainfall during the two events. In Figure 5-5 a strong alignment between rainfall and streamflow isotopic composition is evident, with the initial $\delta^{18}O$ values ranging between -3.5 ‰ and -4 ‰, especially during the early stages of the rainfall event. This relationship indicates a rapid hydrological response and minimal lag between precipitation and streamflow generation. This likely reflects rapid flow pathways becoming active, such as overland or preferential flow downstream of Wetland 1 and Wetland 2. The initial depletion in streamflow $\delta^{18}O$ reaching a minimum of -4.1 ‰ reflects the rapid mobilisation of isotopically lighter water, likely as a result of recent rainfall or water stored in the shallow subsurface. As the event progressed, the streamflow $\delta^{18}O$ levels became increasingly enriched, peaking at -2.75 ‰, indicative of contributions from evaporatively enriched wetland water displaced by incoming rainfall.

In Figure 5-6 the alignment of the $\delta^{2}H$ streamflow and rainfall is poor relative to the $\delta^{18}O$ values. The initial rainfall $\delta^{2}H$ values (recorded during the initial stages of the rainfall event) range between -7.5 ‰ and -12 ‰, whilst the initial streamflow $\delta^{2}H$ values range between -12.5 ‰ and -15.5 ‰. Throughout the rainfall event the rainfall $\delta^{2}H$ values are more

enriched than those of the streamflow δ^2H values. This is inline with the findings from the $\delta^{18}O$ sampling.

Figure 5-7 and Figure 5-8 however, lack overlapping rainfall data, restricting direct stormflow analysis; however, the consistently enriched streamflow isotope signature points to dominant contributions from wetland outflow rather than direct rainfall runoff. The timing of the April event, occurring during the seasonal shift toward drier conditions, further supports reduced catchment saturation and a greater dependence on wetland-derived flows that have undergone longer retention and evaporative modification.

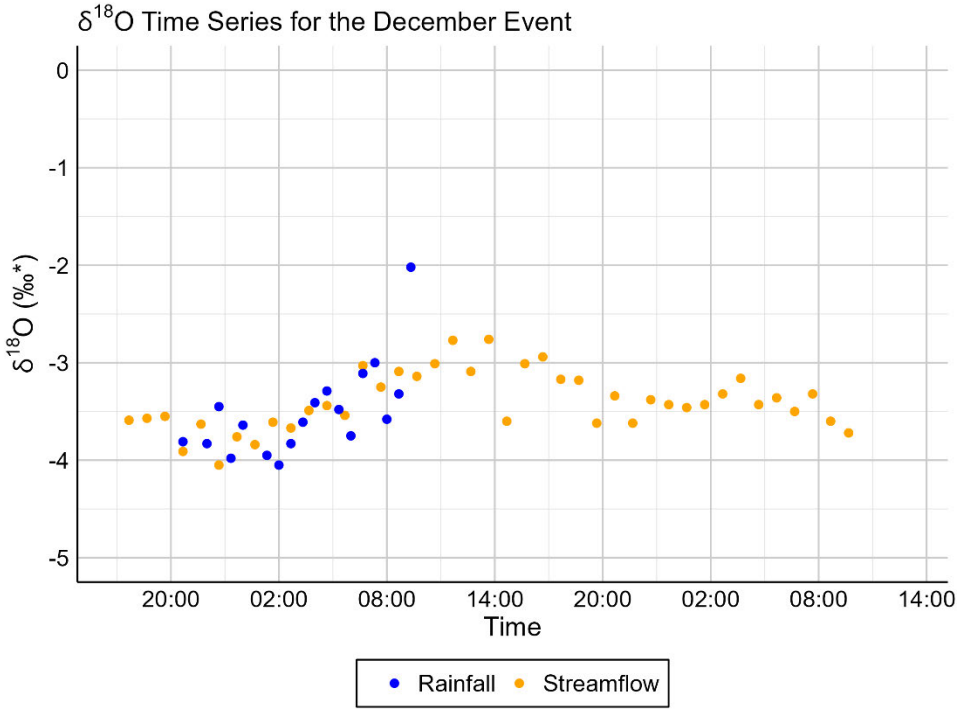

Figure 5-5: December 2023 - time series of the stream flow and rainfall $\delta^{18}O$

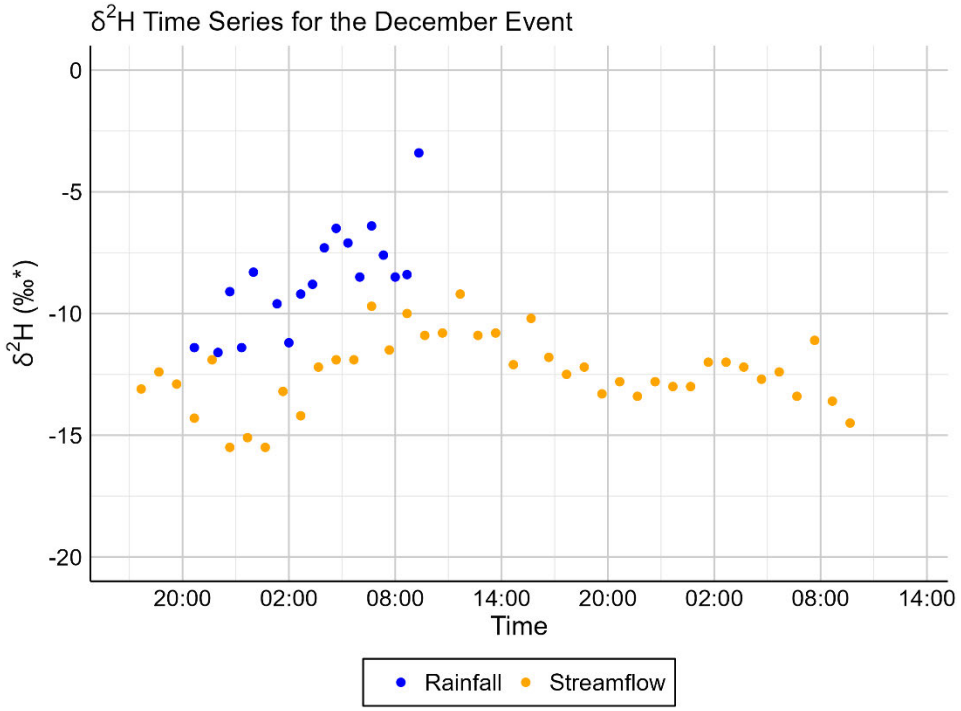

Figure 5-6: December 2023 - time series of the stream flow and rainfall δ^2H

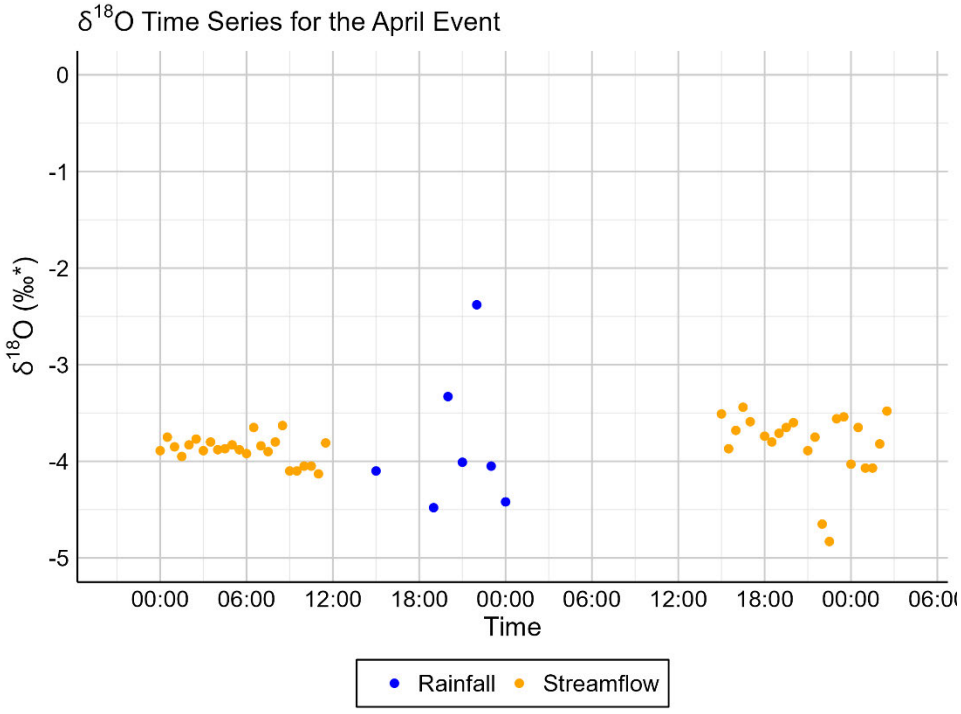

Figure 5-7: April 2024 - time series of the stream flow and rainfall $\delta^{18}O$

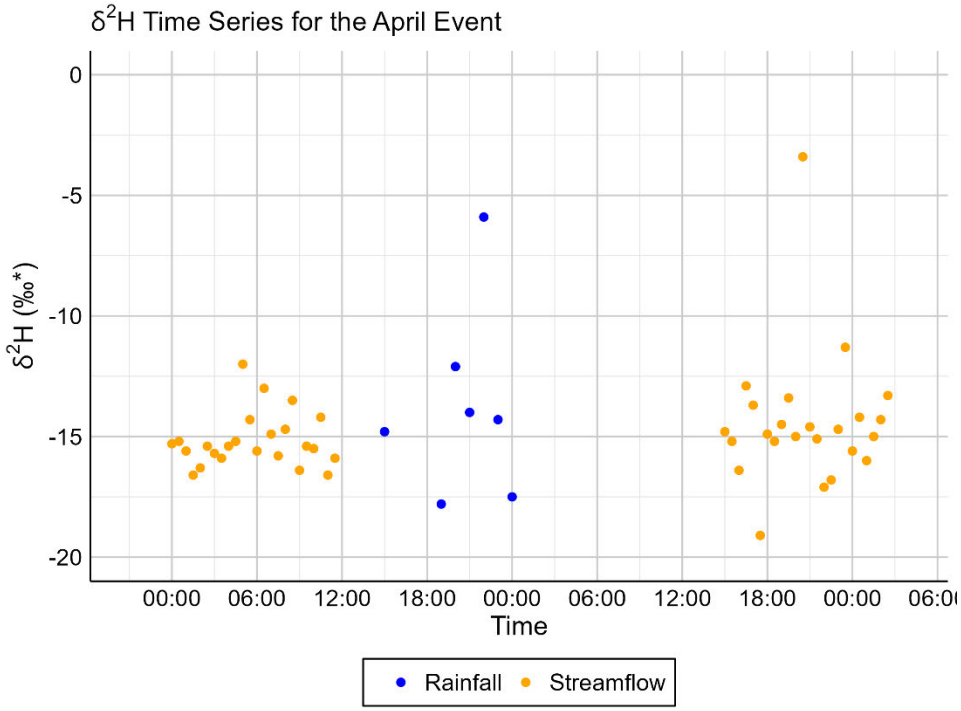

Figure 5-8: April 2024 - time series of the stream flow and rainfall δ^2H

5.1.2 Long-term monitoring

The long-term monitoring results for the stable isotopes, EC and temperature of the monitoring points are presented in the sections below.

5.1.2.1 Stable Isotopes

The stable isotope plot, Figure 5-9, shows $\delta^{18}O$ and $\delta^{2}H$ values for all of the water samples collected over two years from each of the water sources (precipitation, surface water and groundwater), differentiated by wet and dry seasons. This plot includes all of the samples taken from each source throughout the catchment. The majority of samples taken cluster near the GMWL, indicating water of meteoric origin with minimal evaporative fractionation. It should be noted that the sampling of the wet season of 2023 and the dry season of 2024 was incomplete. This was due to the dates on which sampling began and finished potentially affecting the results. Overall, the isotopic data highlight a relatively stable system dominated by meteoric water with limited seasonal and interannual variability.

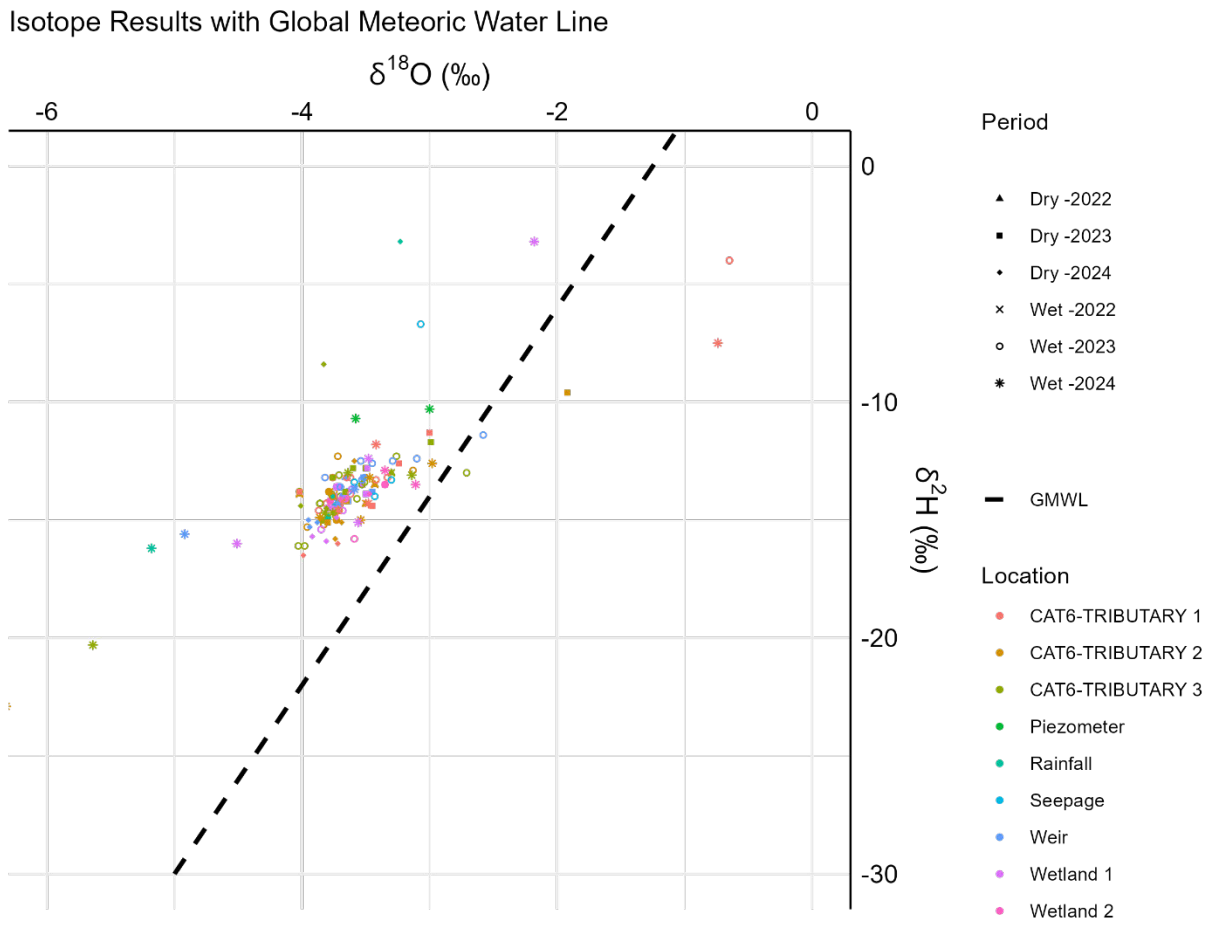

Figure 5-9: Long-term isotope results for the wet and dry seasons during the monitoring period

The long-term isotopic monitoring of the three tributaries (CAT6-Tributaries 1, 2, and 3) is presented below in Figure 5-10. The rainfall trendline was determined from the rainfall samples in Figure 5-9. The equation (Equation 20) seen below is consistent among all of the long-term analyses of individual locations in the catchment. The rainfall trendline serves as a baseline, showing minor evaporative modification consistent with regional precipitation.

$$\delta^2H = 4.38\delta^{18}O + 3.72 \quad (20)$$

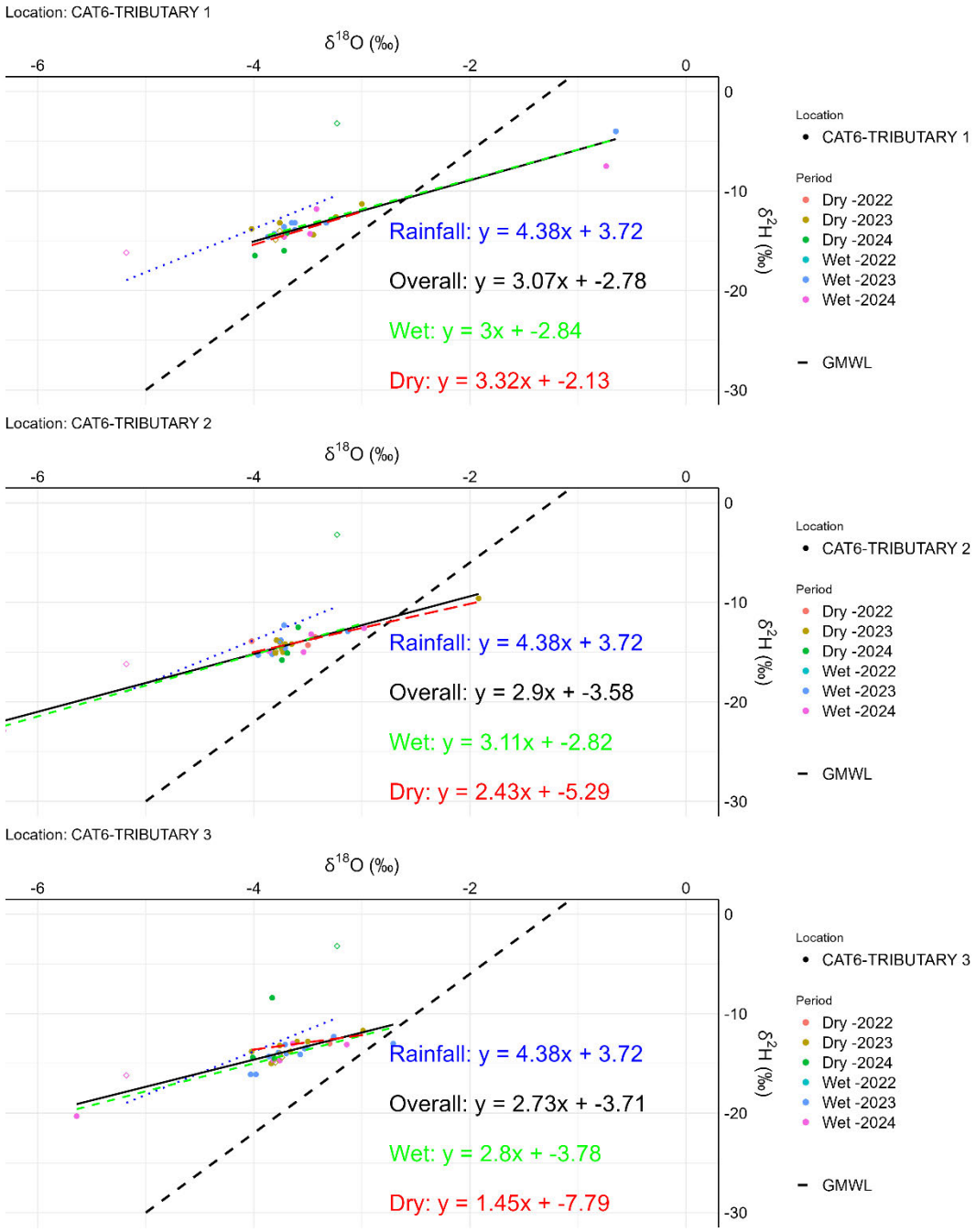

Figure 5-10: Isotopic data from upstream hydrological components

Figure 5-10 shows distinct hydrological patterns influenced by both seasonal dynamics and shallow groundwater influence. All three of the tributaries display isotopic samples and trendlines that fall below the rainfall trendline, indicating contributions from shallow groundwater. Across all three of the tributaries, the wet season trendlines have steeper slopes and higher intercepts than those observed during dry seasons, suggesting a large degree of hydrological connectivity and more direct rainfall contributions during wetter conditions. In

contrast, dry season trendlines show reduced slopes and lower intercepts, reflecting contributions from sources with longer residence times, such as shallow groundwater.

$$\delta^2H = 3.07\delta^{18}O - 2.78 \quad (21)$$

$$\delta^2H = 3\delta^{18}O - 2.84 \quad (22)$$

$$\delta^2H = 3.32\delta^{18}O - 2.13 \quad (23)$$

The eastern tributary presents contrasting hydrological behaviour to the other tributaries, with the steepest overall trendline (Equation 21), indicating a stronger connection to the rainfall and less isotopic modification compared to the other tributaries. During the wet seasons, the trendline (Equation 22) remains relatively close to rainfall inputs. This indicates efficient and rapid runoff generation via near-surface flow paths and minimal interaction with subsurface storage. During the dry seasons, the slope remains steep (Equation 23), unlike the other tributaries. This tributary shows quick recovery after an event and minimal isotopic alteration. This could be due to short soil water residence or quick-draining slopes. Based on these results, Tributary 1 has the most direct hydrological response among the three, with less influence from stored water.

$$\delta^2H = 2.9\delta^{18}O - 3.58 \quad 24$$

$$\delta^2H = 3.11\delta^{18}O - 2.82 \quad 25$$

$$\delta^2H = 2.43\delta^{18}O - 5.29 \quad 26$$

CAT6-Tributary 2 (mid tributary) displays an overall trendline found in (Equation 24), indicating a relatively gentle slope. This suggests substantial mixing with pre-event water stored in the shallow subsurface or riparian zones, where some isotopic enrichment may occur due to evaporative processes in surface soils. During wet seasons (Equation 25) the slope becomes slightly steeper (3.11), suggesting more direct contributions from recent rainfall and the activation of rapid flow paths, such as overland or shallow subsurface flow. In contrast, the dry season trendline (Equation 26) shows a shallower slope (2.43) and a more negative intercept (-5.29). This is consistent with water sourced from deeper soil layers or slowly draining hillslopes, where evaporative fractionation and residence times are more pronounced.

$$\delta^2 H = 2.73\delta^{18}\mathrm{O} - 3.71 \quad (27)$$

$$\delta^2 H = 2.8\delta^{18}\mathrm{O} - 3.78 \quad (28)$$

$$\delta^2 H = 1.45\delta^{18}\mathrm{O} - 7.79 \quad (29)$$

CAT6-Tributary 3 (west tributary) has the shallowest overall slope among the three tributaries (Equation 27), indicating a strong influence from older, stored water and less direct rainfall contribution. The wet season trendline (Equation 28) shows only a slight increase in slope, suggesting that even during rainfall events, the streamflow is still influenced by pre-event water stored in the upper catchment soils. The dry season trendline (Equation 29) has a much shallower slope, with a very low intercept. This would indicate that the dominant contributions to streamflow are as a result of soil moisture stores with a long residence time or groundwater recharge zones at higher elevations of the catchment. This tributary shows the greatest reliance on contributions from subsurface storage during dry seasons.

The long-term isotopic monitoring of the wetlands and the groundwater are presented below in Figure 5-11. These represent the hydrologic features found in the middle of the catchment.

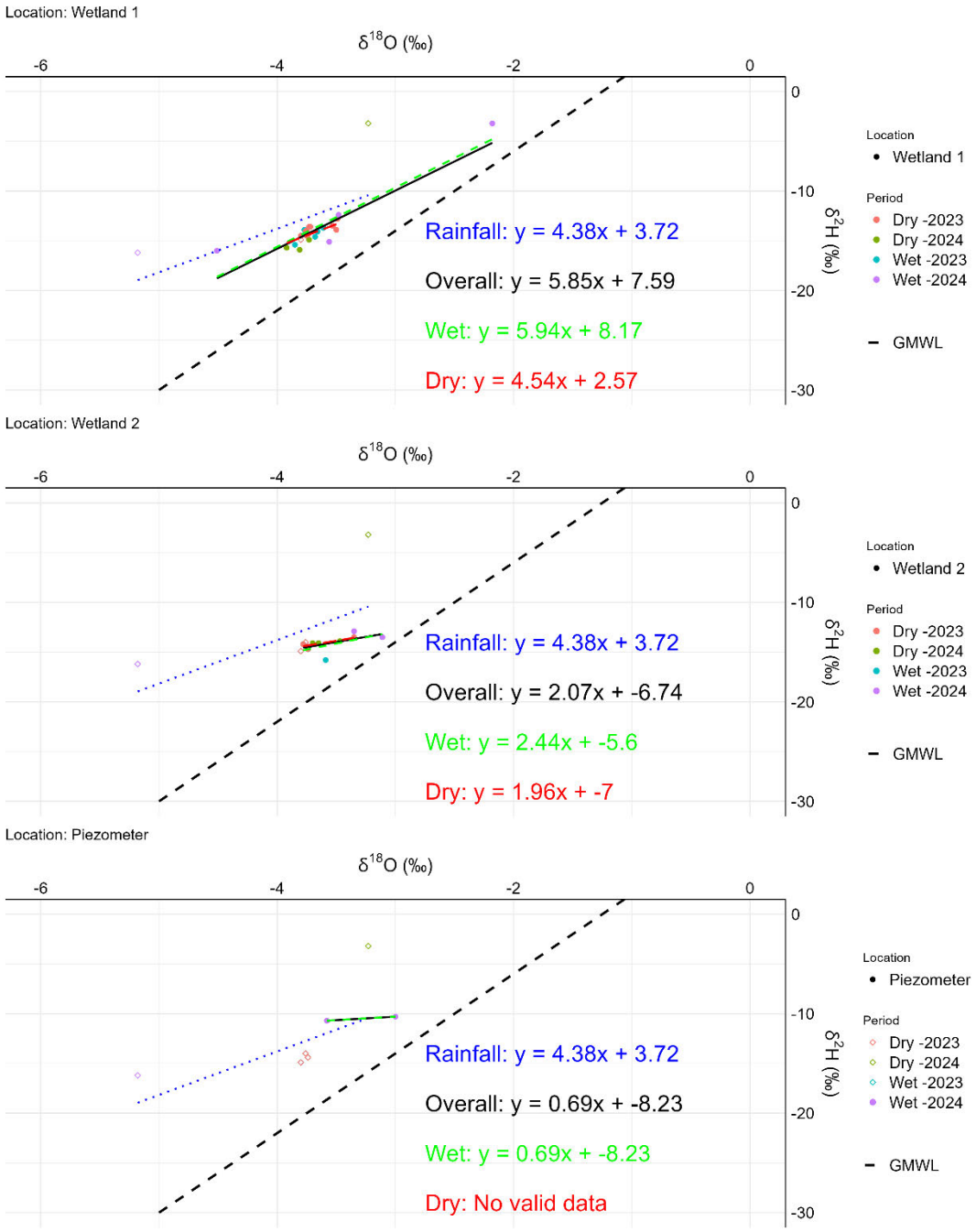

Figure 5-11: Isotopic data from mid-catchment hydrological components

$$\delta^2H = 5.85\delta^{18}O + 7.59 \quad (30)$$

$$\delta^2H = 5.94\delta^{18}O + 8.17 \quad (31)$$

$$\delta^2H = 5.54\delta^{18}O + 2.57 \quad (32)$$

The Wetland 1 overall trendline (Equation 30) compared to the rainfall trendline, displays both a steeper slope and a higher intercept. This indicates that the water has undergone evaporative enrichment and mixing of stored wetland water with event water. The high intercept (7.59) suggests the presence of fully evaporated surface water contributing to streamflow, highlighting Wetland 1's role as a significant storage and mixing zone. During wet seasons, the trendline's (Equation 31) slope increases, showing that fresh rainfall inputs are rapidly incorporated into the wetland, although some evaporative influence continues. The dry season trendline (Equation 32) has a reduced slope and lower intercept than the wet season, suggesting dominance of evaporated surface water and reduced inflow from tributaries during low-flow conditions. These findings highlight the wetland's buffering role and responsiveness to hydrological inputs across the wet and dry season.

$$\delta^2H = 2.07\delta^{18}\mathrm{O} - 6.74 \quad (33)$$

$$\delta^2H = 2.44\delta^{18}\mathrm{O} - 5.6 \quad (34)$$

$$\delta^2H = 1.96\delta^{18}\mathrm{O} - 7 \quad (35)$$

Wetland 2 shows a very different isotopic profile when compared to Wetland 1. The overall trendline (Equation 33) has a very flat slope and very negative intercept, indicating contributions from older stored water, potentially groundwater, that has undergone minimal evaporative enrichment but substantial isotopic depletion during recharge. This suggests that Wetland 2 plays a more passive hydrological role, with longer residence times and slower turnover of stored water. During wet seasons, the trendline (Equation 34) increases slightly in slope, suggesting a modest influence from rainfall, though older water still dominates. In dry conditions, the trendline (Equation 35) remains shallow and depleted, consistent with extended storage and evaporation effects, with minimal contribution from recent surface runoff. Overall, Wetland 2 appears to serve as a long-term storage reservoir, contributing older and isotopically distinct water during both wet and dry seasons.

$$\delta^2H = 0.69\delta^{18}\mathrm{O} - 8.23 \quad 36$$

The piezometer site shows a distinctive isotopic signature dominated by subsurface or groundwater processes. The overall trendline (Equation 36) has a very shallow slope and very low intercept, reflecting water that is isotopically unaltered by surface evaporation and instead

shaped by recharge processes, possibly during cooler periods. This suggests that the piezometer consistently samples a stable, deep groundwater source.

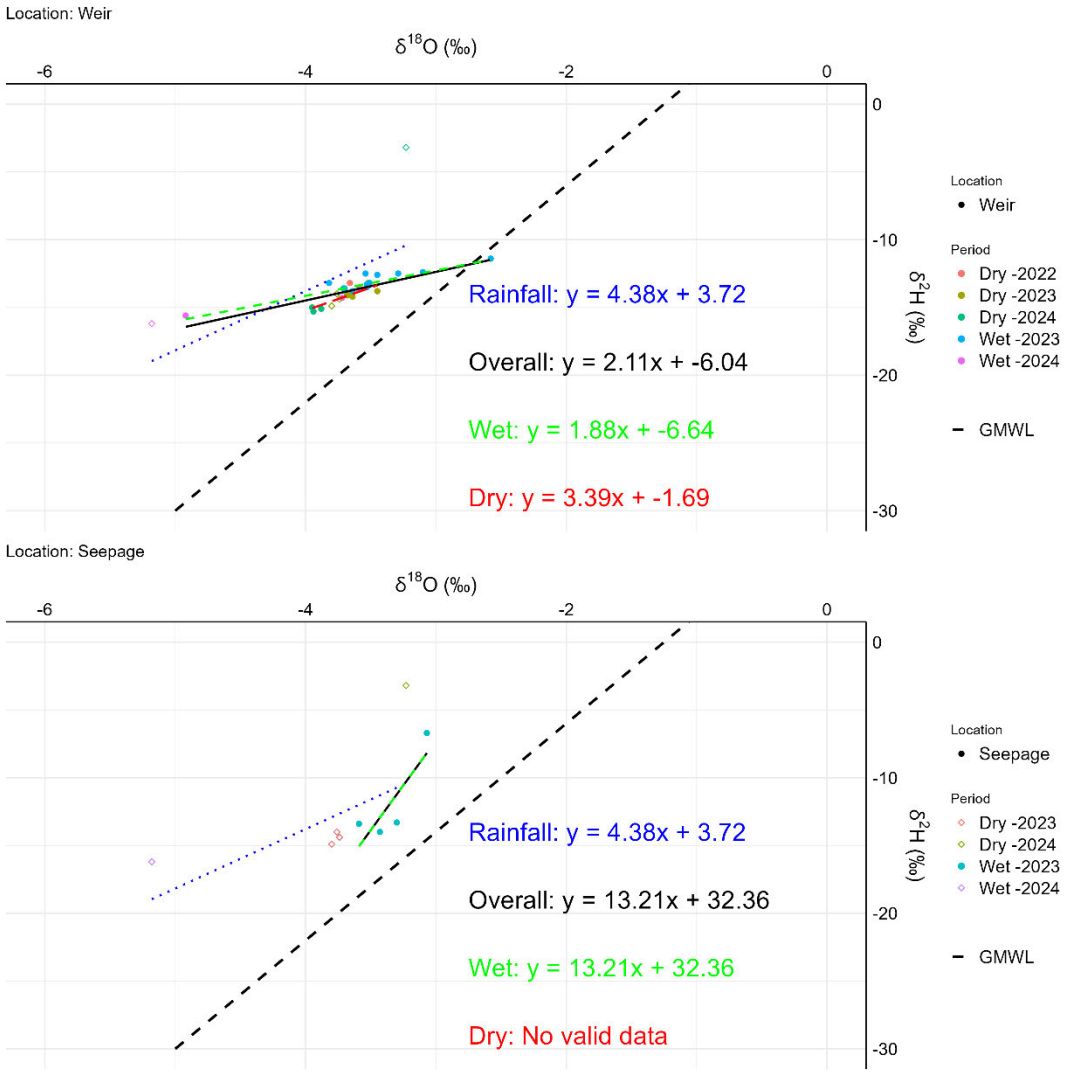

Figure 5-12: Isotopic data from lower catchment and outlet hydrological components

$$\delta^2H = 13.21\delta^{18}O + 32.36 \quad (37)$$

Seepage was only observed during the wet season due to periods of elevated rainfall that likely raised the local water table or saturated surface soils sufficiently to initiate lateral flow. The isotopic signature of this sample site shows an exceptionally steep slope and very high intercept (Equation 37). This is indicative of strong evaporative fractionation prior to mobilisation. Despite the absence of surface storage, the enrichment suggests that the water contributing to seepage may have percolated through shallow soil layers or accumulated temporarily in the unsaturated zone, undergoing evaporative modification before emerging. This episodic behaviour, limited to the wet season, highlights the role of transient near-surface flow paths in

delivering evaporatively enriched water to the stream system under saturated catchment conditions.

$$\delta^2H = 2.11\delta^{18}\mathrm{O} - 6.04 \quad (38)$$

$$\delta^2H = 1.88\delta^{18}\mathrm{O} - 6.64 \quad (39)$$

$$\delta^2H = 3.39\delta^{18}\mathrm{O} - 1.69 \quad (40)$$

The isotopic composition at the weir reflects the integrated signal of all upstream contributions. The overall trendline (Equation 38) indicates substantial mixing of wetland flows, tributary inputs and possibly groundwater. The negative intercept suggests the presence of isotopically depleted components, likely from older subsurface water or long-residence wetland flows entering the weir's stilling pond. During the wet seasons the slope decreases slightly (Equation 39), showing increased dominance of rainfall inputs; however, the wetland signals remain evident. In dry seasons, however, the slope increases significantly (Equation 40), suggesting that the system becomes dominated by the tributary streamflow and low elevation groundwater contributions, whilst the wetland buffering influence diminishes. The more positive intercept during this time indicates a reduction in depleted source contributions. These observations highlight the dynamic role of the weir as a downstream integrator that reflects both long-term storage and short-term flow events.

From Figure 5-13 a timeseries of $\delta^{18}O$ at various points of the catchment can be seen. This figure shows relatively stable $\delta^{18}O$ values at most of the sites, with minimal seasonal fluctuation despite changes in rainfall inputs. Most of the samples' $\delta^{18}O$ values are similar to the rainfall during the wet season, with no strong evaporative signatures observed except at the seepage site. This consistency suggests that the $\delta^{18}O$ signal is buffered by stable water sources within the catchment. This is likely due to continual contributions to streamflow from shallow or intermediate-depth groundwater. Groundwater, having longer residence times and being less affected by immediate atmospheric or surface conditions, provides a more stable isotopic signal. These stable groundwater contributions likely buffer isotopic variability in streamflow and sustain baseflow during dry seasons, which helps explain the relatively consistent $\delta^{18}O$ values despite seasonal rainfall fluctuations.

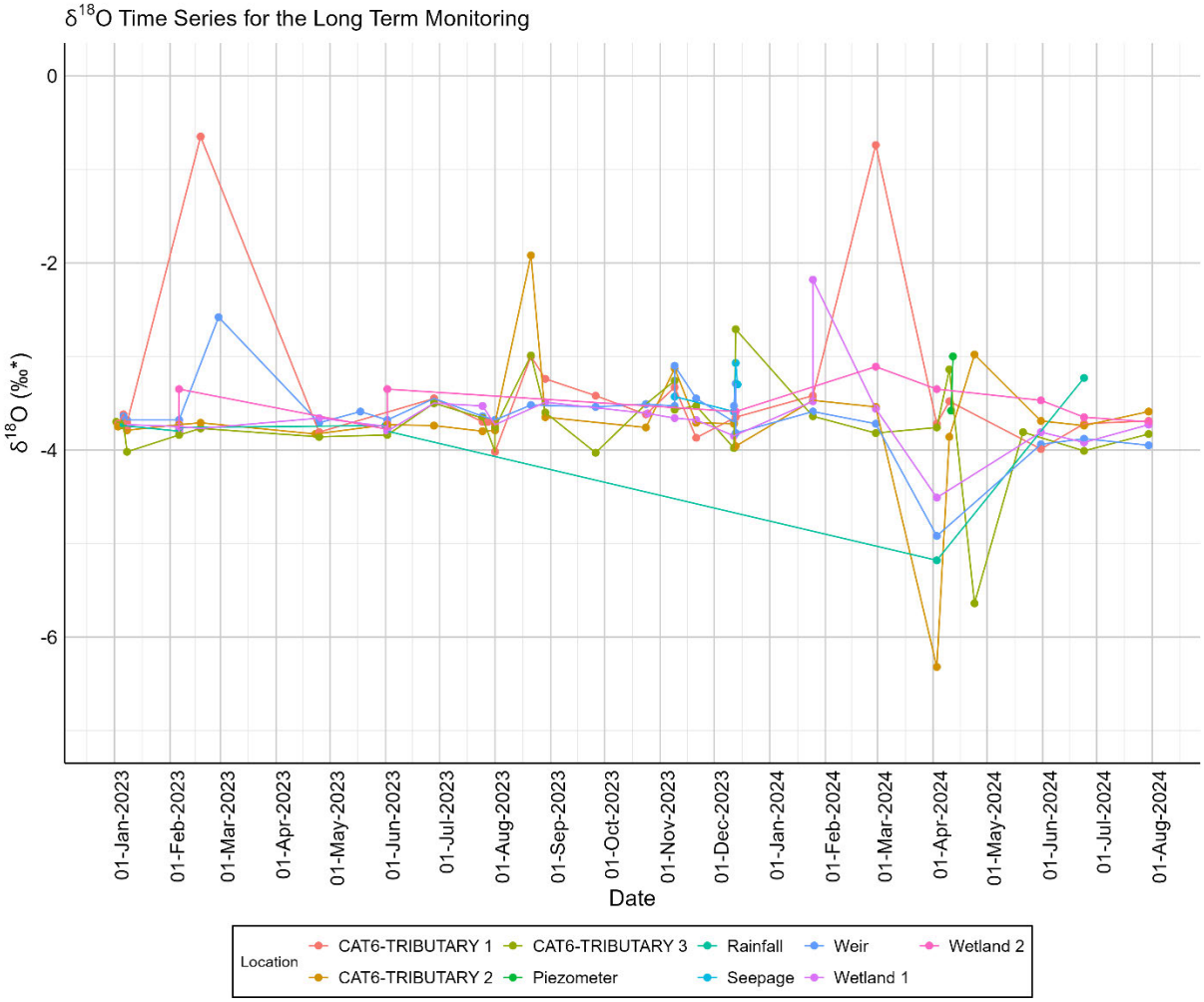

Figure 5-13: Timeseries of $\delta^{18}O$ by location throughout the catchment for the duration of monitoring

From Figure 5-14 a timeseries of $\delta^{18}O$ at various points of the catchment can be seen. The $\delta^{2}H$ values show limited variation across the catchment, with most samples closely following the rainfall during the wet season. Slightly more depleted values in the tributaries and wetlands suggest recharge during cooler conditions or precipitation at higher elevations, highlighting a significant groundwater influence. The seepage site, however, shows clear signs of evaporation, with enrichment in both $\delta^{2}H$ and $\delta^{18}O$ likely caused by an extended period where it was exposed to the atmosphere during the wet season. Overall, the consistent $\delta^{2}H$ values across the catchment indicate that groundwater plays a key role in stabilising streamflow and

baseflow, buffering the system against short-term changes in the climate.

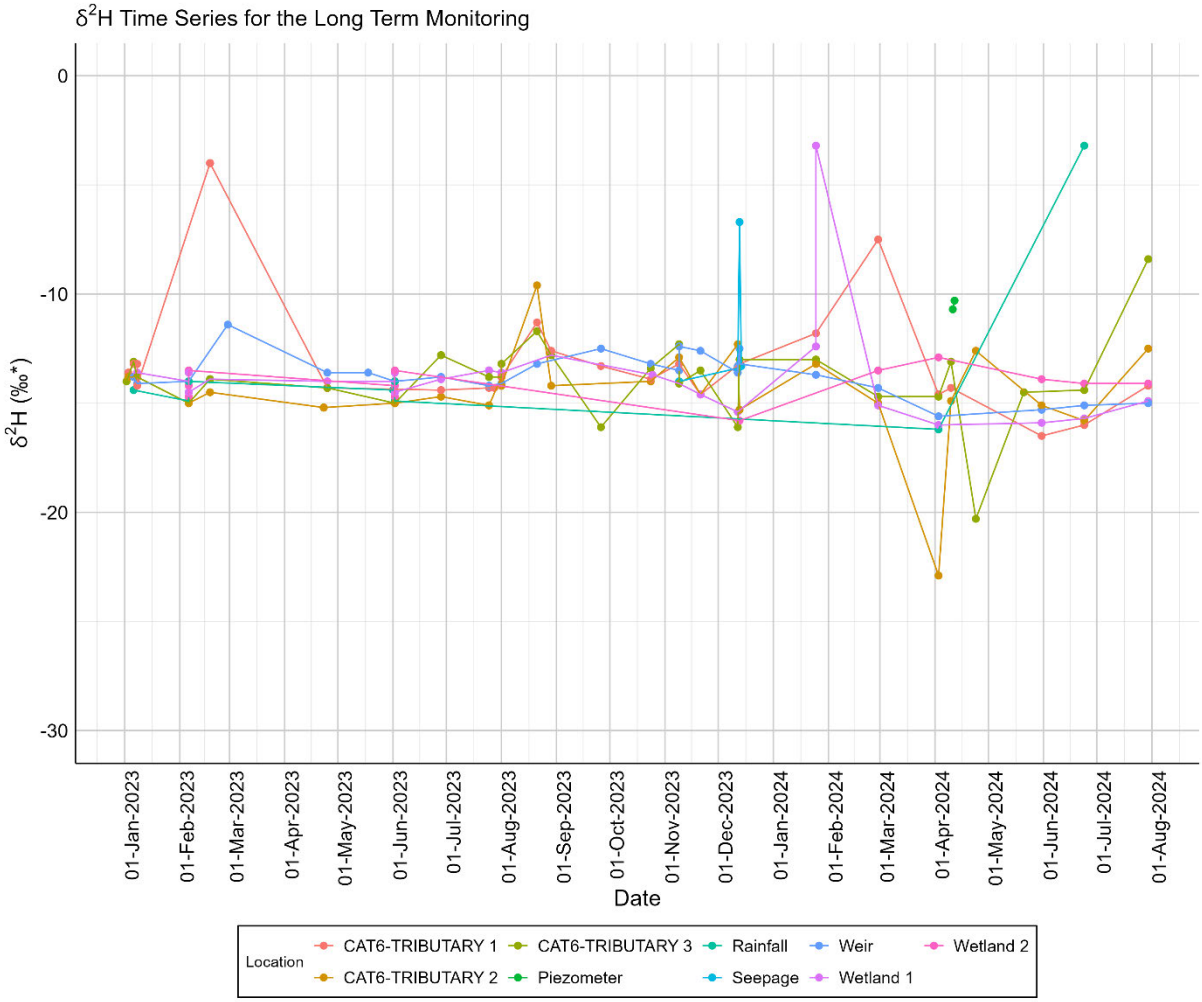

Figure 5-14: Time series of δ^2H by location throughout the catchment for the duration of monitoring

5.1.2.2 EC and Temperature

Figure 5-15 presents the variations in water temperature for each of the long-term monitoring locations in Catchment 6 for the entire sampling duration (approximately 1 year, spanning from March 2023 to July 2024). For the duration of sampling, the water temperatures exhibit clear seasonal fluctuations; the peak temperatures occur during the summer months (wet season) and the water temperatures decrease during the winter months (dry season), as expected for a temperate, high-altitude system.

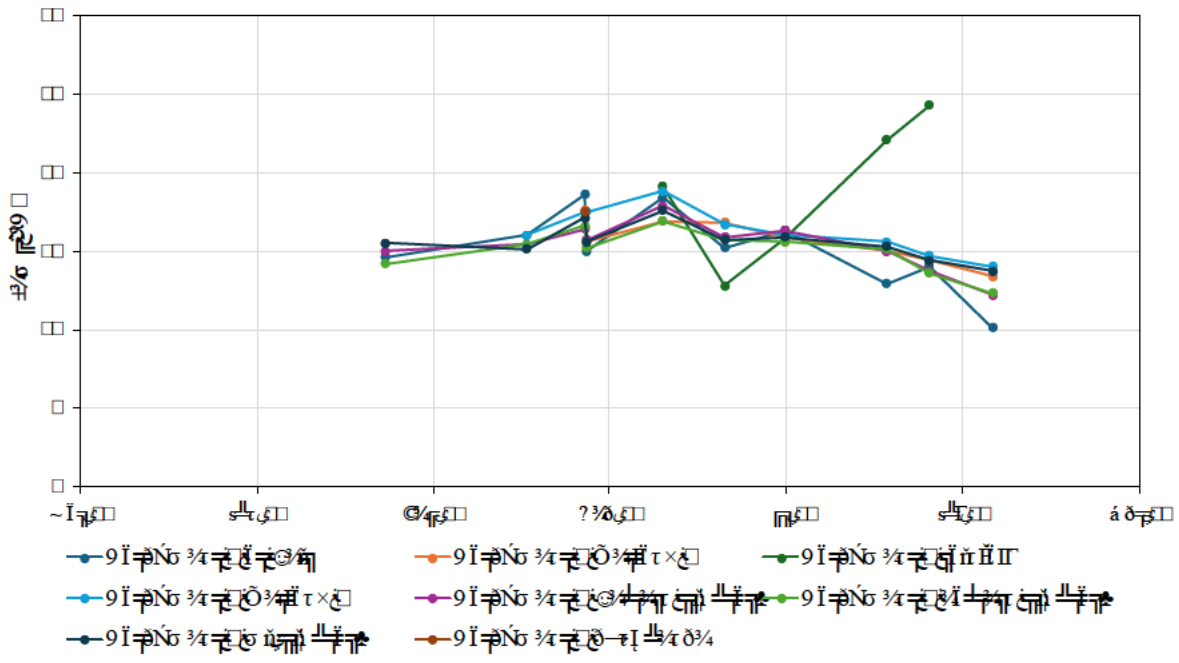

Figure 5-15: Plot of temperature at the long-term sampling points

Water temperature across the majority of sampling sites ranged between 10 °C and 18 °C throughout the monitoring period, with modest seasonal fluctuations. The three tributaries and Wetland 1 exhibited similar temperature ranges and variation patterns, generally aligning with rainfall events and broader seasonal temperature trends. Wetland 2 and the weir site consistently recorded lower temperatures compared to upstream locations, particularly during the warmer months. Amongst all sites, Wetland 2 exhibited the lowest recorded water temperatures over the monitoring period. Rainfall-temperature data displayed higher variability. Notably, two anomalous readings were recorded in July 2024, both exceeding 25 °C. These values diverge from the general trend and differ significantly from the surrounding data points. These elevated values are likely as a result of the elevated ambient temperatures and indirect solar heating of the collected water in the rainfall sampler.

Figure 5-16 presents a timeseries of the EC at the same points at which the temperature was measured. The EC concentration of a water body or source is often used as a proxy for the total dissolved solids (TDS), reflecting the ionic strength of the water. These data can provide insight into the hydrological flow paths, the groundwater-surface water interactions occurring and the spatial variability of the catchment.

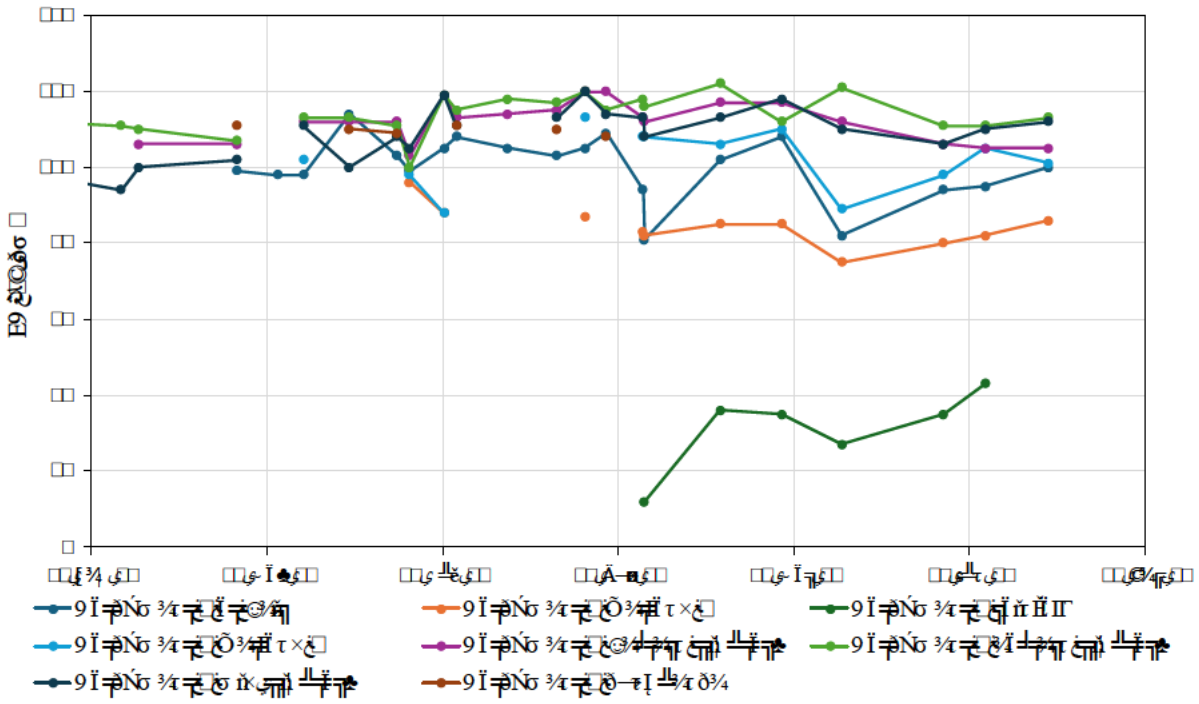

Figure 5-16: EC trends across the long-term monitoring sites

The EC measurements across the catchment, shown in Figure 5-16, showed consistent spatial and temporal patterns. In the upper portion of the catchment, including the three tributaries, Wetland 1 and the tributary confluence site, EC values remained relatively stable over the monitoring period. These sites recorded EC ranges typically between 100 and 120 µS/cm, with only minor fluctuations observed across time. In contrast, Wetland 2 consistently recorded lower EC values than the other monitoring sites. The EC at Wetland 2 ranged between 75 and 90 µS/cm, indicating a distinct chemical signature compared to upstream and downstream locations.

The weir site downstream of Wetland 2 occasionally recorded EC values higher than those measured within the wetland, particularly during the periods of August to November 2023 and March 2024. These elevated values suggest a temporal variation in inflows to the lower catchment, especially during baseflow periods.

Rainfall EC measurements showed substantial variability across the monitoring period. The lowest recorded EC values were approximately 10 µS/cm in late 2023, increasing to over 40 µS/cm by mid-2024. A sharp increase in rainfall EC was observed between June and July 2024, concurrent with an increase in rainfall temperature. This is likely due to increased levels of smoke resulting from the fire break burning taking place in the research catchments and the surrounding area during these months.

Across the catchment, EC values showed a general spatial pattern: high values in the tributaries, followed by a reduction through Wetland 1, moderate EC at the confluence and lower values in Wetland 2. The weir EC values showed more temporal variability, occasionally exceeding upstream values.

Figure 5-17 presents the monthly trends of the EC measured at two monitoring points: upstream of the confluence and Wetland 1, and downstream of Wetland 1 to the catchment outlet. Figure 5-18 presents a scatter plot of the rainfall vs. EC of the data aggregated by catchment position (upstream and downstream), with the resulting trend lines.

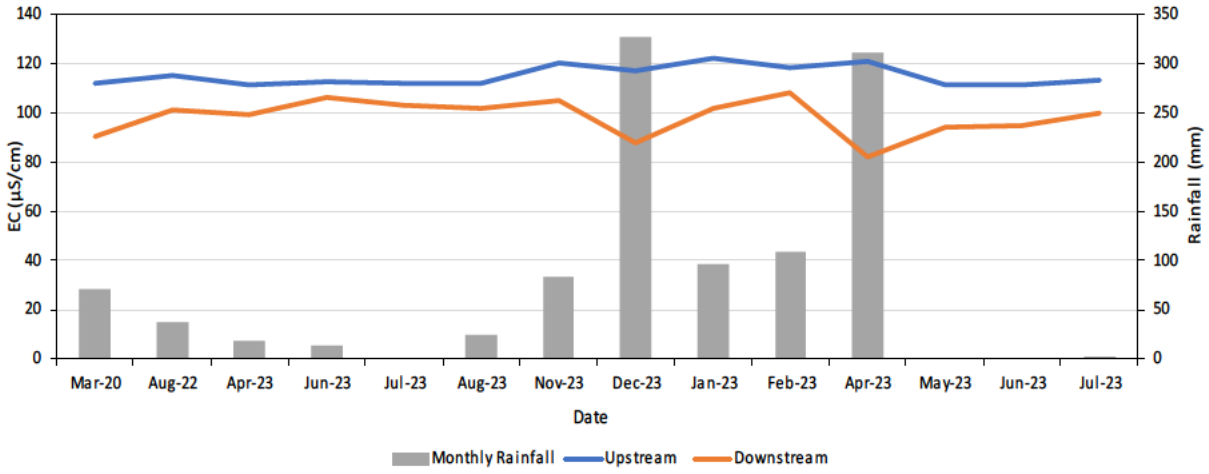

Figure 5-17: Up- and downstream comparison of EC data during the sampling period

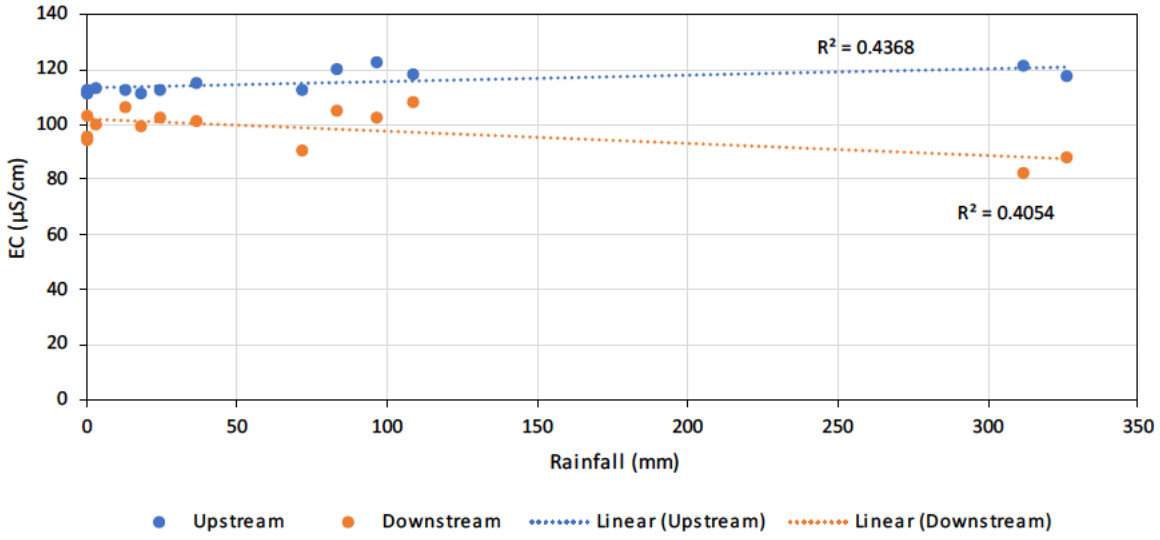

Figure 5-18: Up- and downstream EC correlation analysis

The data show a moderate seasonal variation in EC values, likely influenced by both rainfall and the hydrological processes occurring in Wetland 1. During the wetter summer months (December 2023 to March 2024) EC values at upstream sites are consistently higher than those at downstream sites. This trend suggests that groundwater contributions are a dominant source of streamflow in the upper catchment during the wet season, consistent with deeper flow paths and longer residence times leading to higher ionic concentrations (Scanlon et al., 2002; Winter et al., 1998). In contrast, downstream EC values are notably lower during this period, likely due to the dilution of wetland storage by surface runoff and the buffering capacity of Wetland 1.

In the late dry season, especially from June to July 2024, this pattern reverses whereby downstream EC values begin to exceed those upstream. This shift likely indicates a seasonal change in the wetland's role, transitioning from a dilution-dominated system to a solute source. As evapotranspiration increases and rainfall inputs decline, wetland water is concentrated through evaporative enrichment, releasing stored solutes and contributing higher EC flows downstream (Reddy *et al*., 2003). Reduced flow volumes and increased residence time during this period enhance solute accumulation from internal wetland processes and seepage from adjacent saturated soils and hillslopes.

Figure 5-18 further illustrates this dynamic, showing the relationship between EC and cumulative rainfall. A positive correlation between rainfall and EC is observed at the upstream site ($R^2 = 0.44$), suggesting that rainfall enhances groundwater recharge and subsurface flow contributions rich in dissolved ions. Conversely, a negative correlation is observed downstream ($R^2 = 0.41$), indicating that increasing rainfall events are associated with EC dilution, likely due to increased surface runoff mixing with stored low-EC water in Wetland 1. These contrasting responses reinforce the role of Wetland 1 as a dynamic biogeochemical buffer, modulating the impact of rainfall on water quality as it moves downstream through the catchment.

5.1.3 End-member mixing analysis

To determine the percentage contribution of the groundwater and rainfall to the streamflow, a two-member EMMA model was used, using the rainfall and streamflow data from the December event sampling. Due to the absence of groundwater samples, a proxy value was used. For the stable isotopes groundwater value, the proxy was based on the assumption that the pre-event streamflow was comprised solely of groundwater; therefore, the results from the

pre-event streamflow water were used. Meanwhile, for the EC groundwater value in lieu of a measured value, the streamflow from the eastern tributary for the dry season was used as a proxy. The wetland values were obtained from the measurements taken from Wetland 1 prior to the rainfall event. The results from this analysis can be seen in Figure 5-19. This analysis was not completed for the April sampling as no EC values of the rainfall were measured for this rainfall event and also due to there being no streamflow isotope samples during the rainfall period.

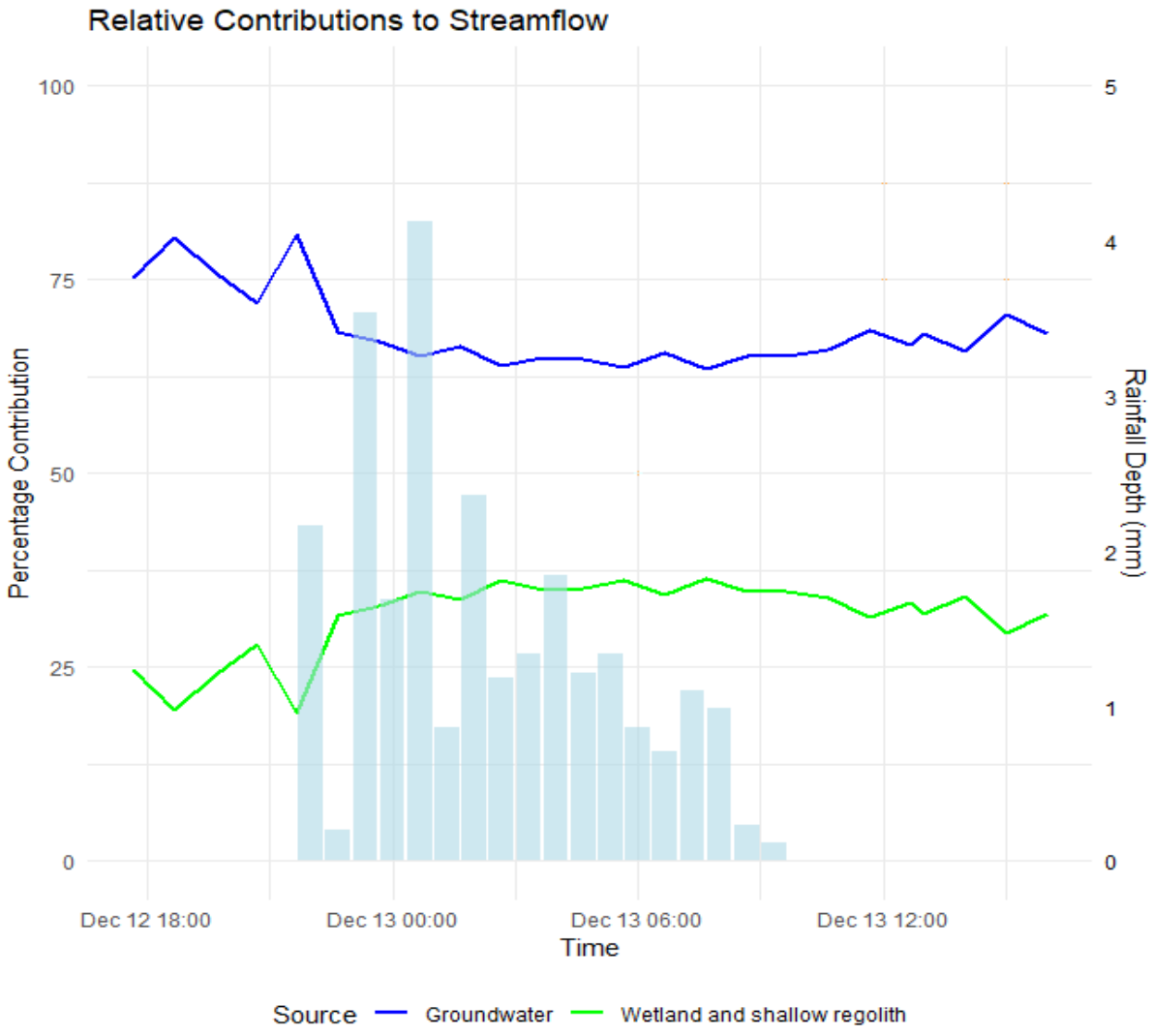

Figure 5-19: December 2023 isotope EMMA results

From the figure above, a rapid increase in the fraction of wetland contributions can be seen towards the beginning of the rainfall event. The wetland contributions increase toward the middle of the event, followed by the groundwater slowly increasing in its contributions over the course of two days once rainfall has ceased. The initial spike in the wetland is likely due to the overland and shallow subsurface flow entering the stream network. The later recovery of

the wetland contribution is likely the water from upstream having entered the stream network after having exceeded the wetland storage in Wetland 1. It should be noted, however, that the groundwater remains the dominant contributor to streamflow throughout the rainfall event.

5.1.4 ^{222}Rn Results

The locations of the ^{222}Rn sampling sites are presented below in Figure 5-20.

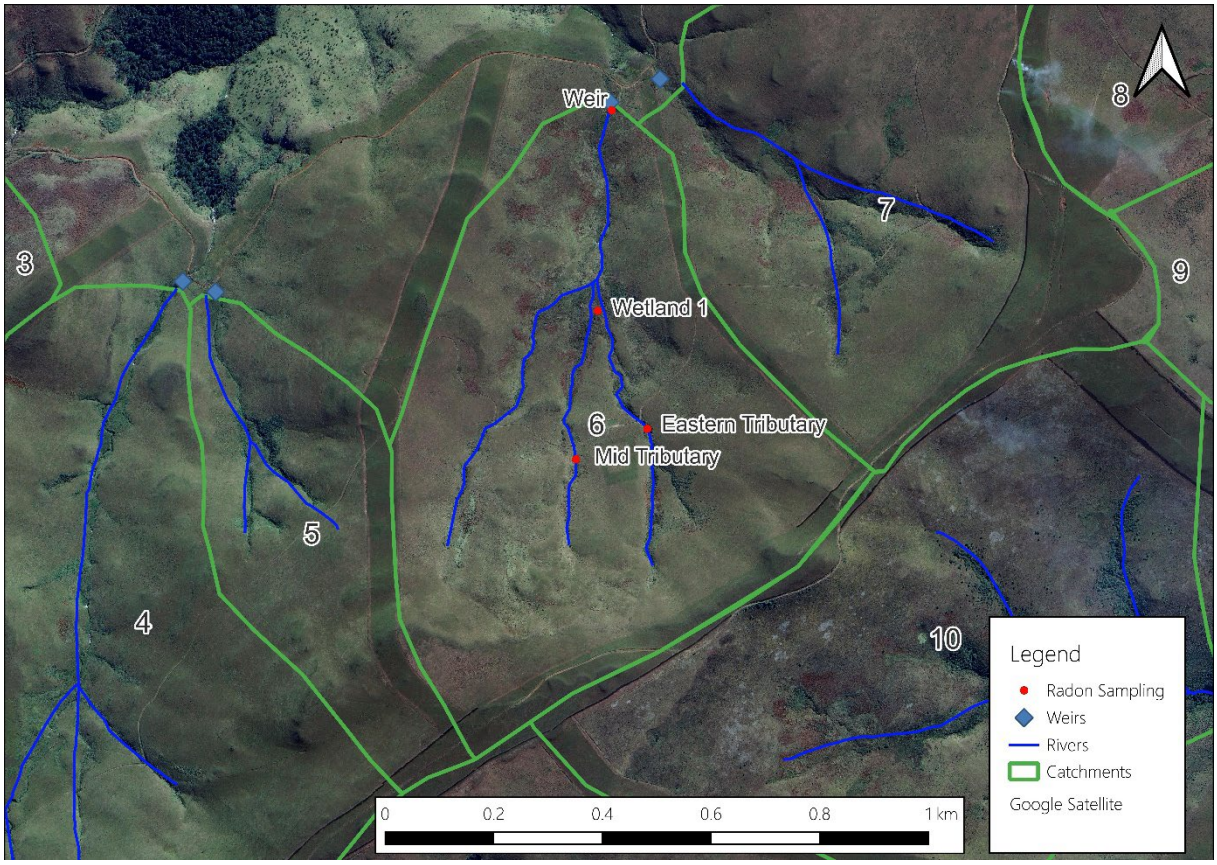

Figure 5-20: ^{222}Rn results and approximate locations

These samples were collected from above the water's surface at each location over the course of a day. Four measurements were taken at each of the sample locations.

Table 5-1: CP Catchment 6 ^{222}Rn results

Location name	Temp	^{222}Rn in air		^{222}Rn in water	
	°C	Bq/m^3		Bq/m^3	
Weir	18.6	481	± 73	393	± 59
Wetland 1	18.7	140	± 39	110	± 30
Mid-tributary	17.1	280	± 55	230	± 46
East tributary	16.6	242	± 57	242	± 47

Table 5-1 presents the results of the ^{222}Rn sampling from the four key hydrological locations within catchment 6 (as seen in Figure 5-20), alongside water temperature readings used for the conversion of the ^{222}Rn in air, as per the methodology laid out in Section 4.1.1.2. These data provide valuable insights into the relative contribution of groundwater to surface water systems, as ^{222}Rn is a well-established natural tracer of subsurface flow (Cook *et al*., 2012; Gilfedder *et al*., 2015).

The highest ^{222}Rn concentration in both air and water is observed at the weir, located near the outlet of the catchment. The elevated concentration (393 ± 59 Bq/m³ in water) at this site strongly suggests a sustained groundwater discharge into the stream prior to it exiting the catchment. ^{222}Rn concentrations of this level are typically associated with subsurface flow paths with long residence times and therefore remain in contact with either bedrock or soil for long periods. This therefore allows for groundwater to accumulate significant levels of ^{222}Rn (Burnett and Dulaiova, 2012). This, coupled with a high air concentration of ^{222}Rn for this site (481 ± 73 Bq/m³), further implies that the streamflow is actively undergoing degassing of the ^{222}Rn as it exits the lower wetland system and flows into the stilling pond at the weir.

The lowest ^{222}Rn concentrations (110 ± 30 Bq/m³ in water) are recorded at the Wetland 1 site, with the sampled values being consistent with surface water inputs dominating the contributions. This wetland acts as a transitional zone/mixing basin fed by three tributaries, all

of which descend their channels with relatively steep slopes. As ^{222}Rn is a noble gas, it is prone to rapid degassing during turbulent flow (Gilfedder *et al*., 2015). The steep topography above Wetland 1 likely promotes turbulent conditions and therefore vigorous aeration, leading to a large degree of ^{222}Rn loss before the water reaches Wetland 1. Furthermore, due to the wetland water having slow moving waters that result in longer residence times, the ^{222}Rn undergoes a high degree of degassing. In addition to the losses due to degassing, the low ^{222}Rn levels sampled indicate that direct groundwater contributions to Wetland 1 itself are minimal. This reinforces Wetland 1's role as a primarily surface-fed system.

The two tributary sites show intermediate levels of ^{222}Rn, but with an interesting distinction: the eastern tributary exhibits a concentration of 242 ± 47 Bq/m³ in water, whilst the mid-tributary's concentration was 230 ± 46 Bq/m³ in water. It should be noted, however, that the eastern tributary's ^{222}Rn in air and ^{222}Rn in water concentrations are nearly identical. This may indicate that the rate of ^{222}Rn degassing from the streamflow is at equilibrium with the surrounding air, as well as limited recent degassing. In contrast, the mid-tributary may be influenced to a larger degree by a mix of shallow interflow and groundwater that has a shorter residence time than that of the eastern tributary.

Overall, these radon data demonstrate the large degree of spatial variability of the groundwater–surface water interactions occurring throughout the catchment. The tributaries were found to be contributing differentially to downstream flow, and Wetland 1 was found to function primarily as a mixing zone with limited direct groundwater input. In contrast, the weir was found to reflect cumulative baseflow-dominated discharge from the entire system.

5.1.5 OPTRAM model

The OPTRAM model was performed on Sentinel-2 satellite imagery for the dry and wet seasons of the research period. A preliminary analysis was conducted to determine the method of regression line generation that fit the data best in order to obtain the wet and dry edge equations and values, as per Section 4.2. The results of this analysis were that the linear regression line fit the data best. The resulting dry and wet edge equations, which delineate the moisture extremes, formed the basis for calculating fractional soil moisture content across the study area, and are presented in Figure 5-21.

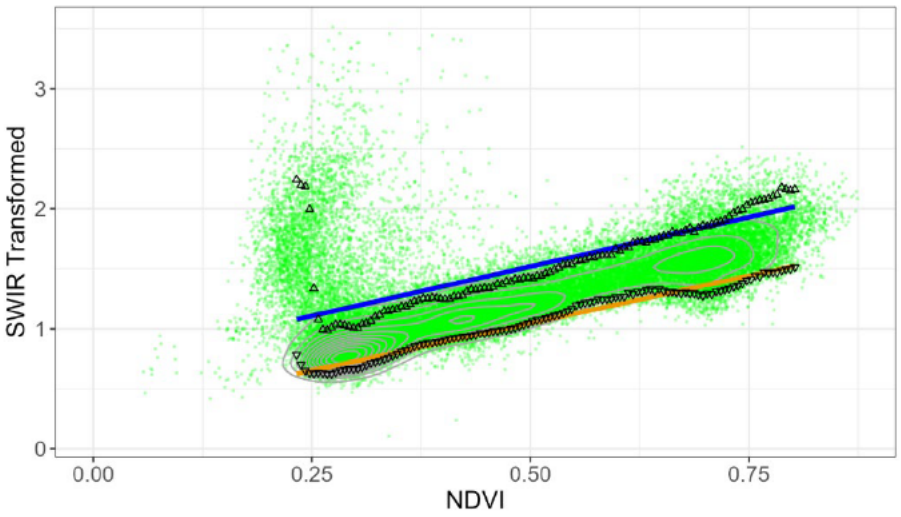

Figure 5-21: CP Catchment 6 linearly fitted trapezoid plot showing the NDVI against the SWIR transformed values

The results from the OPTRAM model were then combined for the respective periods. Figure 5-22 and Figure 5-23 present the spatial distribution of estimated soil moisture during the wet and dry seasons respectively. In both maps, darker colours (blue to purple) represent higher soil moisture content, while lighter hues (yellow to green) indicate drier conditions. The spatial resolution of the satellite imagery is approximately 20 m × 20 m, meaning that moisture must be present over areas at least that large to be detected reliably.

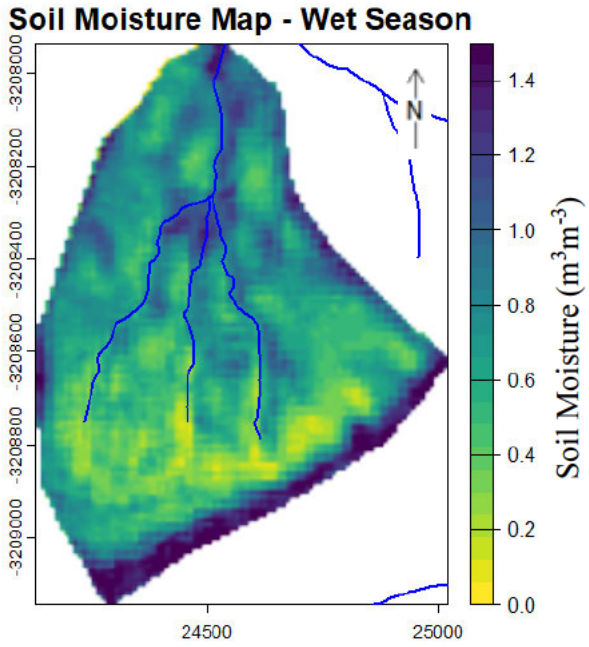

Figure 5-22: Soil moisture for the wet season across CP Catchment 6

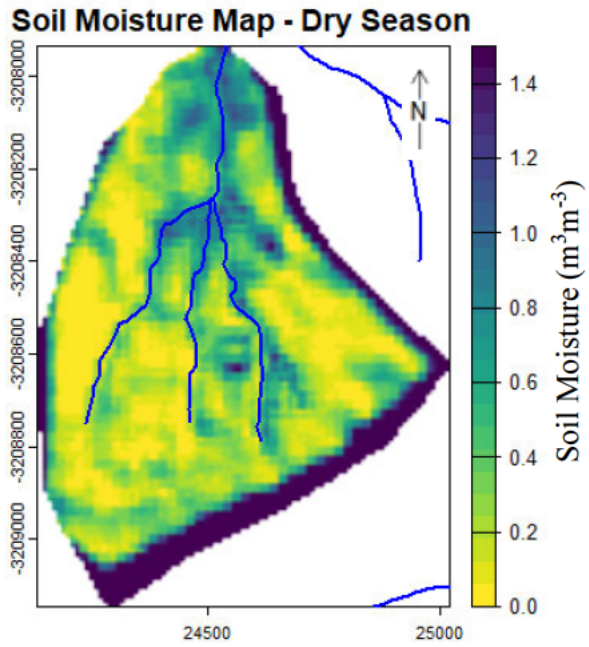

Figure 5-23: Soil moisture for the dry season across CP Catchment 6

In the wet season (Figure 5-22), elevated soil moisture is observed across most of the catchment. This is especially evident in the headwaters of the tributaries and along the stream channels. An area of high moisture extends from the southern plateau into the headwaters of the three tributaries, indicating possible lateral subsurface flow or saturation-excess overland flow. The two wetlands are also distinguishable due to their consistently high soil moisture signatures. These wetlands appear as dark-coloured areas (green to blue).

During the dry season (Figure 5-23), the soil moisture throughout the catchment is reduced compared to the wet season, as shown by the lighter colours. However, both the wetlands and the temporarily saturated valley bottom show higher soil moisture values compared to the surrounding areas. These wetlands act as sources of sustained shallow groundwater discharge or capillary rise, helping to support streamflow and local vegetation during dry seasons. Higher soil moisture zones can be seen to remain on the southern boundary plateau, confirming the presence of localised groundwater-surface water interaction or subsurface connectivity sustaining the tributaries in the dry season.

The NDMI were combined for the wet and dry seasons. Figure 5-24 and Figure 5-25 present the spatial distribution of the NDMI during the wet and dry seasons respectively. It should be noted that due to the lack of overlap in the values of the wet and dry season NDMI, the scales are different for each image. These NDMI images for the wet season and dry seasons

complement the OPTRAM results for the respective season by providing a vegetation-based moisture proxy.

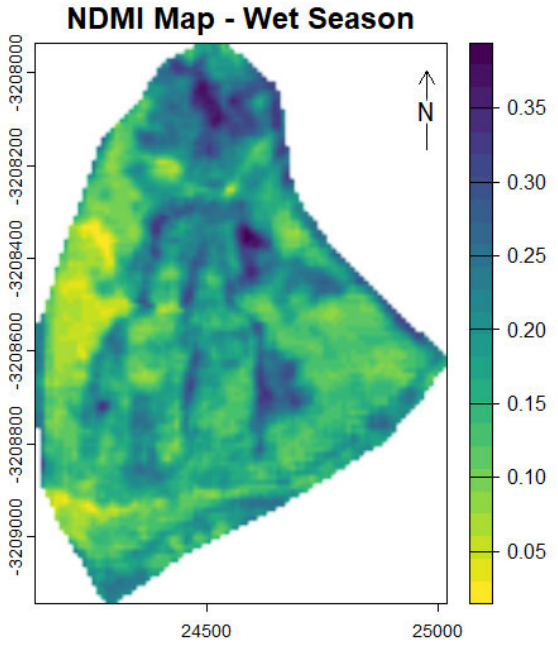

Figure 5-24: NDMI for the wet season across CP Catchment 6

The entirety of the catchment has positive NDMI values as seen on the scale to the right of the figure, indicating water availability with an increase towards the stream channels. The western bank can be seen to have limited vegetative moisture, indicating water stress, potentially due to limited soil moisture storage capacity.

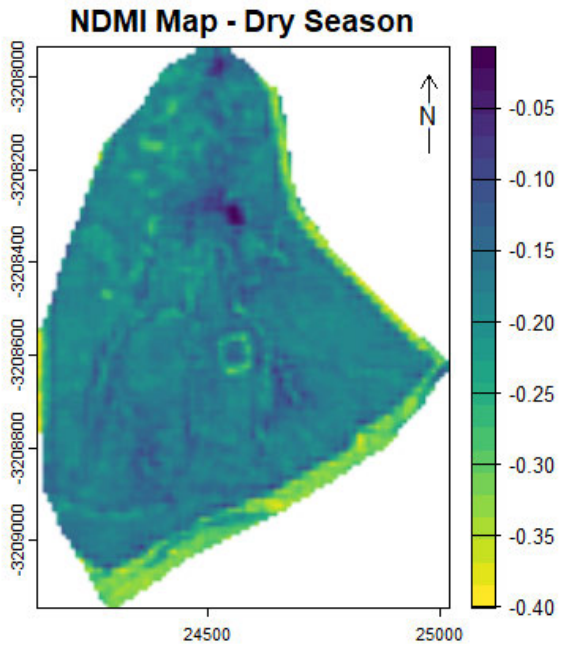

Figure 5-25: NDMI for the dry season across CP Catchment 6.

Most of the catchment displays negative NDMI values as seen on the scale to the right of the figure, indicating limited water availability. In regions where the NDMI values increase, indicating higher moisture in vegetation, a corresponding increase is observed in the same regions where OPTRAM detected elevated soil moisture. This trend is particularly noticeable around wetlands and the temporarily saturated valley bottom. This agreement between OPTRAM and NDMI further supports the interpretation that the wetlands and adjacent riparian zones retain moisture and continue to support surface water-groundwater interactions, even during the dry season.

5.2 Fountainhill Estate Catchments

The data analysed was obtained at 15-minute intervals; however, it was aggregated daily to match the rainfall data. These results are presented in the section below.

5.2.1 Daily Water Quality

Figure 5-26 presents EC and rainfall data from the monitoring Probe 1 site over the duration of monitoring (November 2020 to May 2021). This site is located downstream of agricultural land south of Wartburg.

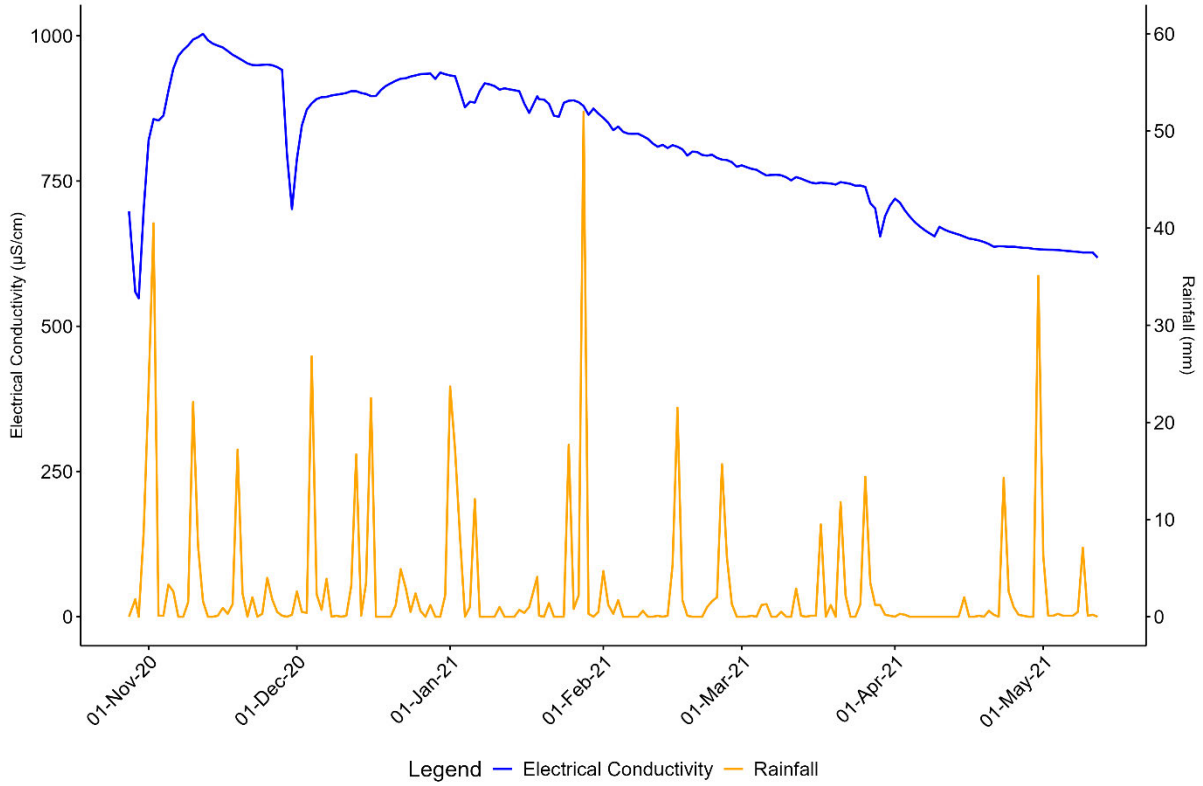

Figure 5-26: EC data for Probe 1 (inlet)

Electrical conductivity (EC) values at Probe 1 range from approximately 620.9 µS/cm to 1007 µS/cm. The highest values were recorded in the early part of the monitoring period, after which the EC began to taper off. Throughout the monitoring period, EC values generally remained elevated, with minor fluctuations and a gradual decreasing trend from January to April 2021. Several rainfall events occurred during this period, including distinct peaks in November, December, early February and late April, but these events had limited impact on EC values. Short-term declines in EC were observed after some rainfall events, but EC typically rebounded quickly. Throughout the EC record, there are two periods that can be seen where the EC values drop precipitously with no rainfall event. The first of these occurred on 28 November 2020 and the second occurred on 28 March 2021. During this period, the EC values dropped to 7 µS/cm and 6 µS/cm respectively. Both events are due to issues in collecting the data wirelessly from the probe, necessitating in the probe needing to be removed from it's casing until the data was manually downloaded. However, due to the daily aggregation, this drop has been smoothed. The ensuing increase in EC values after the probe was returned to its position in the stream is likely due to the probe settling into the sediment that was observed at the bottom of the well.

Figure 5-27 shows the EC for the Probe 2 inlet stream with the largest catchment area outside the estate boundaries. From this figure, the EC values are far higher than expected from a natural stream; however, they are far steadier than the previous site for Probe 1. This could be partly due to the attenuation of stormwater from the dam upstream and the mixing of sources at the confluence upstream of the monitoring site, diluting the EC values.

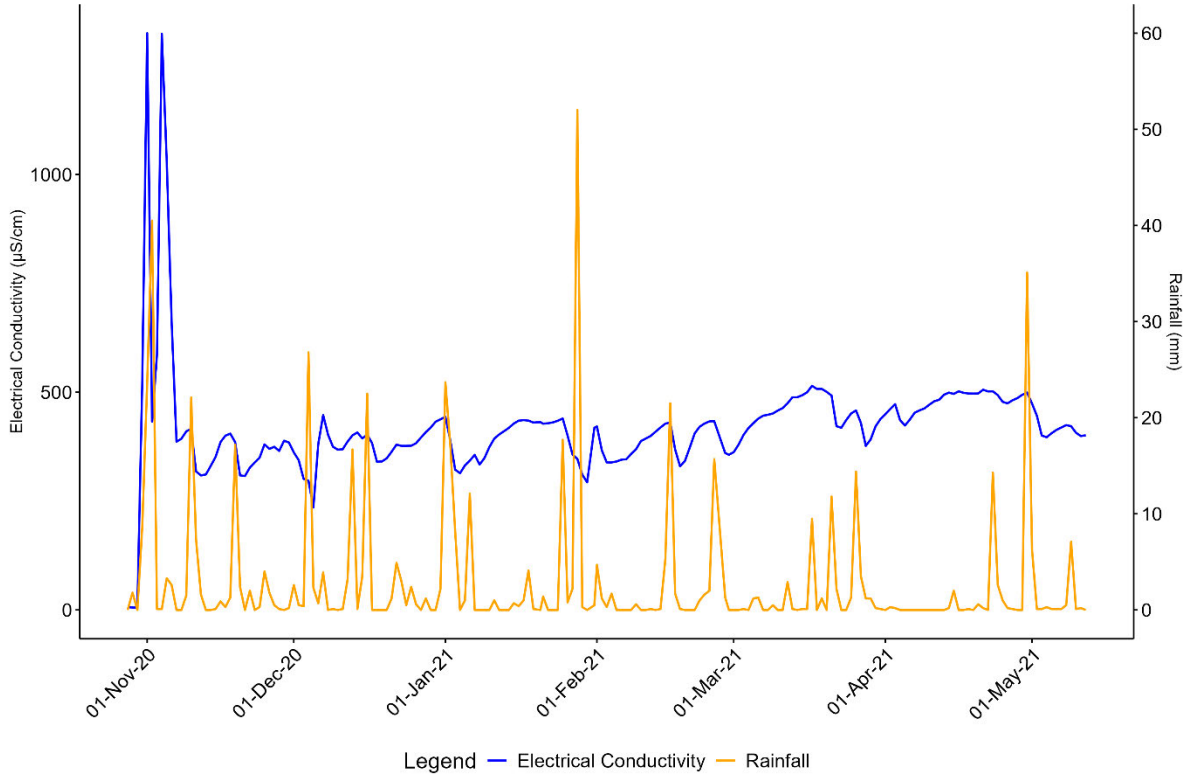

Figure 5-27: EC data for Probe 2 (inlet)

The elevated EC values observed (generally ranging from 250 - 500 µS/cm with occasional spikes ranging up to (1400 µS/cm), suggest that the stream's water chemistry is strongly influenced by ion-rich baseflow. This data and the exhibiting trends highlight the dilution effect the rainfall events have on the subsurface contributions, thereby influencing the stream's EC patterns.

Figure 5-28 presents the EC for Probe 3, located at the inlet stream along the estate boundary downstream of a Eucalyptus plantation. EC values ranged from approximately 71 µS/cm to 200 µS/cm throughout the monitoring period. The data from this site shows a clear and immediate EC response to rainfall events, with sharp declines observed shortly after precipitation peaks. The magnitude of this decline corresponds to the magnitude of the rainfall. These dilution events were typically followed by rapid rebounds in the measured EC levels, returning toward pre-event conditions within a few days.

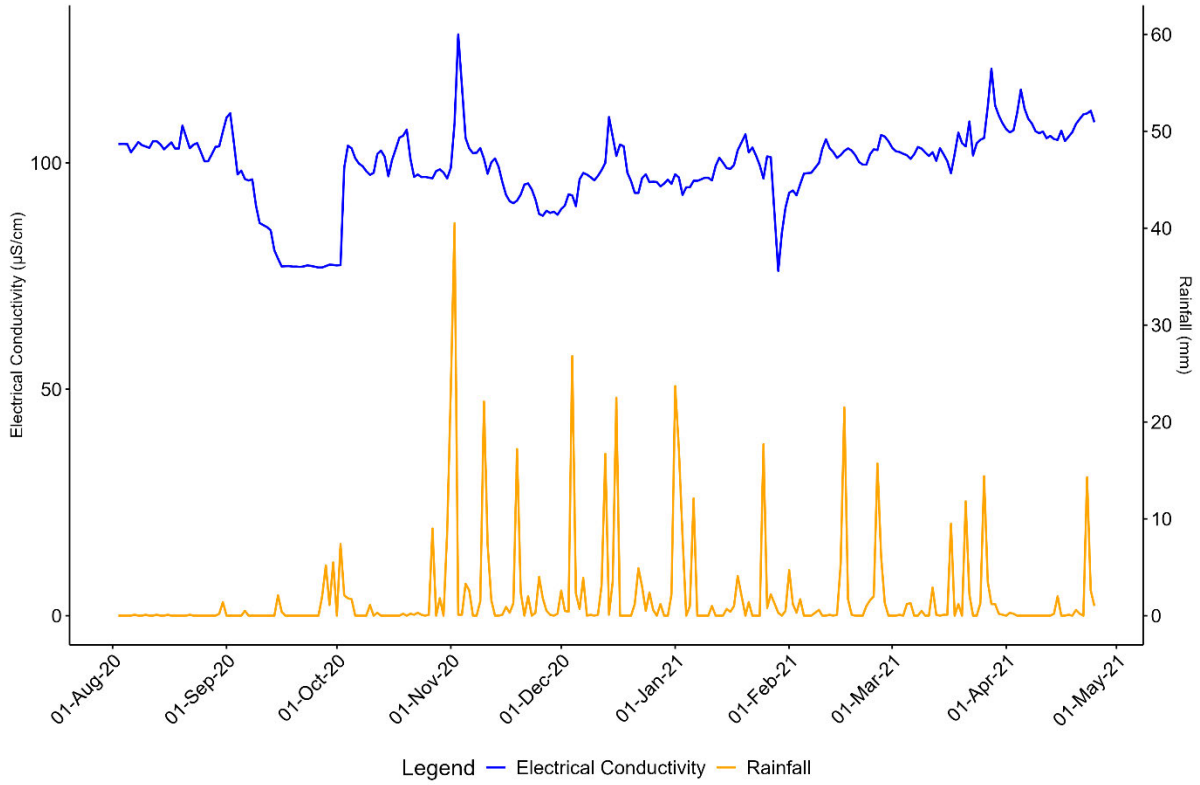

Figure 5-28: EC data for Probe 3 (inlet)

During the wet season, there is a gradual upward trend in EC observed. From January to May 2021, the streamflow's EC levels stabilise around 100 µS/cm, with there being fewer sharp fluctuations observed, and no sustained increase or decrease is evident. Overall, the data from Probe 3 reflect a site that is highly responsive to rainfall events and exhibits the lowest baseline EC values monitored relative to more groundwater-dominated locations in the catchment. For the period of 08 September to 02 October 2020, the EC levels can be seen to be abnormally low, this is likely due to the streamflow ceasing.

Figure 5-29 shows EC and rainfall patterns for Probe 4, located downstream of agricultural lands and upstream reservoirs. Despite its downstream position, where solute concentrations might typically be expected to accumulate, EC values at Probe 4 generally ranged between 286 µS/cm and 492 µS/cm, which were lower than those observed at Probe 1 and Probe 2.

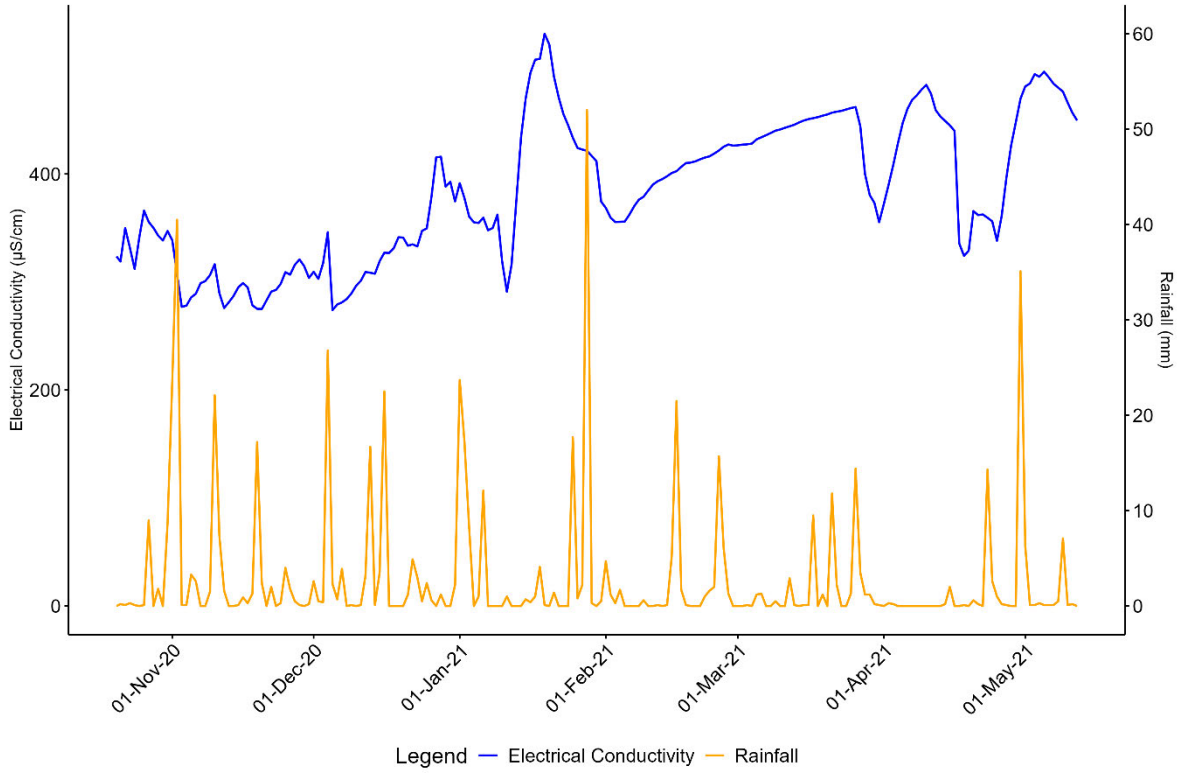

Figure 5-29: EC data for Probe 4 (outlet)

The EC signal at Probe 4 demonstrates clear event-based responses to rainfall. Following several high rainfall events, sharp, short declines in EC were recorded, consistent with dilution by low-conductivity rainfall and surface runoff. These reductions were typically short in duration (less than one day), with EC values rebounding to pre-event levels within hours to days of the event.

Between 9 January and 26 January 2021, a marked increase in EC levels observed (from 280 µS/cm – 542 µS/cm), followed by a sharp decline (542 µS/cm – 472 µS/cm) , with little recorded rainfall. This anomaly suggests the influence of additional water sources such as agricultural runoff or spilling from an upstream reservoir/dam. Additionally, the increase in EC may be a result of evaporation of the stilling pond in which Probe 4 was installed, if the weir is blocked or below the level of spilling. Due to the high level of reeds and other riparian plants growing in the stilling pond, the decomposing plants result in high degrees of organic matter within the pond. A disturbance of this organic matter by an animal in the stilling pond or potentially upstream may have resulted in an accumulation of organic matter and suspended particulate matter at the observation level of the sensor, which may also have resulted in this anomaly. During the latter portion of the wet season (January to March) EC values exhibited an overall increasing trend, with short-term decreases following rainfall events. After three

consecutive rainfall events in late March 2021 resulted in a sharp decrease in EC (from 463.5 µS/cm to 302.1 µS/cm), likely due to dilution from event water, the following increase may be a result of older water from upstream reservoir storage reaching capacity and spilling into the streamflow.

Compared to upstream probes, Probe 4 displayed less variability in EC and the magnitude of dilution events appeared more subdued. This pattern suggests a greater degree of buffering or mixing along the flow path between upstream sources and this downstream location. The lower overall EC values may reflect dilution from upstream tributaries or storage elements (e.g. wetlands, reservoirs) that reduce solute concentrations through mixing or settling processes before water reaches Probe 4.

Figure 5-30 presents the EC and rainfall patterns recorded at Probe 6, a site situated within a stagnant water body that lacks significant upstream or downstream flow connectivity. The stagnant nature of this portion of the site has a profound effect on the water chemistry of this site. The EC values at this location range broadly between 0 µS/cm to 844.1 µS/cm. These consistently elevated values reflect the cumulative effects of evaporative enrichment, nutrient accumulation and the limited flushing capacity inherent to stagnant systems. Rainfall events led to temporary dilution, followed by rapid rebounds in EC.

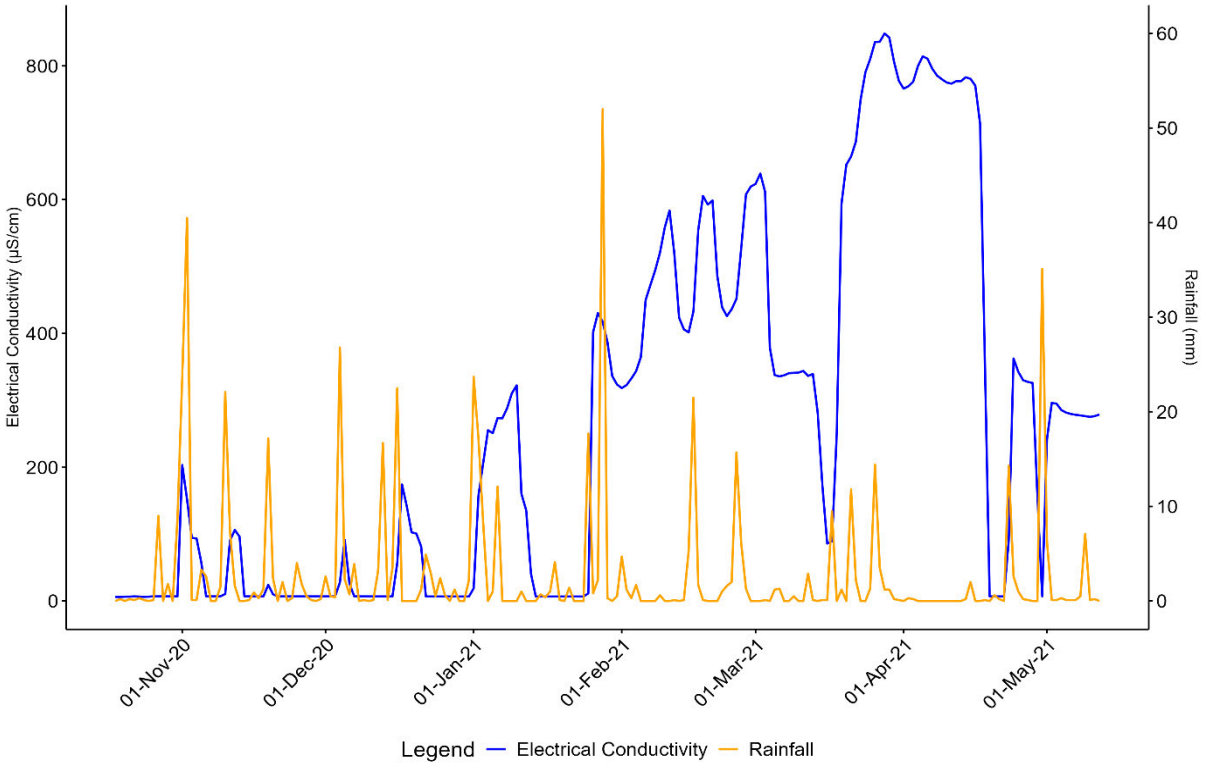

Figure 5-30: EC data for Probe 6 (inlet)

Figure 5-31 presents monthly EC measurements recorded at each of the monitoring sites across FHE (Probe 1 through Probe 6) over the period of monitoring (beginning in August/September 2020, depending on the probe's specific installation date, to May 2021) prior to the loss of the equipment due to extreme rainfall events. Clear seasonal patterns are evident, with higher EC values observed in the wet season and transition into the dry season (November 2020 to March 2021). This trend suggests the water with high EC values was introduced from shallow subsurface groundwater flows as well as agricultural and urban stormwater runoff during wetter periods.

When comparing the probes, distinct differences in EC behaviour are apparent. The lowest EC values (< 100 µS/cm) are consistently measured by Probe 3 throughout the duration of the monitoring. This trend indicates contributions from water sources with shorter residence times, such as shallow groundwater or localised recharge regions that undergo minimal enrichment. However, Probe 6 shows the greatest degree of fluctuation of all the probes, often fluctuating between 0 during dry seasons and 844.1 µS/cm during the wet season. This variability is due to its location within an urban stormwater and seepage-dominated channel that frequently dries out during low rainfall periods (refer to Section 5.2.1).

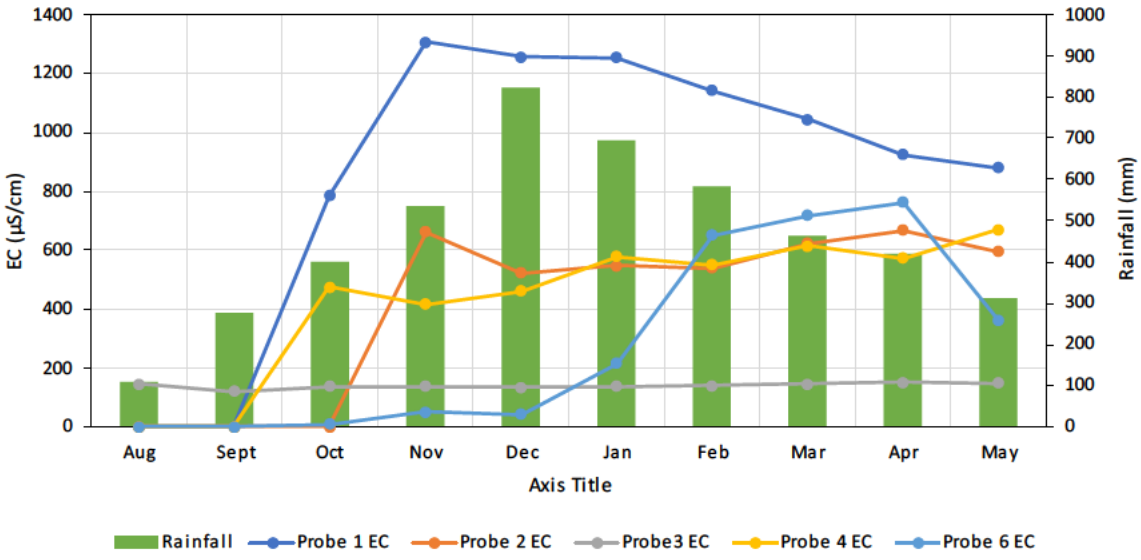

Figure 5-31: Monthly EC values for each probe with the monthly rainfall

5.2.2 OPTRAM model

When performing the preliminary analysis to determine the method of regression line generation that fits the data best, the linear regression was found to be unsuitable (Figure 5-34).

When assessing the exponential regression line method, it was found to perform better. The results of this analysis are presented in Figure 5-33.

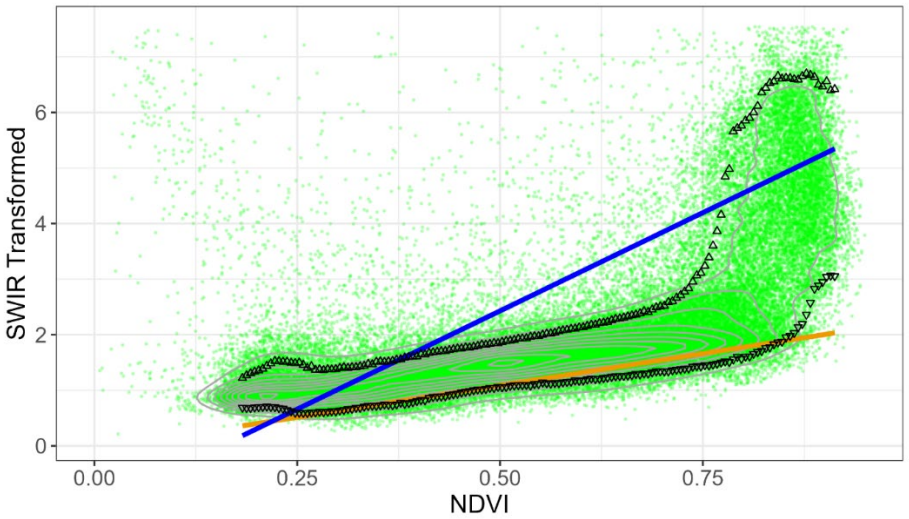

Figure 5-32: FHE linearly fitted trapezoid plot showing the NDVI against the SWIR transformed values

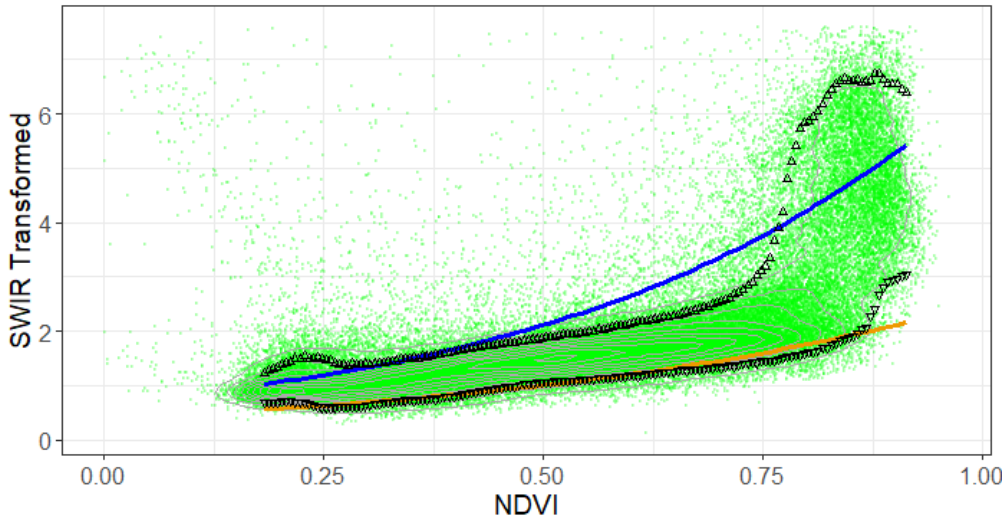

Figure 5-33: FHE exponentially fitted trapezoid plot showing the NDVI against the SWIR transformed values

Figure 5-34 depicts the spatial distribution of soil moisture across the upper catchments of the FHE during the dry season of 2024, as derived from Sentinel-2 satellite imagery using the OPTRAM model. The maps below also delineate the estate boundaries, inflow subcatchments and monitoring probe locations and names.

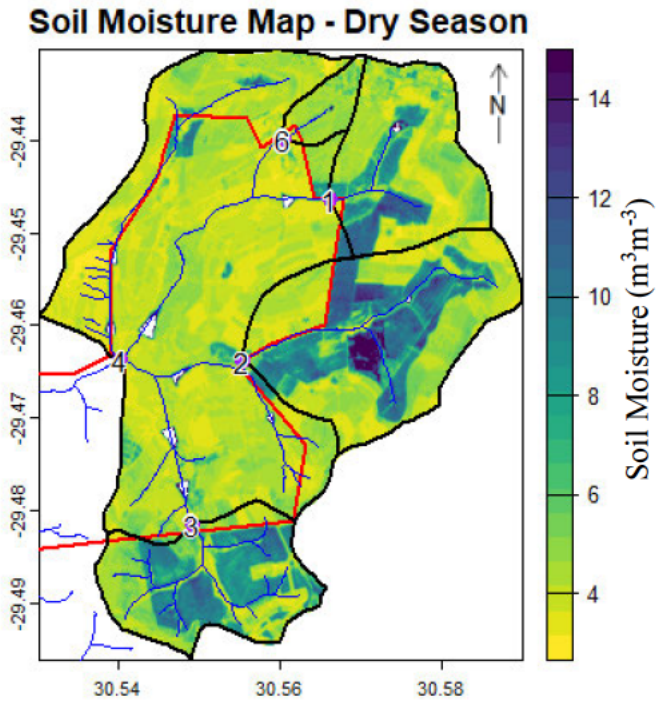

Figure 5-34: Map of the soil moisture for the dry season across FHE upper catchments

During the dry season (Figure 5-34) the soil moisture levels are low (<5.5 $m^3.m^{-3}$) throughout most of the upper portions of the estate, as shown by the lighter colours. However, the nearby and neighbouring farms can be seen to have elevated soil moisture levels compared to those inside the estate boundaries, as shown by the blue to green colours. This is particularly true of the fields upstream of Probes 1, 2 and 3. Whilst Probe 4 doesn't show any definitively highlighted sources, the dams can be seen just upstream of the site on each of the tributaries. These dams are thought to act as buffers and storage for most of the event-generated runoff and streamflow.

Figure 5-35 shows soil moisture for the wet season, derived from the OPTRAM model. When compared to the dry season, the wet season soil moisture values are all elevated, the majority of values across the estate being above 6, as shown by green and blue shades. This is particularly evident in the lower portions of the catchment and around tributaries, suggesting widespread moisture accumulation due to seasonal rainfall. The previously dry zones in the dry season show expected increases in soil moisture, while consistently wetter zones upstream of Probes 1, 2 and 3 remain relatively more saturated. Additionally, areas adjacent tothe farm dams and along the western boundary display a notable rise in moisture levels, indicating potential runoff capture and soil infiltration during wetter periods.

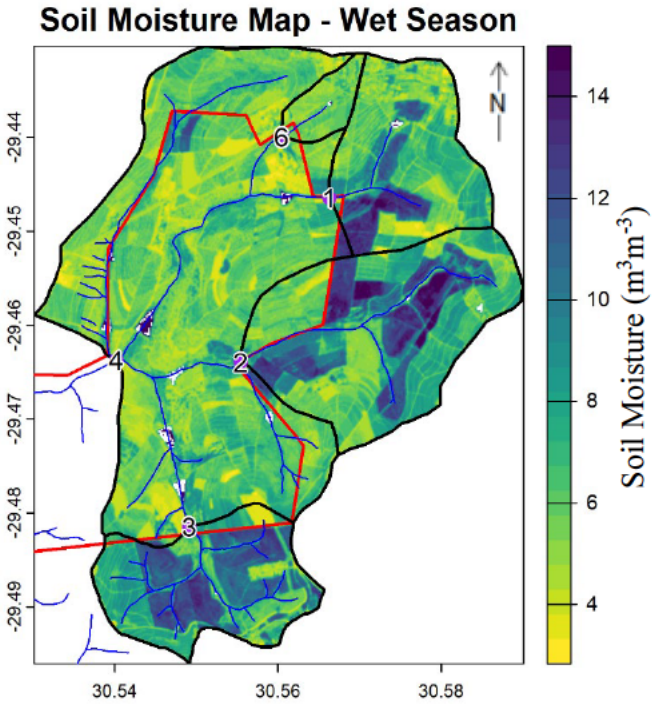

Figure 5-35: Map of the soil moisture for the wet season across FHE upper catchments

Figure 5-36 presents the NDMI for the dry season period. This indicates spatial heterogeneity in surface moisture, with slightly negative values (between -0.2 – 0) dominating most of the estate, suggesting vegetation experiencing moisture stress or bare soil conditions. Localised areas of higher NDMI, especially along the tributaries and upstream of Probes 1 and 2, align with areas of higher soil moisture observed in the OPTRAM results, reinforcing the indication of localised wet zones, likely due to irrigation.

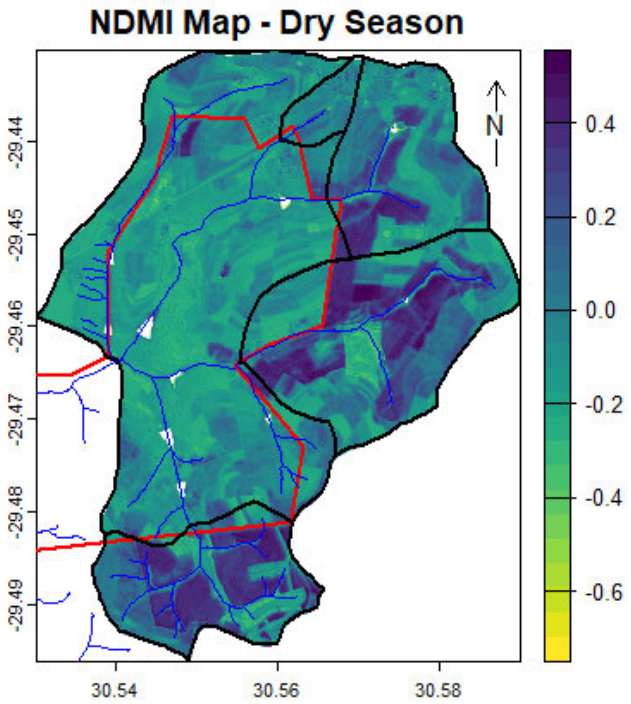

Figure 5-36: Map of the NDMI for the dry season across FHE upper catchments

Figure 5-37 presents the NDMI for the wet season period. When the wet season results are compared to the dry season results, most of the values can be seen to have increased to positive values. This increase in the values within the bounds of the estate indicates a reduction in the moisture stress. The generally higher NDMI values, especially on the banks and fields above the tributaries, align with areas of higher soil moisture observed in the OPTRAM results. This indicates that the vegetation in these areas have benefited from improved moisture conditions, likely due to increased precipitation and potential lateral water contributions from adjacent terrain or water-retaining features such as dams.

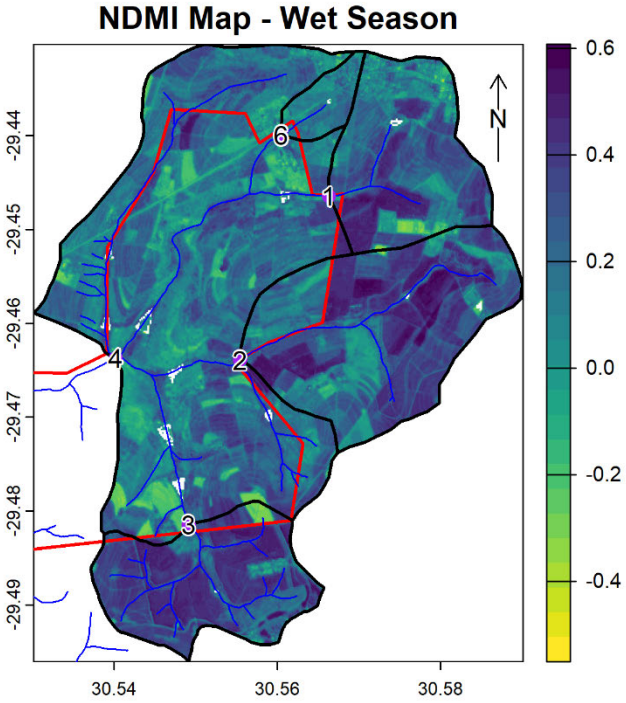

Figure 5-37: Map of the NDMI for the wet season across FHE upper catchments

5.2.3 Hydropedology

The hydropedological map created as a result of the desktop hydropedological study is presented below in Figure 5-38. This map was created using the soil form map and the soil depth map provided by FHE, refer to Figure 3-19 and Figure 3-20 respectively. As the soil study was done before the start of this study and a published paper could not be found on the survey, general hydropedological classes for the soil forms were used. These were obtained from van Tol and Bouwer (2024). In the event of a soil form belonging to two or more potential hydropedological classes, the soil's location relative to geological and hydrological features, its position on the slope and the depth of the soil were considered to determine the most likely class it belonged to.

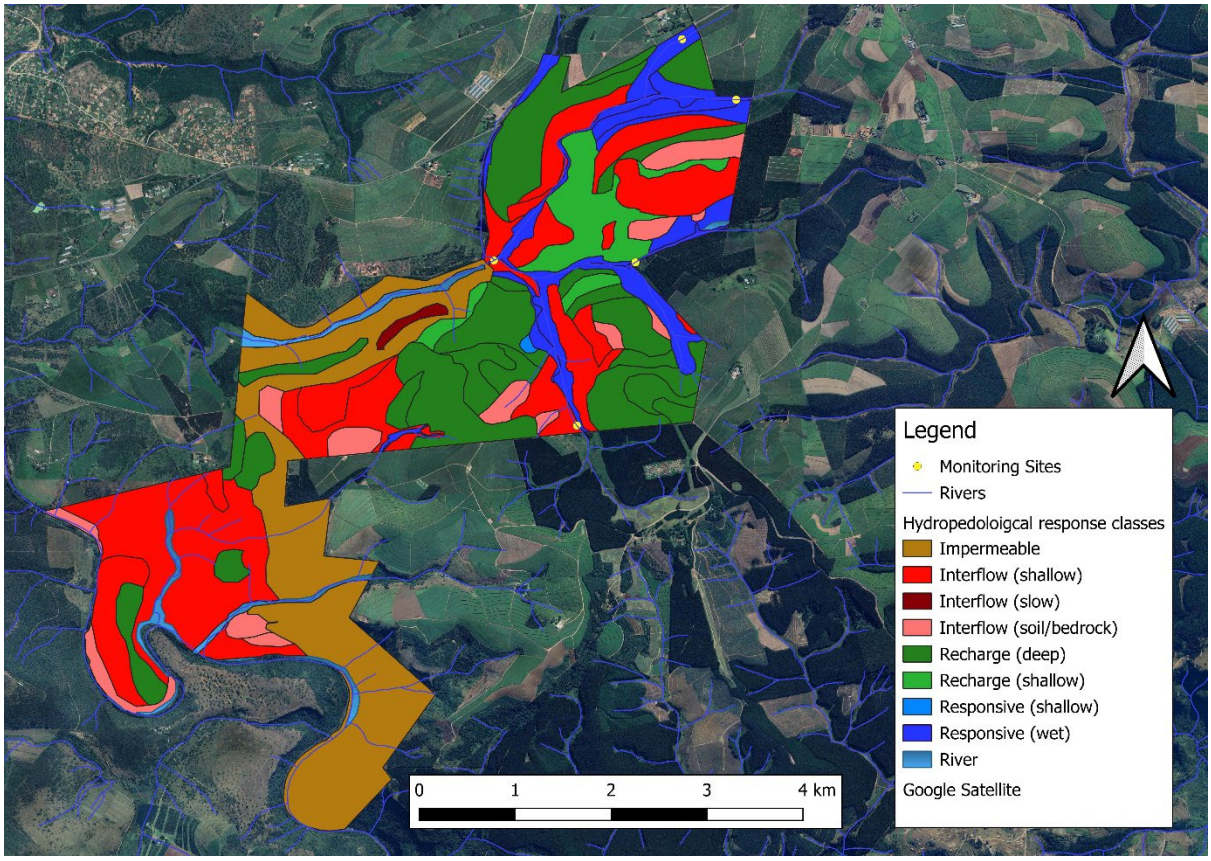

Figure 5-38: FHE hydropedological map

DISCUSSION

This chapter presents and compares the findings from the two study sites from the previous chapter. These sites differ in their topography, climate, land use, soil properties and location in the primary catchment. Understanding how land use and land use changes influence hydrological responses is one of the key focuses of this chapter. Through comparing the results from the previous chapter, we focus on emphasising the differences in the dynamics of surface water and groundwater exchange that are taking place within each catchment, and how they are affected by various factors.

6.1 Flow Path Dynamics and Subsurface Connectivity

6.1.1 CP Catchment 6

The CP Catchment 6 monitoring results show a hydrological system where the rainfall events, the wetland storage and the subsurface processes strongly influence the surface water-groundwater interactions.

The event-based monitoring revealed distinct differences in streamflow responses to rainfall events from the wet season and transition to the dry season (late wet season). The event-based rainfall and streamflow sampling of the December 2023 rainfall event showed an apparent dilution effect across all measured parameters in response to rainfall. This resulted from the rapidly generated stormwater runoff reducing the EC levels in the streamflow. These values were then seen to recover over a period of two days as groundwater contributions, enriched with higher EC values, became the dominant source. The results of the monitoring conducted for the April 2024 rainfall event indicated that rainfall thresholds for runoff generation were not met, with EC levels remaining stable due to limited surface runoff and a predominance of groundwater inputs. These observations suggest that streamflow in Catchment 6 during high-intensity rainfall events is temporarily dominated by surface water contributions, which rapidly transition back to groundwater-fed streamflow following the end of the rainfall event.

Event-based monitoring in CP Catchment 6 showed clear seasonal variability in the streamflow responses to rainfall, showing the changes in the dominant hydrological pathways. During the December 2023 event, 28.2 mm of rainfall was received, triggering rapid stormflow generation, evident in the dilution of electrical conductivity (EC), which dropped from 95 μS/cm to the minimum EC value of 80 μS/cm within three and a half hours. Simultaneously, the streamflow isotopic signatures closely aligned with meteoric water (average event rainfall values of δ^2H =

-8.6 ‰, $\delta^{18}O$ = -3.5 ‰), indicating a direct and rapid hydrological connection between rainfall and streamflow.

The stable isotope analysis further refined the understanding of hydrological flow paths. The first day's streamflow closely resembled the characteristics of the meteoric water. This trend indicates that there is a rapid hydrological connectivity between rainfall and the streamflow generated. Over the subsequent days, contributions from older subsurface and wetland water became pronounced, indicative of buffering effects (Uhlenbrook *et al*., 2005) within Wetland 1 and Wetland 2. These contributions begin within four hours of the rainfall event commencing. This was followed by the chemical and isotopic composition of the streamflow, which began to reflect contributions from older water sources, particularly wetland and subsurface stores, as EC gradually recovered to 93 µS/cm and isotopic signatures shifted toward more depleted values ($\delta^{2}H$ = -12.8 ‰, $\delta^{18}O$ = -3.4 ‰) over the course of two days, consistent with groundwater and wetland contributions. These dynamics suggest the reassertion of baseflow contributions (seen in the EMMA, Section 5.1.3) and were consistent with hydrological processes such as capillary fringe mobilisation and groundwater ridging (Sklash and Farvolden, 1979; Waswa and Lorentz, 2015).

In contrast, the April 2024 event, characterised by lower rainfall depths (2.8 mm rainfall total), did not meet runoff generation thresholds. This is consistent with a system where groundwater and wetland sources dominate flow during low-intensity precipitation events (Spencer *et al*., 2021; Kebede *et al*., 2021). EC values remained relatively stable throughout the event (between 94 µS/cm – 98 µS/cm) and isotopic signatures indicated persistent contributions from wetland-modified water sources ($\delta^{2}H$ = -14.8 ‰, $\delta^{18}O$ = -3.8 ‰), with minimal input from recent precipitation. This suggests limited surface runoff and a sustained dominance of older groundwater and wetland stores.

The high degree of responsiveness measured during the events could be attributed to a variety of factors. The first of these is the steeper slope (> 25°) of the upper reaches of the catchment compared to the lower reaches (< 15°). This, coupled with steep banks on either side of the tributaries, increases the runoff generated and a short time for it to be converted to streamflow. The steep slope in the upper portions of the catchment contributes to faster stormflow travel times and a reduction in storage volume in the wetland system (Tetzlaff et al., 2014; Lazo et al., 2019; Harrison et al., 2022). These effects are further intensified during more significant rainfall events, when changes in shallow subsurface conditions and increased overland flow

enhance hydrological responses. Such conditions promote greater connectivity between different hydropedological soil groups, facilitating more efficient lateral water movement. This increased connectivity is consistent with groundwater ridging processes, which play a key role in generating and sustaining stormflow. The shallow recharge regions also align with the fill and spill mechanism proposed as the shallow aquifers spoken about are often depressions in the underlying bedrock. These fill during a rainfall event until reaching a maximum capacity, after which they release water as subsurface and this results in greater interflow generated. This increase in the flow generated contributes to the stormflow peaks (Geris and Tetzlaff, 2015; van Tol *et al*., 2010; Tetzlaff *et al*., 2014). The relationship between the topography and the flow generated by the hydropedological soil groups was documented for Catchment 6 by Harrison *et al.*, (2022). Harrison *et al*., (2022) found that the middle wetland shown in Figure 3-3 remained saturated for longer when compared to other wetlands in the Cathedral Peak research catchments with a gentler slope and a concave catchment shape (Harrison *et al*., 2022). This may be due to capillary rise or from depressions in the underlying bedrock that continue to contribute to the wetland for a period of time after the wet season. The regolith may also be responsible as it may act as a "sponge" that retains water whilst slowly releasing it, which may take longer to be released during the dry season. These results support previous tracer-based studies indicating that rapid streamflow responses can be predominantly driven by groundwater contributions, rather than solely by surface runoff (Sklash and Farvolden, 1979; Jones *et al*., 2006; Klaus and McDonnell, 2013). This study also aligns with the findings of the study conducted by Jones *et al*. (2006) where the groundwater contributions were close to 75%.

The results presented in previous sections (Section 5.1) agreed with Tetzlaff *et al*., (2014). Tetzlaff *et al*. (2014) found that the baseflow within the stream network consists primarily of pre-event water, with more significant rainfall events increasing contributions from the wetland systems to the stream network; however, it was found that the groundwater remained the dominant contributor.

The long-term monitoring of EC and water temperature across CP Catchment 6 shows clear spatial patterns and seasonal dynamics indicative of consistent baseflow inputs and hydrological connectivity. These trends indicate that most of the catchment streamflow is dominated by subsurface and groundwater-fed sources, with some important distinctions between key hydrological features.

Across the upper reaches of the catchment (the tributaries, Wetland 1 and the tributary confluence) the EC values remained relatively stable throughout the monitoring period,

generally ranging between 100–120 µS/cm. This narrow range suggests that these sites are fed by chemically similar and well-mixed groundwater sources, likely derived from common geological formations and weathering processes within the catchment (see Section 3.1.4). The chemical similarity supports the notion of a high degree of hydrological connectivity among these upstream sites, with baseflow contributions maintaining the ionic composition year-round (Winter *et al*., 1998).

Wetland 2, however, consistently exhibited lower EC values (75–90 µS/cm), distinguishing it as the most chemically unique site in the system. Several mechanisms could account for this difference, including biogeochemical processing within the wetland (e.g., plant uptake), dilution from surface storage and longer water residence times promoting ion adsorption to sediments (Reddy *et al*., 2003). The role of Wetland 2 as a chemical buffer or filter is consistent with wetland systems studied in other papers (Kadlec and Wallace, 2009; Mander *et al*., 2017), where it contributes to the attenuation of ionic loads before discharge at the downstream weir.

The EC values at the weir occasionally exceeded those of Wetland 2, particularly during August–November 2023 and March 2024. This pattern suggests intermittent inputs of higher EC water, potentially from deeper groundwater sources with longer residence times, or from surface runoff and subsurface seepage occurring downstream of Wetland 2. These findings highlight the significance of localised flow paths and episodic contributions that can influence stream chemistry, even beyond major hydrological control points like wetlands. While often difficult to capture in water balance models, such contributions are critical during baseflow-dominated periods and reflect the complex interactions between surface and subsurface hydrological processes (Wels *et al*., 1991; Stieglitz *et al*., 2003, Tetzlaff *et al*., 2007).

Rainfall EC measurements showed a large degree of variation during the monitoring period, ranging from as low as 10 µS/cm in late 2023 to greater than 40 µS/cm by mid-2024. The normally low EC is expected for high-altitude sites like Cathedral Peak, where rainfall is a result of relatively clean atmospheric sources (Weathers and Likens, 1997). The observed increase in rainfall EC through the 2024 dry season may be a result of increased dust or pollutants in the atmosphere (Likens and Bormann, 1974). During the period of June–July 2024, a sharp increase can be seen in the rainfall's EC measurement along with elevated rainfall temperatures, potentially resulting from convective storm activity and atmospheric washout.

In terms of water temperature, most sampling sites exhibited modest fluctuations, typically ranging between 10–18 °C. This low degree of variation indicates strong thermal buffering, a

common characteristic of hydrological systems dominated by groundwater inflow (Constantz, 1998). These systems display thermally stable discharge, as opposed to systems dominated by surface runoff, which closely follow the ambient air temperature. The similarity in temperature trends across the three tributaries and Wetland 1 further supports the argument for efficient hydrological mixing and shallow subsurface contributions. These sites closely match the rainfall temperature trends, highlighting the rapid response to recharge events and the limited thermal lag existing between these systems.

By contrast, the downstream components of the catchment, Wetland 2 and the weir, recorded consistently lower water temperatures. This was particularly apparent during the summer months when upstream locations, the tributaries and Wetland 1, warmed more noticeably than the downstream locations. This cooling effect may result from discharge from deeper groundwater sources or longer residence times within Wetland 2. This allows for greater thermal equilibration with ambient soil and subsurface conditions. The downstream location of the weir, combined with shading and reduced solar exposure as a result of the surrounding mountains and banks (Story *et al*., 2003; Zierl *et al*., 2007), likely contributes to the consistently lower temperatures observed there.

Two anomalously high rainfall temperature readings (exceeding 25 °C) were recorded in July 2024. These could result from a variety of reasons, such as sensor exposure errors, calibration drift or the warming of shallow rain collectors under transient warm air conditions. In the event that these temperatures are not due to an error, it may be due to convective storm events, albeit rare during winter, highlighting the importance of sensor validation and contextual weather data in interpreting hydroclimatic signals.

Together, the long-term EC and temperature records underscore the dominance of groundwater and shallow subsurface processes in sustaining streamflow throughout CP Catchment 6. They also illustrate the important role of wetlands in modulating both the chemical and thermal signatures of water, particularly Wetland 2, which exhibits buffering effects distinct from upstream systems. These findings highlight not only the spatial complexity of source contributions but also the seasonal variability driven by rainfall characteristics and antecedent moisture conditions.

The long-term monitoring also demonstrated stable isotopic signals attributed to meteoric origin and dominance by shallow or intermediate-depth groundwater, further highlighting the buffering roles of wetlands and subsurface systems. The long-term stable isotope data show

that the majority of samples cluster near the Global Meteoric Water Line (GMWL). This indicates that the meteoric origin for most water sources within the catchment has a minimal evaporative fractionation under typical conditions. Tributaries demonstrate variable isotopic signatures based on their specific hydrological dynamics. For example, Tributary 1 displays minimal isotopic modification during both wet and dry seasons, suggesting rapid runoff generation and shorter water residence times. Tributary 2 exhibits greater mixing with pre-event water stored in shallow subsurface zones, emphasising slower flow paths and increased evaporative fractionation during dry seasons. Tributary 3 relies heavily on older stored water sources, featuring isotopic depletion and long residence times, particularly during the dry season.

Wetlands play distinct roles in modulating isotopic composition and streamflow. Wetland 1, as a mixing zone, prominently incorporates rainfall-derived water during wet seasons while showing evaporative enrichment during drier conditions due to longer retention times. Wetland 2, on the other hand, acts as a long-term storage reservoir with significant contributions from isotopically depleted groundwater and minimal evaporative influence. These contrasting roles of the two wetlands highlight the spatial complexity of wetland contributions to streamflow.

Long-term monitoring across various catchment locations consistently reinforces the dominance of groundwater-derived baseflow, which buffers the seasonal isotopic variability. This stability helps sustain streamflow during dry seasons and maintains consistent isotopic signals throughout the catchment.

In comparison to the dynamic short-term responses observed in event-based sampling, the long-term isotope trends emphasize the resilience of CP Catchment 6's hydrological system. The stable contributions from groundwater and wetlands mitigate the impacts of seasonal rainfall variability, ensuring consistent baseflow conditions throughout the year. These insights align with findings from Spencer *et al.* (2021) and Kebede *et al.* (2021), which emphasize the stabilizing role of subsurface storage systems and wetlands in sustaining streamflow. However, the unique hydrological configuration of CP Catchment 6, particularly the roles of its wetlands and the pronounced connectivity of Tributary 1, sets it apart from other high-altitude catchments studied in the literature.

The integration of ^{222}Rn tracing and remote sensing soil moisture modelling (OPTRAM and NDMI) provides novel insights into the subsurface connectivity and dominant hydrological flow paths in CP Catchment 6. These tools enable a spatially explicit interpretation of

groundwater–surface water exchange processes, highlighting the role of variable terrain, geology and wetland function in shaping lateral and vertical flow dynamics.

The ^{222}Rn sampling results revealed distinct spatial differences in groundwater contributions across the catchment. The highest ^{222}Rn concentrations were observed at the weir (393 ± 59 Bq/m³ in water), strongly indicating sustained and cumulative baseflow input from the broader catchment area. Elevated air concentrations of ^{222}Rn (481 ± 73 Bq/m³) suggest active degassing during stream discharge, affirming the presence of deeper, long-residence-time groundwater that had accumulated ^{222}Rn through extended contact with bedrock or soil (Burnett and Dulaiova, 2012; Gilfedder *et al*., 2015). This aligns well with isotopic and EC signals observed at the weir during dry seasons, where baseflow dominance was previously established.

In contrast, the lowest ^{222}Rn concentrations were recorded at Wetland 1 (110 ± 30 Bq/m³ in water), supporting its role as a surface water mixing zone with minimal direct groundwater input. The topographic steepness of the tributaries feeding Wetland 1 likely enhances turbulent flow and degassing before water reaches the wetland, thus further reducing detectable ^{222}Rn levels. This interpretation is consistent with event-based isotope and EC results that showed rapid rainfall-runoff connectivity through the tributaries and a delayed but sustained contribution from wetland and subsurface stores.

Intermediate ^{222}Rn concentrations in the eastern (242 ± 47 Bq/m³ in water) and mid (230 ± 46 Bq/m³ in water) tributaries revealed important distinctions in subsurface flow paths. The relatively higher and equilibrium-like air and water ^{222}Rn levels in the eastern tributary suggest contributions from a deeper or more stable groundwater source, possibly a perched aquifer or fracture flow system. This is further supported by its isotopic depletion during dry seasons, indicating the presence of older water with limited evaporative influence. In contrast, the mid-tributary appears to reflect a combination of shallow interflow and shorter residence groundwater, contributing more dynamically to Wetland 1.

Remote sensing via OPTRAM and NDMI confirmed and expanded these interpretations, especially in highlighting lateral and near-surface flow processes. During the wet season, the OPTRAM-derived soil moisture maps showed widespread high moisture levels across the catchment, with particularly saturated zones extending from the southern plateau into the tributary headwaters. These patterns suggest the operation of lateral subsurface connectivity, including saturation-excess overland flow and fill and spill mechanisms contributing to catchment wetting. This is consistent with field-based observations of rising streamflow and

EC recovery after storm events, indicating activation of shallow groundwater pathways (Sklash and Farvolden, 1979; Tromp-van Meerveld and McDonnell, 2006).

During the dry season, OPTRAM and NDMI both showed moisture retention within the wetlands and valley bottom zones, affirming their role as hydrological buffers. These areas maintained elevated soil and vegetation moisture levels while the surrounding uplands dried, underscoring the wetlands' contributions to baseflow via capillary rise or shallow groundwater discharge. Notably, the southern plateau maintained higher dry-season soil moisture, likely sustained by shallow perched water tables or localised upwelling. These findings reinforce interpretations from temperature and EC trends showing persistent wetland influence and groundwater baseflow at the weir.

The spatial agreement between high NDMI values and OPTRAM-inferred soil moisture hotspots supports the presence of sustained root-zone water availability, indicating that surface water-groundwater interactions persist even in the dry season. Such agreement between two independent proxies strengthens the assertion that flow path dynamics in CP Catchment 6 are shaped by a combination of topographic controls, wetland buffering and lateral subsurface connectivity.

Overall, the ^{222}Rn and remote sensing data provide strong corroboration of the processes inferred from EC, isotopes and temperature data. They reveal a hydrological system that is not only spatially heterogeneous but also responsive to seasonal dynamics, where tributary headwaters, wetland zones and valley bottoms exhibit unique, but integrated, flow path behaviours. These findings highlight the need for multi-method approaches in complex catchments where both vertical (deep vs. shallow groundwater) and lateral connectivity determine streamflow generation and resilience to rainfall variability.

6.1.2 Fountainhill Estate

Across all sites, EC values exceed those expected for natural, unimpacted streams (30–150 µS/cm; Edokpayi *et al*., 2018), implicating anthropogenic and subsurface contributions as key drivers of water quality.

Probe 1, located in an area surrounded by intensive agriculture and near human settlements, displayed the highest and most variable EC values (620.9 – 1006.6 µS/cm). These elevated levels suggest sustained inputs of dissolved ions from fertiliser use, soil disturbance, irrigation return flow and potentially greywater discharges from the nearby town (Kumar and Puri, 2012). The site is dominantly influenced by baseflow and lateral subsurface inputs rather than surface

runoff. Clear dilution effects were observed following large rainfall events, which triggered sharp, short-term decreases in EC due to low-conductivity rainwater inflow. However, smaller events often produced limited response, reinforcing the role of antecedent soil moisture and rainfall magnitude in attenuating hydrological pathways (Levy *et al*., 2018). Seasonal EC declines from January to May likely reflect reduced agricultural input and falling groundwater levels post-harvest, with intermittent spikes following rainfall suggesting rewetting-induced solute mobilisation (Scanlon *et al*., 2002).

Probe 2, situated on a tributary with the largest upstream catchment outside the estate, exhibited a more stable EC baseline (250–500 µS/cm), with periodic spikes up to 1400 µS/cm. The stability suggests a strong and sustained subsurface baseflow contribution, influenced by land use dominated by sugarcane and eucalyptus plantations. These land uses are known to alter infiltration rates and subsurface flow patterns, potentially increasing ionic concentrations through soil water leaching (Scott *et al*., 2005). The periodic EC spikes following rainfall indicate episodic flushing of accumulated salts and nutrients from the plantation soils. Unlike Probe 1, where EC responses to rain are more immediate and volatile, Probe 2's response is more buffered, likely due to deeper infiltration and delayed lateral flow paths through the plantation slopes.

Probe 3, with the lowest EC values (71–199.6 µS/cm), represents a relatively responsive and less mineral-enriched system. Sharp EC declines after rainfall events point to strong surface runoff influence, with rapid post-event recovery suggesting quick drainage and limited residence time. The low baseline EC implies limited subsurface contribution or flow through less mineralised soil/rock pathways (Winter *et al*., 1998). A gradual EC increase during the wet season suggests cumulative solute build-up, while the January to May stabilisation period reflects reduced rainfall intensity and agricultural inputs.

Probe 4, downstream of agricultural fields and upstream of reservoirs, recorded EC values of 286–492 µS/cm. These reflect continuous ion loading from both subsurface flow and occasional overland runoff. Clear EC dilution-rebound cycles were observed following major rainfall events, with fast recoveries pointing to strong subsurface connectivity (Tweed *et al*., 2009). A notable increase in EC during the early wet season, despite rainfall, suggests spillover from upstream reservoirs enriched with solutes and nutrients accumulated during dry seasons (Schilling and Zhang, 2004). The seasonal decline from January to May corresponds with periods of lower fertiliser application rates and groundwater drawdown. This is consistent with

reduced subsurface ion transport. This site shows a mixed system where baseflow, rainfall and dam releases collectively shape water quality.

Probe 6, located in a stagnant water body with minimal hydrological connectivity, presents a contrasting pattern. EC levels ranged widely (0 µS/cm – 844 µS/cm), heavily influenced by evaporation, limited flushing and cumulative nutrient loading. The absence of continuous flow promotes evaporative enrichment and nutrient buildup from agricultural runoff and lateral seepage. Rainfall events occasionally induce sharp EC declines, as the well is flushed as the highly evaporated pre-event water is diluted with event-based runoff, but these are short-lived, with rapid rebounds due to renewed solute accumulation and potential sediment–water interactions (Olden and Naiman, 2010). Seasonal trends show the dry season as a period of intensified EC due to evaporation and nutrient concentration, while wet-season inputs temporarily dilute but do not sustainably flush the system. Anaerobic conditions and internal biogeochemical cycling further contribute to elevated EC during stagnation.

When comparing the FHE sites, Probe 3 stands out for its low EC and strong rainfall responsiveness, reflecting a less groundwater-dominated, faster-flushing hydrological regime. Probe 6, in contrast, shows the highest variability and sustained solute accumulation due to its isolated, evaporative setting. Probes 1, 2 and 4 all highlight the role of baseflow enriched by agricultural activity, with differing degrees of rainfall buffering and dilution depending on upstream storage and connectivity.

Soil moisture and vegetation indices provide important context for interpreting EC responses. OPTRAM-derived soil moisture maps for the dry season show low moisture (<5.5 $m^3.m^{-3}$) across the estate. Meanwhile, the adjacent farms, especially those that are upstream of Probes 1, 2 and 3, maintain higher moisture, suggesting irrigation or terrain-driven water retention. These patterns correspond with the elevated EC in these tributaries. During the wet season, widespread soil moisture increases were observed, particularly in lower catchment areas and near dams, consistent with rainfall accumulation and runoff. NDMI results mirror these trends with the dry season values ranging between -0.2 and 0, indicating vegetation moisture stress, while during the wet season, the increases in the NDMI indicate an increase in the water availability and suggest zones of potential runoff capture and lateral flow contributions, particularly near tributary headwaters and reservoir margins.

These findings demonstrate that EC is a powerful integrator of hydrological and land use processes in this system. Stream chemistry reflects not only the influence of immediate rainfall

and flow events but also the legacy of agricultural inputs, groundwater dynamics and landscape connectivity. Understanding these interactions is crucial for managing water quality in smallholder-dominated, agriculturally impacted headwater catchments like those in the Wartburg region.

6.2 Conceptual Models

6.2.1 CP Catchment 6

The CP Catchment 6 monitoring results show a hydrological system where the rainfall events, the wetland storage and the subsurface processes strongly influence the surface water-groundwater interactions. Incorporating long-term monitoring data into the conceptual model highlights the importance of seasonally stable groundwater and wetland contributions in buffering hydrological variability, ensuring sustained streamflow, and influencing isotopic composition across the catchment. A key element of the conceptual model is the critical role of wetlands in regulating catchment hydrology. Wetland 1 exhibited strong evaporative enrichment and mixing with fresher water inputs during wet seasons, but gradually transitioned to a source of solutes during dry seasons due to reduced inflow and evaporative processes. Wetland 2, on the other hand, offered more passive hydrological contributions, serving as a long-term storage reservoir with limited rainfall influence. The piezometer data, although limited, show isotopically stable groundwater contributions from deep recharge zones that provide sustained baseflow during dry conditions. ^{222}Rn monitoring added further evidence of groundwater dominance, showing spatial variability in subsurface inputs. The high ^{222}Rn concentrations at the weir demonstrated significant groundwater contributions sustained through deep bedrock flow paths, while Wetland 1 primarily functioned as a surface-fed mixing zone. Differentiation in ^{222}Rn concentrations between tributaries also underscored variation in flow mechanisms, with the eastern tributary potentially fed by deeper fractures or perched aquifers, while the mid-tributary displayed a mix of shallow interflow and shorter residence-time groundwater.

Using the results from all of the analyses conducted as presented in Section 6.1.1, as well as the previous hydropedology done by Harrison *et al.* (2022), a conceptual map was created for both the wet and dry seasons. These conceptual models are presented below in Figure 6-1.

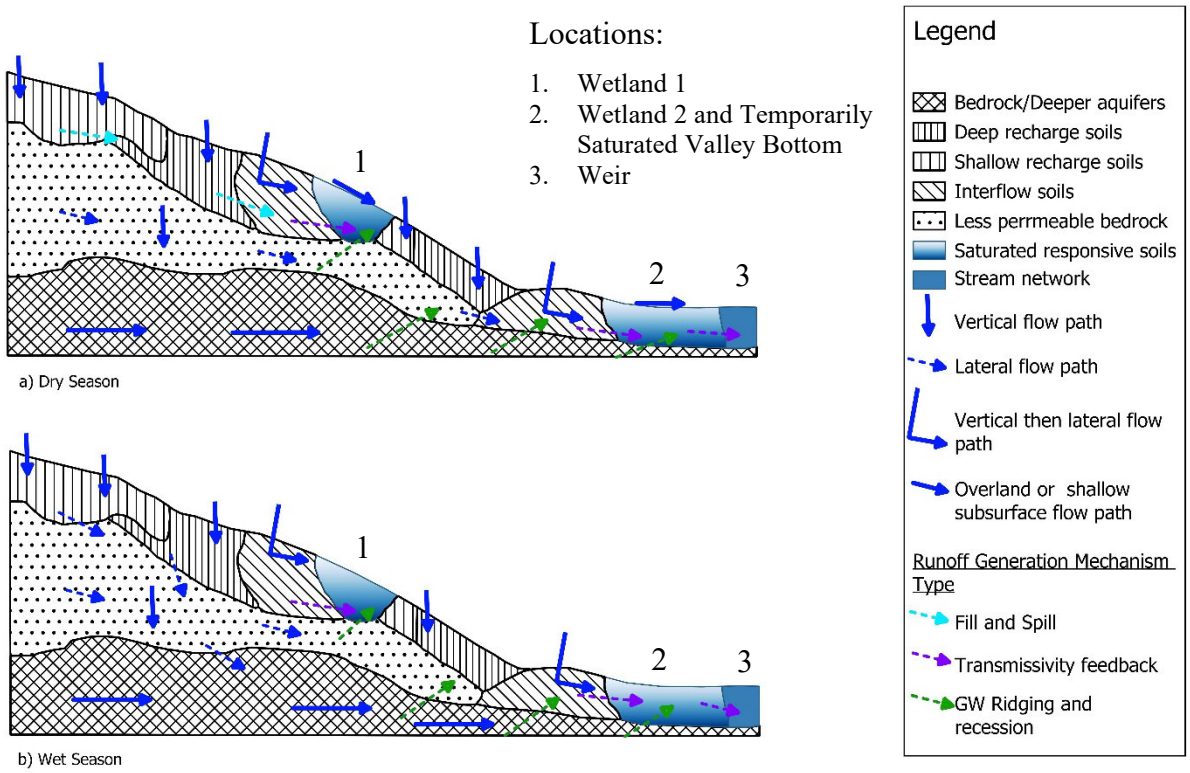

Figure 6-1: CP Catchment 6 conceptual model for the wet and dry season

6.2.2 FHE

From the hydropedological map shown in Figure 5-38, the typical descriptions of soil groups and the typical hillslopes, the conceptual models found below in Figure 6-2 were proposed. The hydropedological interpretations of the two typical hillslopes are as follows: when the precipitation falls in the upper reaches of the catchments studied, it enters into recharge group soils. Depending on the depth of the soil, the water from the deep recharge zones is assumed to enter the bedrock aquifers and travel towards the river. Water generated from the shallow recharge soils moves laterally to the next hydropedological group. The water entering the interflow soils from precipitation is expected to predominantly move along the interface between two horizons, with water from the shallow recharge soils continuing to move laterally along the soil-bedrock interface. In the estate catchments, these soils are often located on the mid-slope between the recharge and responsive soils. The responsive soils make up the majority of the wetlands, often saturated for most of the year. The OPTRAM model results corroborate this. Analysing this distribution of the surface runoff, lateral flow and infiltration will allow for a more holistic understanding of the effect various changes will have on hydrological processes and responses (Windhorst *et al.*, 2014). This will be important when developing water balances as it will allow for better management of the water resources and

modelling of flows within the site. It will also allow for better streamflow inputs to be used in various modelling of the catchment sites

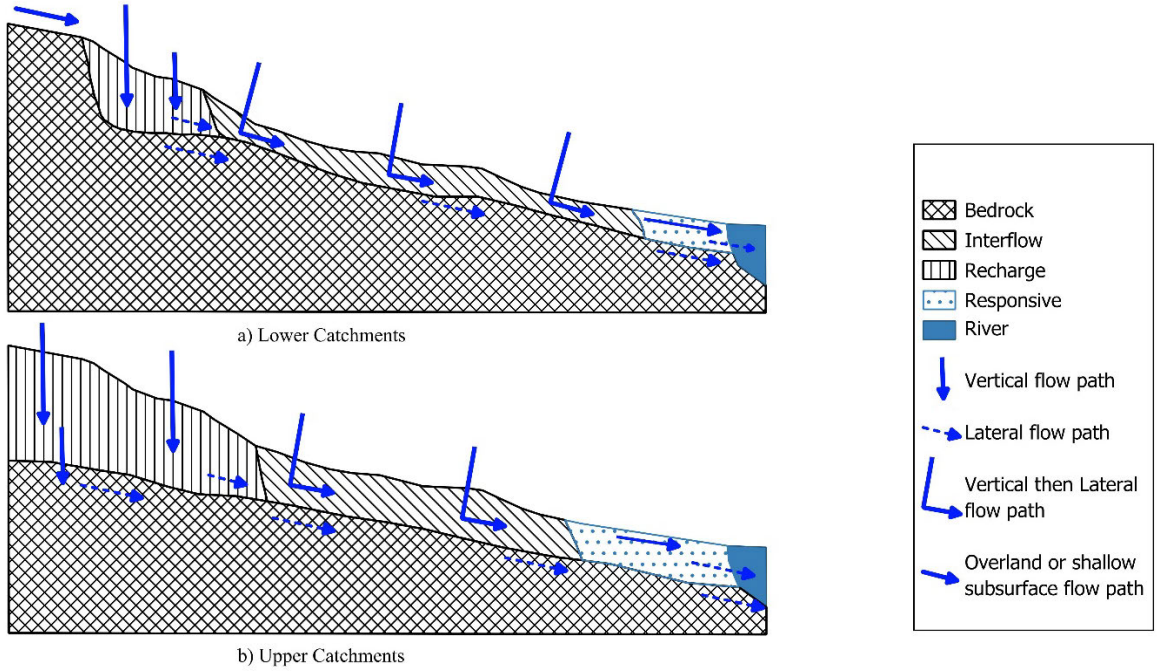

Figure 6-2: FHE upper and lower catchment conceptual models

6.3 Comparison Of Findings from An Agricultural and A Near Pristine Catchment

The hydrological and geochemical differences between CP Catchment 6 and the FHE site underscore the contrasting influence of land use, topography and subsurface connectivity on surface water–groundwater interactions. Both sites are seen to be groundwater-driven hydrological systems. However, the types of groundwater contributions differ due to differences in the type and degree of anthropogenic influences/activities. These differences are also due to their geomorphological contexts.

CP Catchment 6 is situated in a near-pristine, steep montane environment with a maximum slope of 117.2° and is dominated by natural hydrological processes. The EC values of this site generally remain low and stable across most of the monitoring sites throughout the catchment (ranging between 100 µS/cm and 120 µS/cm). This trend indicates dilute groundwater inputs and well-buffered streamflow conditions. Wetland 2, with its consistently low EC values (75 µS/cm and 90 µS/cm), demonstrates long residence times and biogeochemical uptake, buffering stream chemistry during both dry and wet seasons.

In contrast, FHE is a human-impacted agricultural landscape. The measured EC values (especially at Probe 1, where they range between 621 µS/cm and 1007 µS/cm) are elevated to levels far greater than normally found in natural, unimpacted streams (Edokpayi *et al*., 2018) and exhibit a large degree of variation. This indicates inputs from fertiliser use, irrigation return flows and greywater discharge. The sites that lie downstream of sugarcane and eucalyptus plantations show episodic EC spikes post-rainfall, indicating solute flushing from disturbed soils. The seasonal decline in EC following the harvest season suggests a close coupling between land management and subsurface hydrological responses.

Rainfall-driven hydrological responses further illustrate the differences in flow path dynamics. In CP Catchment 6, the steep slopes and shallow soils result in rapid stormflow generation, evident in the December 2023 event, followed by gradual recovery due to groundwater contributions. FHE, by contrast, exhibits variable rainfall responses governed by antecedent soil moisture and land use. The site-specific differences between the FHE monitoring probe sites reflect the heterogeneity introduced by agricultural land modification (compacting of soils due to heavy machinery, tilling of fields, etc.), irrigation systems and flatter terrain.

Both systems are underpinned by significant groundwater contributions. In CP Catchment 6, the deep groundwater flow paths contribute to baseflow year-round. However, in FHE, the groundwater bears a strong anthropogenic signature, enriched with ions leached from agricultural soils. While lateral groundwater movement supports baseflow in tributaries, stagnant regions accumulate solutes over time due to reduced flushing and increased residence time effects.

While CP Catchment 6 currently exhibits near-pristine conditions, historical land use experiments (e.g. burning and afforestation trials since 1945) (Toucher *et al*., 2016; Harrison *et al*., 2022) may have subtly altered soil formation and hydropedology (Harrison *et al*., 2022). These changes influence subsurface connectivity by affecting soil structure, biotic activity and permeability (Phillips *et al*., 2013). In FHE, historic agricultural practices have more visibly altered hydrological properties through tillage, irrigation and landscape modification (Kuzyakov and Zamanian, 2019).

The greatest difference between the two sites is the degree of anthropogenic influence. The natural topography, shallow subsurface pathways and wetland buffering primarily control CP Catchment 6's hydrological responses. In contrast, the FHE site shows a system heavily influenced and modified by agriculture and infrastructure. This finding aligns with broader

findings that agricultural and urban land uses amplify runoff, alter the hydrological flow paths and increase solute loads (Zhang and Schilling, 2006; Hallema *et al*., 2017). Furthermore, the interaction between hydropedology, historical land use and ecosystem functioning is critical to understanding catchment-scale hydrological behaviour (Shafroth *et al*., 2010; Thorp *et al*., 2010).

6.4 Effect of Land Use Changes on Surface Water-Groundwater Interactions

Land use and its transformation over time are critical determinants of surface water–groundwater interactions, as they influence the soil structure, infiltration capacity and biogeochemical pathways within a catchment, thereby altering the hydrological connectivity (Scanlon *et al*., 2007; Sophocleous, 2002). The contrasting characteristics of CP Catchment 6 and FHE show how the natural and anthropogenic processes influence and shape these interactions.

CP Catchment 6 is a benchmark for understanding catchments with a low degree of disturbance. Although historically the research catchments of Cathedral Peak were subjected to experimental land use treatments since the mid-20th century, the catchment has mostly been restored to a near-pristine state (Toucher *et al*., 2016). This promotes well-connected subsurface flow paths through undisturbed soils and hydropedologically active hillslope and wetland dynamics. Subsurface interflow, driven by fill and spill mechanisms and groundwater ridging, dominates streamflow contributions during non-storm periods, with stable EC values and minimal solute accumulation providing evidence of efficient vertical and lateral recharge (Tetzlaff *et al*., 2013; Soulsby *et al*., 2006). Over decades, vegetation and soil structure recovery have restored infiltration rates and buffered surface flow dynamics (Phillips *et al*., 2013).

In contrast, FHE highlights the hydrological consequences of intensive land use and legacy effects from historical agricultural practices. Irrigation, ploughing and afforestation, both on the estate and in the surrounding farms, with deep-rooted non-native species such as *Eucalyptus* species, have altered the soil structure, reducing infiltration capacity in some areas and promoting preferential flow in others. These modifications result in periodic connectivity between the surface and subsurface, with EC signatures at Probes 1 to 3 reflecting strong anthropogenic influence via solute-rich return flows, delayed groundwater responses and shallow interflow after large rainfall events. Additionally, stagnant saturated zones like that of Probe 6 show signs of evaporative enrichment and poor flushing capacity; this is often seen in

disconnected systems under evaporative stress (Foster and Chilton, 2003; Harrison *et al*., 2022).

The spatial variability of land cover at FHE, including sugarcane, pastures and residential areas, produces fragmented hydrological behaviour. Recent studies have shown that land use heterogeneity disrupts subsurface pathways and connectivity, resulting in low recharge and uneven distribution of hydraulic gradients (Hallema *et al*., 2017; Dunjó *et al*., 2004). Additionally, impervious surfaces, such as roads, roofs, cars, parks and soil compaction from heavy machinery in agricultural operations, reduce infiltration, increasing the surface runoff generated during storm events while at the same time limiting the groundwater recharge (Zhang and Schilling, 2006).

The historic effects of land use continue in both catchments, but with different outcomes. In CP Catchment 6, the historical land use experiments may have promoted weathering of the bedrock and pedogenesis via root action, promoting deeper soils and increasing the soil water retention capacity (Kuzyakov and Zamanian, 2019; Phillips *et al*., 2013), whilst at FHE, the continued anthropogenic influences likely hinder the recovery of natural hydropedological function, favouring rapid surface transport of solutes and altered flow paths that short-circuit deeper recharge (Scanlon *et al*., 2007).

These findings are consistent with observations from other studies around the world, which show that land use change can significantly alter the hydrological processes of a catchment, shifting the balance between infiltration, storage and runoff (DeFries and Eshleman, 2004). Agricultural intensification and deforestation have consistently been linked to higher surface runoff coefficients and reduced baseflow contributions in numerous catchments worldwide. Additionally, ecosystems that are subjected to increasing degrees of anthropogenic influence often decrease the resilience of subsurface flow systems, reducing their buffering capacity during extreme rainfall events (Tetzlaff *et al*., 2014; Shafroth *et al*., 2010).

In trying to manage water resources, an important step is the modelling of the catchment to understand how potential changes will affect a catchment. One of the models commonly used for this is the Agricultural Catchments Research Unit (ACRU) model. The ACRU model is a "physical conceptual agrohydrological" model (Clark, *et al*., 2012). The schematic of the model can be seen below in Figure 6-3. As can be seen from this image, the model doesn't account for interflow mechanisms or complex groundwater flow mechanisms. The findings from the study have shown that CP Catchment 6 is a highly complex catchment, and thus, when

trying to use models such as ACRU, challenges are often faced. Whilst hillslope hydrological routing can be used within ACRU, models are often unable to accurately model the groundwater flow mechanisms as they increase in complexity. This highlights the need for modules within hydrological models for the incorporation of groundwater flow mechanisms to increase and improve their representation of the natural system.

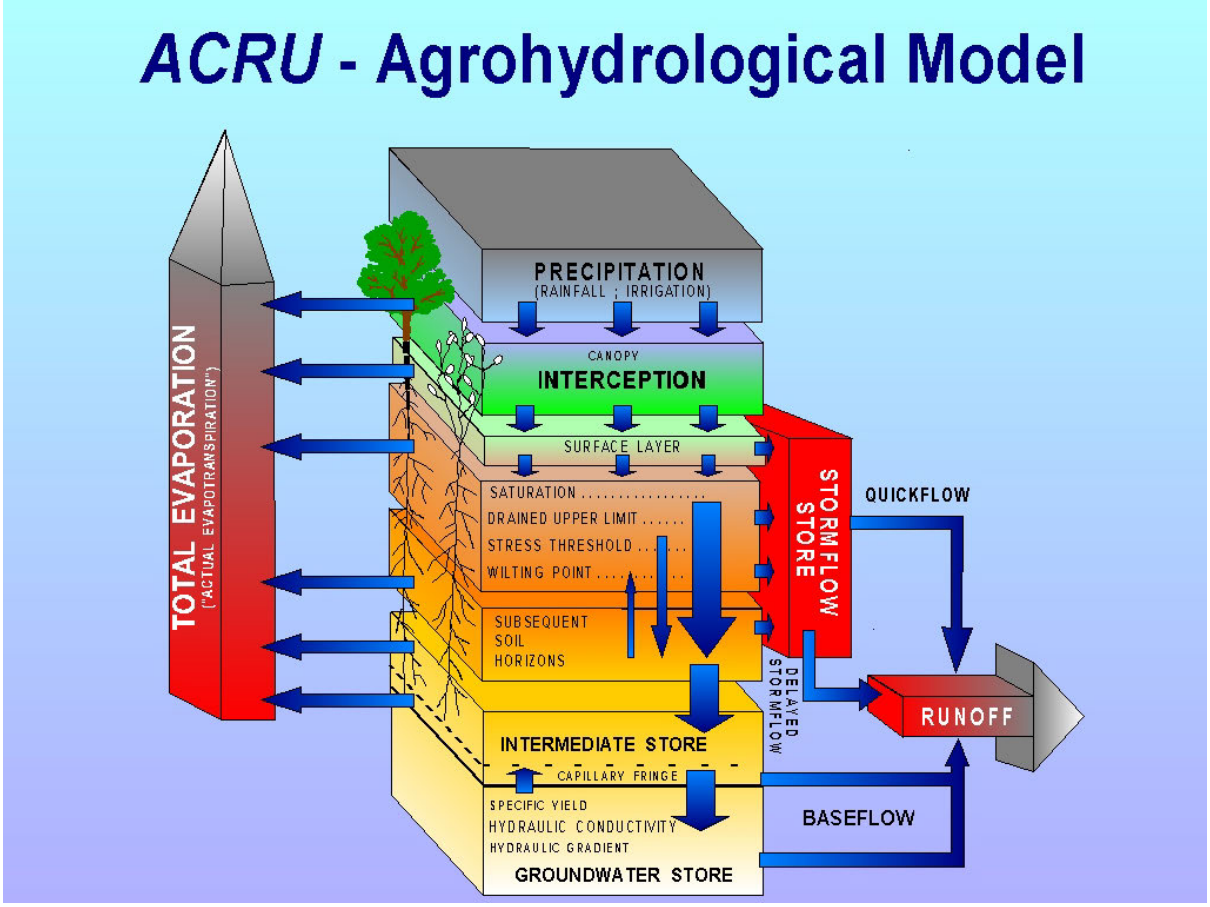

Figure 6-3: ACRU Model Schematic (Clark *et al*., 2012)

6.5 Limitations

While this research contributes to understanding the surface water-groundwater interactions occurring in the upper reaches of the FHE, certain limitations should be acknowledged to contextualise the findings. Due to the extreme rainfall events in 2022, parts of the monitoring network installed by SRK Consulting were destroyed or damaged. This resulted in a large portion of data being lost as it was stored locally on the monitoring probes and had yet to be downloaded for various reasons. It should be noted that whilst the EC was an effective tracer for determining agricultural influences, due to the original intention for the monitoring sites to record and monitor inflows and outflows, the sites did not cover the hillslope scale nor study the internal sources of water.

A further limitation of this research was the fact that the different locations could not be sampled for their stable isotopic compositions. This limitation was imposed because of an injury sustained early in the fieldwork into the Cathedral Peak Research catchments. This injury precluded any further sampling in this area. This could have influenced the extent of the study hence the reliance on existing datasets.

CONCLUSION

This study comprehensively examines surface water–groundwater interactions and hydrological processes in two contrasting South African catchments. These sites are the near-pristine CP Catchment 6 in the Drakensberg Mountains and the agriculturally impacted FHE near Wartburg. By combining hydrometric data, environmental tracers (electrical conductivity, stable isotopes and ^{222}Rn), remote sensing (the OPTRAM model and the NDMI index) and hydropedological assessments, this research advances understanding of how topography, land use and subsurface characteristics govern hydrological connectivity, flow generation and water quality.

At CP Catchment 6, the steep slopes, natural vegetation and well-connected wetlands allow for a hydrologically efficient system with rapid stormflow generation and sustained baseflow during dry seasons. Stable isotope data confirmed a consistent meteoric origin of groundwater with minimal evaporative influence. At the same time, ^{222}Rn and EC measurements highlighted the role of subsurface flow paths and groundwater ridging in sustaining streamflow. Wetlands emerged as dynamic buffers, alternating between evaporative enrichment during dry seasons and rapid mixing during storm events, modulating flow and solute transport. These findings validate and extend the conceptual models proposed by Tetzlaff *et al*. (2014) and Harrison *et al*. (2022), underscoring the significance of lateral and vertical subsurface flow mechanisms, including "fill and spill" dynamics. The OPTRAM model effectively mapped recharge zones and lateral flow paths, confirming its utility in montane, data-rich environments.

In contrast, the FHE catchments exhibit hydrological fragmentation due to intensive agricultural land use, including irrigation, soil compaction, fertiliser application and the construction of farm dams. EC data revealed spatially and temporally variable water quality, with episodic solute flushing linked to rainfall events and antecedent moisture conditions. Remote sensing data, coupled with limited in-situ monitoring, was shown to delineate both the seepage zones and subsurface pathways successfully. Farm dams were found to both buffer the water quality fluctuations and alter natural flow regimes. The desktop hydropedological analysis showed that slope position, soil type and historic land management practices significantly influence infiltration capacity, runoff generation and solute transport, particularly in areas affected by afforestation and historic tillage.

The comparative analysis of CP Catchment 6 and FHE highlights how geomorphology and land use shape hydrological resilience and catchment functioning. CP Catchment 6 exemplifies

robust hydrological connectivity supported by natural gradients and wetland buffering, while FHE illustrates disrupted flowpaths, reduced infiltration and increased surface runoff due to anthropogenic alteration. Wetlands at CP Catchment 6 act as active hydrological buffers, whereas those at FHE often function as stagnant solute-accumulating zones with limited flushing capacity.

These findings have important implications for hydrological modelling and water resource management. In montane catchments like CP Catchment 6, models must incorporate interflow, fractured bedrock pathways and dynamic wetland-groundwater exchanges. Existing frameworks such as ACRU require refinement to include these processes explicitly. In agriculturally modified systems like FHE, modelling approaches must account for land use legacy effects, altered infiltration dynamics and spatially variable connectivity.

This research demonstrates the value of integrated, multidisciplinary approaches, combining field observations, environmental tracers, remote sensing and hydropedology for characterising catchment-scale hydrological processes. It emphasises the need for long-term monitoring and targeted interventions such as soil restoration, wetland rehabilitation and improved irrigation practices to enhance sustainability. In the context of growing pressures from land use change and climate variability, such insights are critical for developing resilient water management strategies across South Africa's diverse and dynamic landscapes.

7.1 Recommendations

Given the scope and time constraints of this Master's thesis, several opportunities exist for expanding and refining future work. A longer observation period, coupled with sustained monitoring at both study sites, is essential to enhance the understanding of surface water–groundwater interactions under varying climatic and land use conditions.

At CP Catchment 6, continued high-resolution monitoring of streamflow using stable isotopes and ^{222}Rn is recommended. Increasing the temporal resolution of sampling, particularly during transitional periods such as the onset and recession of rainfall events, will improve insight into the timing and magnitude of groundwater and wetland contributions to streamflow. In addition, incorporating soil water sampling for stable isotopes and other tracers (e.g. EC, chloride or dissolved organic carbon) would help to characterize the vadose zone and quantify hillslope seepage and lateral flow pathways. This could significantly improve our understanding of the fill and spill dynamics and the partitioning of rainfall between overland flow, interflow and recharge.

For the FHE site, the reestablishment and expansion of the sensor network, both spatially and across different landscape positions, would facilitate a more comprehensive delineation of flow paths and hydrological responses across land use types. Such an approach would also improve the estimation of water budgets and enable more robust hydrological modelling. Additional focus on soil moisture dynamics, infiltration rates and shallow groundwater levels would support efforts to evaluate the impacts of land management practices such as irrigation, tillage and afforestation.

Future research should also aim to refine the understanding of wetland functioning, particularly in relation to biogeochemical processes such as nutrient cycling, solute retention and organic matter dynamics. These factors are critical in determining the water quality buffering role of wetlands. Furthermore, deep groundwater contributions remain insufficiently characterized at both sites. Targeted borehole drilling, geophysical surveys and deeper groundwater sampling would support a more complete conceptual model of catchment-scale hydrology, especially in steep, fractured montane environments like CP Catchment 6.

7.2 Contributions of this research

The research presented in this dissertation formed a component of a Water Research Commission (WRC) Project (C2022/2023-00892) titled "Adding surface water groundwater interaction dimension in runoff generation studies and in catchment water management practices using isotope tracers". This research addressed the following aims and research questions.

Aims:

- To identify sources and pathways of the surface and near-surface (vadose zone) water and groundwater and contributions to normal, high and low flows using stable isotopes,
- To provide an understanding of the mechanisms governing the movement of surface, vadose zone water and groundwater in contributing hillslopes; and
- To update and improve the current conceptual models of the groundwater flows that exist in the catchment studied.

Research Questions:

- Does groundwater play a vital role in generating stormwater and low flows? If so, what is the mechanism of the flow?
- What is the role of land use changes/alterations in impacting the runoff generation mechanisms?

This research identified and validated existing flow paths through the use of a variety of methods both individually and combined. The study was also able to confirm that groundwater is a vital component in the baseflow of the Cathedral Peak all year round, whilst seasonal contribution did vary with changes to rainfall. For the FHE, the study was able to validate the use of EC as a tracer when identifying agricultural runoff and seepage sources, with the coupled use of the OPTRAM model as a qualitative tool requiring little calibration when determining flow paths. The study also sought to update current conceptual models for both sites and, using the data available, was able to generate hillslope conceptual flow models for the FHE in the absence of existing models, whilst for the CP Catchment 6, the current conceptual models were validated as the data confirmed the flow paths.

REFERENCES

Abdul, A.S. and Gillham, R.W., 1984. Laboratory studies of the effects of the capillary fringe on streamflow generation. Water Resources Research, 20(6), pp.691-698.

Abdul, A.S. and Gillham, R.W., 1989. Field studies of the effects of the capillary fringe on streamflow generation. Journal of Hydrology, 112(1-2), pp.1-18.Barbieri, M., 2019. Isotopes in hydrology and hydrogeology. Water, 11(2), p.291.

Allen, M., Babiker, M., Chen, Y., De Coninck, H., Connors, S., Van Diemen, R., Dube, O., Ebi, K., Engelbrecht, F. and Ferrat, M., 2018. Summary for policymakers global warming of 1.5 C: an IPCC special report on the impacts of global warming of 1.5 C above pre-industrial levels and related global greenhouse gas emissions pathways, in the context of strengthening the global response to the threat of climate change. World Meteorological Organization, pp.1-24.

Babaeian, E., Sadeghi, M., Franz, T.E., Jones, S. and Tuller, M., 2018. Mapping soil moisture with the OPtical TRApezoid Model (OPTRAM) based on long-term MODIS observations. Remote Sensing of Environment, 211, pp.425-440.

Barichievy, K.R., 2020. Map number 2020/SLM. Department of Agriculture and Rural Development.

Barichievy, K.R., 2020. Map number 2020/SDM. Department of Agriculture and Rural Development.

Barsch, D. and Caine, N., 1984. The nature of mountain geomorphology. Mountain Research and Development, pp.287-298.

Barthel, R., 2014. HESS Opinions" Integration of groundwater and surface water research: an interdisciplinary problem?". Hydrology and Earth System Sciences, 18(7), pp.2615-2628.

Barthold, F.K., Tyralla, C., Schneider, K., Vaché, K.B., Frede, H.G. and Breuer, L., 2011. How many tracers do we need for end member mixing analysis (EMMA)? A sensitivity analysis. Water Resources Research, 47(8).

Benettin, P., Rodriguez, N.B., Sprenger, M., Kim, M., Klaus, J., Harman, C.J., Van Der Velde, Y., Hrachowitz, M., Botter, G., McGuire, K.J. and Kirchner, J.W., 2022. Transit time estimation in catchments: Recent developments and future directions. Water Resources Research, 58(11), p.e2022WR033096.

Bertrand, G., Siergieiev, D., Ala-Aho, P. and Rossi, P.M., 2014. Environmental tracers and indicators bringing together groundwater, surface water and groundwater-dependent

ecosystems: importance of scale in choosing relevant tools. Environmental earth sciences, 72, pp.813-827.

Beven, K. and Germann, P., 2013. Macropores and water flow in soils revisited. Water Resources Research, 49(6), pp.3071-3092.

Birkel, C. and Soulsby, C., 2016. Linking tracers, water age and conceptual models to identify dominant runoff processes in a sparsely monitored humid tropical catchment. Hydrological Processes, 30(24), pp.4477-4493.

Bischoff-Mattson, Z., Maree, G., Vogel, C., Lynch, A., Olivier, D. and Terblanche, D., 2020. Shape of a water crisis: Practitioner perspectives on urban water scarcity and 'Day Zero'in South Africa. Water Policy, 22(2), pp.193-210.

Boano, F., Harvey, J.W., Marion, A., Packman, A.I., Revelli, R., Ridolfi, L. and Wörman, A., 2014. Hyporheic flow and transport processes: Mechanisms, models, and biogeochemical implications. Reviews of geophysics, 52(4), pp.603-679.

Bonell, M., 1993. Progress in the understanding of runoff generation dynamics in forests. Journal of Hydrology, 150(2-4), pp.217-275.

Bonell, M., Barnes, C.J., Grant, C.R., Howard, A. and Burns, J., 1998. High rainfall, response-dominated catchments: A comparative study of experiments in tropical northeast Queensland with temperate New Zealand. In Isotope tracers in catchment hydrology (pp. 347-390). Elsevier.

Bosch, J. M. (1979). Treatment effects on annual and dry season streamflow at Cathedral Peak. South African Forestry Journal, 108(1), 29-38.

Boulton, A.J., Datry, T., Kasahara, T., Mutz, M. and Stanford, J.A., 2010. Ecology and management of the hyporheic zone: stream–groundwater interactions of running waters and their floodplains. Journal of the North American Benthological Society, 29(1), pp.26-40.

Bourke, S.A., Cook, P.G., Shanafield, M., Dogramaci, S. and Clark, J.F., 2014. Characterisation of hyporheic exchange in a losing stream using radon-222. Journal of hydrology, 519, pp.94-105.

Brammer, D.D., 1996. An evolving perceptual model of hillslopes flow at the Maimai catchment. Advances in Hillslope Hydrology, pp.35-60.

Brodie, R., Sundaram, B., Tottenham, R., Hostetler, S. and Ransley, T., 2007. An overview of tools for assessing groundwater-surface water connectivity. Bureau of Rural Sciences, Canberra, 133.

Bronstert, A., 1999. Capabilities and limitations of detailed hillslope hydrological modelling. Hydrological Processes, 13(1), pp.21-48.

Brunke, M. and Gonser, T., 1997. The ecological significance of exchange processes between rivers and groundwater. Freshwater biology, 37(1), pp.1-33.

Brunner, P., Therrien, R., Renard, P., Simmons, C.T. and Franssen, H.J.H., 2017. Advances in understanding river-groundwater interactions. Reviews of Geophysics, 55(3), pp.818-854.

Burnett, W.C. and Dulaiova, H., 2003. Estimating the dynamics of groundwater input into the coastal zone via continuous radon-222 measurements. Journal of environmental radioactivity, 69(1-2), pp.21-35.

Burnett, W.C., Aggarwal, P.K., Aureli, A., Bokuniewicz, H., Cable, J.E., Charette, M.A., Kontar, E., Krupa, S., Kulkarni, K.M., Loveless, A. and Moore, W.S., 2006. Quantifying submarine groundwater discharge in the coastal zone via multiple methods. Science of the total Environment, 367(2-3), pp.498-543.

Buttle, J.M. and Sami, K., 1992. Testing the groundwater ridging hypothesis of streamflow generation during snowmelt in a forested catchment. Journal of Hydrology, 135(1-4), pp.53-72.

Carlson, T.N., Gillies, R.R. and Perry, E.M., 1994. A method to make use of thermal infrared temperature and NDVI measurements to infer surface soil water content and fractional vegetation cover. Remote Sensing Reviews, 9(1-2), pp.161-173.

Chahinian, N., Moussa, R., Andrieux, P. and Voltz, M., 2005. Comparison of infiltration models to simulate flood events at the field scale. Journal of Hydrology, 306(1-4), pp.191-214.

Chahinian, N., Moussa, R., Andrieux, P. and Voltz, M., 2006. Accounting for temporal variation in soil hydrological properties when simulating surface runoff on tilled plots. Journal of Hydrology, 326(1-4), pp.135-152.

Cherry, J.A. and Freeze, R.A., 1979. Groundwater (p. 370). Englewood Cliffs, NJ: Prentice-Hall.

Chen, Z., Hartmann, A., Wagener, T. and Goldscheider, N., 2018. Dynamics of water fluxes and storages in an Alpine karst catchment under current and potential future climate conditions. Hydrology and Earth System Sciences, 22(7), pp.3807-3823.

Chen, Y., Li, J., Wang, X., Wang, Z., Wei, Y. and Ren, J., 2022. Occurrence characteristics and influencing factors of uranium and radon in deep-buried thermal storage aquifers. Journal of Radioanalytical and Nuclear Chemistry, pp.1-13.

Chetia, T., Baruah, S., Dey, C., Baruah, S. and Sharma, S., 2022. Seismic induced soil gas radon anomalies observed at multiparametric geophysical observatory, Tezpur (Eastern Himalaya), India: an appraisal of probable model for earthquake forecasting based on peak of radon anomalies. Natural Hazards, 111(3), pp.3071-3098.

Christophersen, N. and Hooper, R.P., 1992. Multivariate analysis of stream water chemical data: The use of principal components analysis for the end-member mixing problem. Water resources research, 28(1), pp.99-107.

Clark, D.J., Smithers, J.C., Thornton-Dibb, S.L.C. and Lutchminarain, A., 2012. Deployment, maintenance and further development of SPATSIM-HDSF volume. Water research commission, 1870/2/12.

Cloke, H.L., Anderson, M.G., McDonnell, J.J. and Renaud, J.P., 2006. Using numerical modelling to evaluate the capillary fringe groundwater ridging hypothesis of streamflow generation. Journal of Hydrology, 316(1-4), pp.141-162.

Coles, A.E. and McDonnell, J.J., 2018. Fill and spill drives runoff connectivity over frozen ground. Journal of Hydrology, 558, pp.115-128.

Conant Jr, B., Robinson, C.E., Hinton, M.J. and Russell, H.A., 2019. A framework for conceptualizing groundwater-surface water interactions and identifying potential impacts on water quality, water quantity, and ecosystems. Journal of Hydrology, 574, pp.609-627.

Condon, L.E., Markovich, K.H., Kelleher, C.A., McDonnell, J.J., Ferguson, G. and McIntosh, J.C., 2020. Where is the bottom of a watershed?. Water Resources Research, 56(3), p.e2019WR026010.

Constantz, J., 1998. Interaction between stream temperature, streamflow, and groundwater exchanges in alpine streams. Water resources research, 34(7), pp.1609-1615.

Cook, P.G., 2013. Estimating groundwater discharge to rivers from river chemistry surveys. Hydrological Processes, 27(25), pp.3694–3707.

Cook, P.G., Favreau, G., Dighton, J.C. and Tickell, S., 2003. Determining natural groundwater influx to a tropical river using radon, chlorofluorocarbons and ionic environmental tracers. Journal of Hydrology, 277(1-2), pp.74-88.

Cook, P.G. and Herczeg, A.L. eds., 2012. Environmental tracers in subsurface hydrology.

Craig, H., 1961a. Isotopic variations in meteoric waters. Science, 133(3465), pp.1702-1703.

Craig, H., 1961b. Standard for reporting concentrations of deuterium and oxygen-18 in natural waters. Science, 133(3467), pp.1833-1834.

Craig, H. and Gordon, L.I., 1965. Deuterium and oxygen 18 variations in the ocean and the marine atmosphere, Stable Isotopes in Oceanographic Studies and Paleotemperatures E. In Proceedings of the Third Spoleto Conference, Spoleto, Italy, edited by E. Tongiori (pp. 9-130).

Dansgaard, W., 1964. Stable isotopes in precipitation. tellus, 16(4), pp.436-468.

Dawson, T.E. and Ehleringer, J.R., 1991. Streamside trees that do not use stream water. Nature, 350(6316), pp.335-337.

David, A., Guilbert, N., Hamaguchi, N., Higashi, Y., Hino, H., Leibbrandt, M. and Shifa, M., 2018. Spatial poverty and inequality in South Africa: A municipality level analysis.

DeFries, R. and Eshleman, K.N., 2004. Land-use change and hydrologic processes: A major focus for the future.

Dlamini, L.X., Kotzé, E., Thevenot, M., Feig, G.T., Mathieu, O. and Lévêque, J., 2024. Impact of fire exclusion and aspect on soil carbon fractions in Afromontane grasslands, Cathedral Peak, South Africa. European Journal of Soil Science, 75(4), p.e13528.

Du, E., Jackson, C.R., Klaus, J., McDonnell, J.J., Griffiths, N.A., Williamson, M.F., Greco, J.L. and Bitew, M., 2016. Interflow dynamics on a low relief forested hillslope: Lots of fill, little spill. Journal of Hydrology, 534, pp.648-658.

Dudal, R., 2005. The sixth factor of soil formation. Eurasian Soil Science C/C of Pochvovedenie, 38, p.S60.

Dunjó, G., Pardini, G. and Gispert, M., 2004. The role of land use–land cover on runoff generation and sediment yield at a microplot scale, in a small Mediterranean catchment. Journal of arid environments, 57(2), pp.239-256.

Dunne, T., 1980. Formation and controls of channel networks. Progress in Physical Geography, 4(2), pp.211-239.

Edokpayi, J.N., Odiyo, J.O., Popoola, E.O. and Msagati, T.A., 2018. Evaluation of microbiological and physicochemical parameters of alternative source of drinking water: a case study of nzhelele river, South Africa. The open microbiology journal, 12, p.18.

Ellins, K.K., Roman-Mas, A. and Lee, R., 1990. Using 222Rn to examine groundwater/surface discharge interaction in the Rio Grande de Manati, Puerto Rico. Journal of Hydrology, 115(1-4), pp.319-341.

Elliot, T., 2014. Environmental tracers. Water, 6(11), pp.3264-3269.

EOS Data Analytics (2022). Normalized Difference Moisture Index: Equation And Interpretation. [online] eos.com. Available at: https://eos.com/make-an-analysis/ndmi/.

Everson, C. S., Molefe, G. L., and Everson, T. M. (1998). Monitoring and modelling components of the water balance in a grassland catchment in the summer rainfall area of South Africa. WRC.

Ezugwu, C.N. and Apeh, S., 2017. Groundwater and Surface Water as One Resource: Connectivity and Interaction. IOSR J. Mech. Civ. Eng, 14, pp.54-59.

Feng, X., Faiia, A.M. and Posmentier, E.S., 2009. Seasonality of isotopes in precipitation: A global perspective. Journal of Geophysical Research: Atmospheres, 114(D8).

Forster, C. and Smith, L., 1988. Groundwater flow systems in mountainous terrain: 2. Controlling factors. Water Resources Research, 24(7), pp.1011-1023.

Foster, S.S.D. and Chilton, P.J., 2003. Groundwater: the processes and global significance of aquifer degradation. Philosophical Transactions of the Royal Society of London. Series B: Biological Sciences, 358(1440), pp.1957-1972.

Fountainhill Estate. 2021. Assorted Shapefiles for the Fountainhill Estate. Unpublished spatial dataset. Provided by Fountainhill Estate, KwaZulu-Natal, South Africa.

Freyer, K., Treutler, H.C., Dehnert, J. and Nestler, W., 1997. Sampling and measurement of radon-222 in water. Journal of Environmental Radioactivity, 37(3), pp.327-337.

Friedman, I., Redfield, A.C., Schoen, B. and Harris, J., 1964. The variation of the deuterium content of natural waters in the hydrologic cycle. Reviews of Geophysics, 2(1), pp.177-224.

Fujimoto, M., Ohte, N., Kawasaki, M., Osaka, K.I., Itoh, M., Ohtsuka, I. and Itoh, M., 2016. Influence of bedrock groundwater on streamflow characteristics in a volcanic catchment. Hydrological Processes, 30(4), pp.558-572.

Gao, B.C., 1996. NDWI—A normalized difference water index for remote sensing of vegetation liquid water from space. Remote sensing of environment, 58(3), pp.257-266.

Gat, J.R. and Tzur, Y., 1968. Modification of the isotopic composition of rainwater by processes which occur before groundwater recharge. Weizmann Inst. of Science, Rehovoth, Israel.

Garvelmann, J., Külls, C. and Weiler, M., 2012. A porewater-based stable isotope approach for the investigation of subsurface hydrological processes. Hydrology and Earth System Sciences, 16(2), pp.631-640.

Genereux, D.P., 1998. Quantifying uncertainty in tracer-based hydrograph separations. Water Resources Research, 34(4), pp.915-919.

Genereux, D.P. and Hooper, R.P., 1998. Oxygen and hydrogen isotopes in rainfall-runoff studies. In Isotope tracers in catchment hydrology (pp. 319-346). Elsevier.

Gibert, J., Dole-Olivier, M.J., Marmonier, P. and Vervier, P., 1990. Surface water-groundwater ecotones. The ecology and management of aquatic-terrestrial ecotones, pp.199-225.

Gilfedder, B.S., Frei, S., Hofmann, H. and Cartwright, I., 2015. Groundwater discharge to wetlands driven by storm and flood events: Quantification using continuous Radon-222 and electrical conductivity measurements and dynamic mass-balance modelling. Geochimica et Cosmochimica Acta, 165, pp.161-177.

Gilfedder, M., Rassam, D.W., Stenson, M.P., Jolly, I.D., Walker, G.R. and Littleboy, M., 2012. Incorporating land-use changes and surface–groundwater interactions in a simple catchment water yield model. Environmental Modelling and Software, 38, pp.62-73.

Gioda, A., Mayol-Bracero, O.L., Scatena, F.N., Weathers, K.C., Mateus, V.L. and McDowell, W.H., 2013. Chemical constituents in clouds and rainwater in the Puerto Rican rainforest: Potential sources and seasonal drivers. Atmospheric Environment, 68, pp.208-220.

Girault, F., Perrier, F. and Przylibski, T.A., 2018. Radon-222 and radium-226 occurrence in water: a review. Geological Society, London, Special Publications, 451(1), pp.131-154.

Google. 2024. Google Satellite Imagery. Available at: https://www.google.com/maps (Accessed: 31 May 2025).

Gordijn, P.J., Everson, T.M. and O'Connor, T.G., 2018. Resistance of Drakensberg grasslands to compositional change depends on the influence of fire-return interval and grassland structure on richness and spatial turnover. Perspectives in Plant Ecology, Evolution and Systematics, 34, pp.26-36.

Granger, J. E. (1976). The plant succession and some associated factors in Catchment IX, Cathedral Peak Research Station. PhD, University of Natal, Pietermaritzburg, South Africa.

Gray, B.A., 2017. Towards an improved understanding of the influence of rainguage design, slope and aspect on rainfall measurements: a cross-calibration study (Doctoral dissertation).

Gröning, M., Lutz, H.O., Roller-Lutz, Z., Kralik, M., Gourcy, L. and Pöltenstein, L., 2012. A simple rain collector preventing water re-evaporation dedicated for δ18O and δ2H analysis of cumulative precipitation samples. Journal of hydrology, 448, pp.195-200.Gundersen, L.C. and Wanty, R.B., 2020. Field studies of radon in rocks, soils, and water. CRC Press.

Guswa, A.J., Brauman, K.A., Brown, C., Hamel, P., Keeler, B.L. and Sayre, S.S., 2014. Ecosystem services: Challenges and opportunities for hydrologic modeling to support decision making. Water Resources Research, 50(5), pp.4535–4544.

Hallema, D.W., Sun, G., Caldwell, P.V., Norman, S.P., Cohen, E.C., Liu, Y., Ward, E.J. and McNulty, S.G., 2017. Assessment of wildland fire impacts on watershed annual water yield: Analytical framework and case studies in the United States. Ecohydrology, 10(2), p.e1794.

Harrison, R., van Tol, J. and Amiotte Suchet, P., 2022. Hydropedological Characteristics of the Cathedral Peak Research Catchments. Hydrology, 9(11), p.189.

Hjerdt, K.N., 2002. Deconvoluting the hydrologic response of a small till catchment: Spatial variability of groundwater level and quality in relation to streamflow. State University of New York College of Environmental Science and Forestry.

Holmes, R.M., 2000. The importance of groundwater to stream ecosystem function. In Streams and groundwaters (pp. 137-148). Academic Press.

Hooper, R.P., 2003. Diagnostic tools for mixing models of stream water chemistry. Water Resources Research, 39(3).

Horton, R.E., 1933. The role of infiltration in the hydrologic cycle. Eos, Transactions American Geophysical Union, 14(1), pp.446-460.

Hübner, R., Heller, K., Günther, T. and Kleber, A., 2015. Monitoring hillslope moisture dynamics with surface ERT for enhancing spatial significance of hydrometric point measurements. Hydrology and Earth System Sciences, 19(1), pp.225-240.

Iwagami, S., Tsujimura, M., Onda, Y., Shimada, J. and Tanaka, T., 2010. Role of bedrock groundwater in the rainfall–runoff process in a small headwater catchment underlain by volcanic rock. Hydrological Processes, 24(19), pp.2771-2783.

Jackson, C.R., Bitew, M. and Du, E., 2014. When interflow also percolates: downslope travel distances and hillsclope process zones.

Jewitt, G., 2002. Can integrated water resources management sustain the provision of ecosystem goods and services?. Physics and Chemistry of the Earth, Parts A/B/C, 27(11-22), pp.887-895.

Juan, G., Li, Z., Qi, F., Ruifeng, Y., Tingting, N., Baijuan, Z., Jian, X., Wende, G., Fusen, N., Weixuan, D. and Anle, Y., 2020. Environmental effect and spatiotemporal pattern of stable isotopes in precipitation on the transition zone between the Tibetan Plateau and arid region. Science of the Total Environment, 749, p.141559.

Jung, H., Koh, D.C., Kim, Y.S., Jeen, S.W. and Lee, J., 2020. Stable isotopes of water and nitrate for the identification of groundwater flowpaths: A review. Water, 12(1), p.138.

Kadlec, R.H. and Wallace, S., 2008. Treatment wetlands. CRC press.

Kalbus, E., Reinstorf, F. and Schirmer, M., 2006. Measuring methods for groundwater–surface water interactions: a review. Hydrology and Earth System Sciences, 10(6), pp.873-887.

Kattan, Z., 2008. Estimation of evaporation and irrigation return flow in arid zones using stable isotope ratios and chloride mass-balance analysis: Case of the Euphrates River, Syria. Journal of Arid Environments, 72(5), pp.730-747.

Kebede, S., Charles, K., Godfrey, S., MacDonald, A. and Taylor, R.G., 2021. Regional-scale interactions between groundwater and surface water under changing aridity: evidence from the River Awash Basin, Ethiopia. Hydrological Sciences Journal, 66(3), pp.450-463.

Kebede, S., Hailu, K., Siraj, A. and Birhanu, B., 2023. Environmental isotopes (δ18O–δ2H, 222Rn) and electrical conductivity in backtracking sources of urban pipe water, monitoring the stability of water quality and estimating pipe water residence time. Frontiers in Water, 5, p.1066055.

Kendall, C. and McDonnell, J.J., 1993. Effect of intrastorm isotopic heterogeneities of rainfall, soil water, and groundwater on runoff modeling. IAHS PUBLICATION, pp.41-41.

Kendall, C. and Doctor, D.H., 2003. Stable isotope applications in hydrologic studies. Treatise on geochemistry, 5, p.605.

Kendall, C. and McDonnell, J.J. eds., 2012. Isotope tracers in catchment hydrology. Elsevier.

Kendall KA, Shanley JB, McDonnell JJ. A hydrometric and geochemical approach to test the transmissivity feedback hypothesis during snowmelt. Journal of Hydrology. 1999 Jul 8;219(3-4):188-205.

Kendall, K.A., Shanley, J.B. and McDonnell, J.J., 1999. A hydrometric and geochemical approach to test the transmissivity feedback hypothesis during snowmelt. Journal of Hydrology, 219(3-4), pp.188-205.

Klaus, J. and McDonnell, J.J., 2013. Hydrograph separation using stable isotopes: Review and evaluation. Journal of hydrology, 505, pp.47-64.

Kløve, B., Ala-Aho, P., Bertrand, G., Boukalova, Z., Ertürk, A., Goldscheider, N., Ilmonen, J., Karakaya, N., Kupfersberger, H., Kvœrner, J. and Lundberg, A., 2011. Groundwater dependent ecosystems. Part I: Hydroecological status and trends. Environmental Science and Policy, 14(7), pp.770-781.

Kløve, B., Allan, A., Bertrand, G., Druzynska, E., Ertürk, A., Goldscheider, N., Henry, S., Karakaya, N., Karjalainen, T.P., Koundouri, P. and Kupfersberger, H., 2011. Groundwater dependent ecosystems. Part II. Ecosystem services and management in Europe under risk of climate change and land use intensification. Environmental Science and Policy, 14(7), pp.782-793.

Kollongei, K.J. and Lorentz, S.A., 2014. Connectivity influences on nutrient and sediment migration in the Wartburg catchment, KwaZulu-Natal Province, South Africa. Physics and Chemistry of the Earth, Parts A/B/C, 67, pp.12-22.

Kumar, M. and Puri, A., 2012. A review of permissible limits of drinking water. Indian journal of occupational and environmental medicine, 16(1), pp.40-44.

Kurtz, W., Hendricks Franssen, H.J., Kaiser, H.P. and Vereecken, H., 2014. Joint assimilation of piezometric heads and groundwater temperatures for improved modeling of river-aquifer interactions. Water Resources Research, 50(2), pp.1665-1688.

Kuzyakov, Y. and Zamanian, K., 2019. Reviews and syntheses: Agropedogenesis–humankind as the sixth soil-forming factor and attractors of agricultural soil degradation. Biogeosciences, 16(24), pp.4783-4803.

Land Type Survey Staff, 2003. Land types of South Africa.

Larned, S.T., Gooseff, M.N., Packman, A.I., Rugel, K. and Wondzell, S.M., 2015. Groundwater–surface-water interactions: current research directions. Freshwater Science, 34(1), pp.92-98.

Lazo, P.; Mosquera, G.; McDonnell, J.; Crespo, P. The role of vegetation, soils, and precipitation on water storage and hydrological services in Andean Páramo catchments. J. Hydrol. 2019, 572, 805–819.

Lehmann, P., Hinz, C., McGrath, G., Tromp-van Meerveld, H.J. and McDonnell, J.J., 2007. Rainfall threshold for hillslope outflow: an emergent property of flow pathway connectivity. Hydrology and Earth System Sciences, 11(2), pp.1047-1063.

Lemma, B., Kebede Gurmessa, S., Nemomissa, S., Otte, I., Glaser, B. and Zech, M., 2020. Spatial and temporal 2H and 18O isotope variation of contemporary precipitation in the Bale Mountains, Ethiopia. Isotopes in environmental and health studies, 56(2), pp.122-135.

Levy, M.C., Lopes, A.V., Cohn, A., Larsen, L.G. and Thompson, S.E., 2018. Land use change increases streamflow across the arc of deforestation in Brazil. Geophysical Research Letters, 45(8), pp.3520-3530.

Likens, G.E. and Bormann, F.H., 1974. Acid rain: a serious regional environmental problem. Science, 184(4142), pp.1176-1179.

Liu, F., Wang, S., Wang, L., Shi, L., Song, X., Yeh, T.C.J. and Zhen, P., 2019. Coupling hydrochemistry and stable isotopes to identify the major factors affecting groundwater geochemical evolution in the Heilongdong Spring Basin, North China. Journal of geochemical Exploration, 205, p.106352.

Lorentz, S.A., Thornton-Dibb, S., Pretorius, C. and Goba, P., 2001. Hydrological systems modelling research programme: hydrological processes. Water Research Commission, Pretoria, Report, 637(1), p.01.

Lorentz, S.A., Thornton-Dibb, S., Pretorius, C. and Goba, P., 2004. Hydrological systems modelling research programme: hydrological processes. Water Research Commission, Pretoria, Report, 1086 (1), p.04.

Lorentz, S., Riddell, E.S., Nel, J., Van Tol, J., Fundisi, D., Jumbi, F. and van Niekerk, A., 2020. Groundwater-surface water interactions in an ephemeral savanna catchment, Kruger National Park. Koedoe: African Protected Area Conservation and Science, 62(2), pp.1-14.

Lundin, L., 1982. Soil moisture and ground water in till soiland the significance of soil type for runoff (Doctoral dissertation, Uppsala universitet).

Lundquist, J.D., Pepin, N. and Rochford, C., 2008. Automated algorithm for mapping regions of cold-air pooling in complex terrain. Journal of Geophysical Research: Atmospheres, 113(D22).

Madlala, T., Kanyerere, T., Oberholster, P. and Butler, M., 2021. Assessing the groundwater dependence of valley bottom wetlands in coal-mining environment using multiple environmental tracers, Mpumalanga, South Africa. Sustainable Water Resources Management, 7, pp.1-23.

Mahlangu, S., Lorentz, S., Diamond, R. and Dippenaar, M., 2020. Surface water-groundwater interaction using tritium and stable water isotopes: A case study of Middelburg, South Africa. Journal of African Earth Sciences, 171, p.103886.

Mander, Ü., Tournebize, J., Sauvage, S. and Sánchez-Perez, J.M., 2017. Wetlands and buffer zones in watershed management. Ecological Engineering, 103, pp.289-295.

Marques, A.L., Dos Santos, W. and Geraldo, L.P., 2004. Direct measurements of radon activity in water from various natural sources using nuclear track detectors. Applied radiation and isotopes, 60(6), pp.801-804.

Mazor, E., 2003. Chemical and isotopic groundwater hydrology (Vol. 98). CRC press.

McDonnell, J.J., Sivapalan, M., Vaché, K., Dunn, S., Grant, G., Haggerty, R., Hinz, C., Hooper, R., Kirchner, J., Roderick, M.L. and Selker, J., 2007. Moving beyond heterogeneity and process complexity: A new vision for watershed hydrology. Water Resources Research, 43(7).

McDonnell, J.J., Spence, C., Karran, D.J., Van Meerveld, H.J. and Harman, C.J., 2021. Fill-and-spill: A process description of runoff generation at the scale of the beholder. Water Resources Research, 57(5), p.e2020WR027514.

McDonnell, J.J. and Tanaka, T., 2001. On the future of forest hydrology and biogeochemistry. Hydrological Processes, 15(10), pp.2053-2055.

McGuire, K.J. and McDonnell, J.J., 2006. A review and evaluation of catchment transit time modeling. Journal of Hydrology, 330(3-4), pp.543-563.

McGuire, K.J., Klaus, J. and Jackson, C.R., 2024. Interflow, subsurface stormflow and throughflow: A synthesis of field work and modelling.

Mekonnen, M.M. and Hoekstra, A.Y., 2016. Four billion people facing severe water scarcity. Science advances, 2(2), p.e1500323.

Milly, P.C., Dunne, K.A. and Vecchia, A.V., 2005. Global pattern of trends in streamflow and water availability in a changing climate. Nature, 438(7066), pp.347-350.

Mitsch, W.J. and Gosselink, J.G., 2015. Wetlands. John wiley and sons.

Mohammed, A.M., Krishnamurthy, R.V., Kehew, A.E., Crossey, L.J. and Karlstrom, K.K., 2016. Factors affecting the stable isotopes ratios in groundwater impacted by intense agricultural practices: A case study from the Nile Valley of Egypt. Science of the Total Environment, 573, pp.707-715.

Mucina, L., Rutherford, M.C. and Powrie, L.W., 2006. Vegetation Atlas of South Africa, Lesotho and Swaziland. The vegetation of South Africa, Lesotho and Swaziland, pp.748-789.

Musokwa, M., Mafongoya, P. and Lorentz, S., 2019. Evaluation of agroforestry systems for maize (Zea mays) productivity in South Africa. South African Journal of Plant and Soil, 36(1), pp.65-67.

Nänni, U.W., 1956. Forest hydrological research at the Cathedral Peak research station. Journal of the South African Forestry Association, 27(1), pp.2-35.

Nänni, U. W. (1960). The immediate effects of veld-burning on streamflow in Cathedral Peak catchments. Journal of the South African Forestry Association, 34(1), 7-12.

National Geographic Education. (2023). Surface Water. Retrieved from https://education.nationalgeographic.org/resource/surface-water/ (Accessed August 30 2023).

Ndlovu, M., Clulow, A.D., Savage, M.J., Nhamo, L., Magidi, J. and Mabhaudhi, T., 2021. An assessment of the impacts of climate variability and change in KwaZulu-Natal Province, South Africa. Atmosphere, 12(4), p.427.

Olden, J.D. and Naiman, R.J., 2010. Incorporating thermal regimes into environmental flows assessments: modifying dam operations to restore freshwater ecosystem integrity. Freshwater Biology, 55(1), pp.86-107.

Pachauri, R.K. and Reisinger, A., 2007. Climate change 2007: Synthesis report. Contribution of working groups I, II and III to the fourth assessment report of the Intergovernmental Panel on Climate Change. Climate Change 2007. Working Groups I, II and III to the Fourth Assessment.

Peel, M., Kipfer, R., Hunkeler, D. and Brunner, P., 2022. Variable 222Rn emanation rates in an alluvial aquifer: Limits on using 222Rn as a tracer of surface water–Groundwater interactions. Chemical Geology, 599, p.120829.

Phillips, R.P., Brzostek, E. and Midgley, M.G., 2013. The mycorrhizal-associated nutrient economy: a new framework for predicting carbon–nutrient couplings in temperate forests. New Phytologist, 199(1), pp.41-51.

Popp, A.L., Pardo-Álvarez, Á., Schilling, O.S., Scheidegger, A., Musy, S., Peel, M., Brunner, P., Purtschert, R., Hunkeler, D. and Kipfer, R., 2021. A framework for untangling transient groundwater mixing and travel times. Water resources research, 57(4), p.e2020WR028362.

Reddy, K. and DeLaune, R.D., 2003. Biogeochemistry of wetlands science and applications.

Reddy, K.R., DeLaune, R.D. and Inglett, P.W., 2022. Biogeochemistry of wetlands: science and applications. CRC press.

Riddell, E.S., Nel, J., Van Tol, J., Fundisi, D., Jumbi, F., Van Niekerk, A. et al., (2020), 'Groundwater–surface water interactions in an ephemeral savanna catchment, Kruger National Park', Koedoe 62: https://doi.org/10.4102/koedoe.v62i2.1583

Rouault, M., Roy, S.S. and Balling Jr, R.C., 2013. The diurnal cycle of rainfall in South Africa in the austral summer. International Journal of Climatology, 33(3), pp.770-777.

Rozanski, K., Araguás-Araguás, L. and Gonfiantini, R., 1993. Isotopic patterns in modern global precipitation. Climate change in continental isotopic records, 78, pp.1-36.

Sadeghi, M., Babaeian, E., Tuller, M. and Jones, S.B., 2017. The optical trapezoid model: A novel approach to remote sensing of soil moisture applied to Sentinel-2 and Landsat-8 observations. Remote sensing of environment, 198, pp.52-68.

Sahu, P., Panigrahi, D.C. and Mishra, D.P., 2016. A comprehensive review on sources of radon and factors affecting radon concentration in underground uranium mines. Environmental Earth Sciences, 75, pp.1-19.

Salati, E., Dall'Olio, A., Matsui, E. and Gat, J.R., 1979. Recycling of water in the Amazon basin: an isotopic study. Water resources research, 15(5), pp.1250-1258.

Salih, I.M.M., 2003. Radon in natural waters: analytical methods; correlation to environmental parameters; radiation dose estimation; and GIS applications (Doctoral dissertation, Linköping University Electronic Press).

Scanlon, B.R., Healy, R.W. and Cook, P.G., 2002. Choosing appropriate techniques for quantifying groundwater recharge. Hydrogeology journal, 10, pp.18-39.

Scanlon, B.R., Jolly, I., Sophocleous, M. and Zhang, L., 2007. Global impacts of conversions from natural to agricultural ecosystems on water resources: Quantity versus quality. Water resources research, 43(3).

Schilling, K. and Zhang, Y.K., 2004. Baseflow contribution to nitrate-nitrogen export from a large, agricultural watershed, USA. Journal of Hydrology, 295(1-4), pp.305-316.

Schubert, M., Brueggemann, L., Knoeller, K. and Schirmer, M., 2011. Using radon as an environmental tracer for estimating groundwater flow velocities in single-well tests. Water Resources Research, 47(3).

Schulze, R. E., and George, W. J. (1987). A dynamic, process-based, user-oriented model of forest effects on water yield. Hydrological processes, 1(3), 293-307.

Scott, D.F., Bruijnzeel, L.A. and Mackensen, J., 2005. 25 The hydrological and soil impacts of forestation in the tropics. This page intentionally left blank, p.622.

Seinfeld, J.H. and Pandis, S.N., 2016. Atmospheric chemistry and physics: from air pollution to climate change. John Wiley and Sons.

Shafroth, P.B., Stromberg, J.C. and Patten, D.T., 2002. Riparian vegetation response to altered disturbance and stress regimes. Ecological applications, 12(1), pp.107-123.

Sinergise, S.-H. by (n.d.). Normalized Difference Moisture Index (NDMI). [online] Sentinel-Hub custom scripts. Available at: https://custom-scripts.sentinel-hub.com/sentinel-2/ndmi/.

Silver, M., Beiden, R., Dong, Z., Panov, N. and Karnieli, A., 2024. rOPTRAM: Deriving Soil Moisture from Satellite Imagery in R. Journal of Open Source Software, 9(100), p.7086.

Sklash, M.G. and Farvolden, R.N., 1979. The role of groundwater in storm runoff. Journal of Hydrology, 43(1-4), pp.45-65.

Somers, L.D. and McKenzie, J.M., 2020. A review of groundwater in high mountain environments. Wiley Interdisciplinary Reviews: Water, 7(6), p.e1475.

Sophocleous, M., 2002. Interactions between groundwater and surface water: the state of the science. Hydrogeology journal, 10, pp.52-67.

Soulsby, C., Malcolm, R., Helliwell, R., Ferrier, R.C. and Jenkins, A.J.H.P., 2000. Isotope hydrology of the Allt a'Mharcaidh catchment, Cairngorms, Scotland: implications for hydrological pathways and residence times. Hydrological Processes, 14(4), pp.747-762.

Soulsby, C., Tetzlaff, D., Rodgers, P., Dunn, S., and Waldron, S. (2006). Runoff processes, stream water residence times and controlling landscape characteristics in a mesoscale catchment: An initial evaluation. Journal of Hydrology, 325(1–4), 197–221.

Spence, C. and Woo, M.K., 2003. Hydrology of subarctic Canadian shield: soil-filled valleys. Journal of Hydrology, 279(1-4), pp.151-166.

Spencer, S.A., Anderson, A.E., Silins, U. and Collins, A.L., 2021. Hillslope and groundwater contributions to streamflow in a Rocky Mountain watershed underlain by glacial till and fractured sedimentary bedrock. Hydrology and Earth System Sciences, 25(1), pp.237-255.

Stieglitz, M., Shaman, J., McNamara, J., Engel, V., Shanley, J. and Kling, G.W., 2003. An approach to understanding hydrologic connectivity on the hillslope and the implications for nutrient transport. Global biogeochemical cycles, 17(4).

Story, A., Moore, R.D. and Macdonald, J.S., 2003. Stream temperatures in two shaded reaches below cutblocks and logging roads: downstream cooling linked to subsurface hydrology. Canadian Journal of Forest Research, 33(8), pp.1383-1396.

Stumpp, C., Klaus, J. and Stichler, W., 2014. Analysis of long-term stable isotopic composition in German precipitation. Journal of Hydrology, 517, pp.351-361.

Strydom, T., Nel, J.M., Nel, M., Petersen, R.M. and Ramjukadh, C.L., 2021. The use of Radon (Rn222) isotopes to detect groundwater discharge in streams draining Table Mountain Group (TMG) aquifers. Water SA, 47(2), pp.194-199.

Sukanya, S., Noble, J. and Joseph, S., 2022. Application of radon (222Rn) as an environmental tracer in hydrogeological and geological investigations: An overview. Chemosphere, 303, p.135141.+

Sun, C., Chen, Y., Li, J., Chen, W. and Li, X., 2019. Stable isotope variations in precipitation in the northwesternmost Tibetan Plateau related to various meteorological controlling factors. Atmospheric Research, 227, pp.66-78.

Sun, X., Yang, P., Xiang, Y., Si, X. and Liu, D., 2018. Across-fault distributions of radon concentrations in soil gas for different tectonic environments. Geosciences Journal, 22, pp.227-239.

Tanner, C.C., Sukias, J.P., Headley, T.R., Yates, C.R. and Stott, R., 2012. Constructed wetlands and denitrifying bioreactors for on-site and decentralised wastewater treatment: comparison of five alternative configurations. Ecological Engineering, 42, pp.112-123.

Tanner, J.L. and Hughes, D.A., 2015. Surface water–groundwater interactions in catchment scale water resources assessments—understanding and hypothesis testing with a hydrological model. Hydrological Sciences Journal, 60(11), pp.1880-1895.

Tanner, J., Lorentz, S., Hughes, D., & Gxokwe, S. (2022). Understanding hillslope runoff generation using stable isotopes in a montane grassland catchment, South Africa. Hydrological Processes, 36(5), e14543. https://doi.org/10.1002/hyp.14543

Terblanche, D.E., Pegram, G.G.S. and Mittermaier, M.P., 2001. The development of weather radar as a research and operational tool for hydrology in South Africa. Journal of Hydrology, 241(1-2), pp.3-25.

Tetzlaff, D., Malcolm, I.A. and Soulsby, C., 2007. Influence of forestry, environmental change and climatic variability on the hydrology, hydrochemistry and residence times of upland catchments. Journal of Hydrology, 346(3-4), pp.93-111.

Tetzlaff, D. and Soulsby, C., 2008. Sources of baseflow in larger catchments–Using tracers to develop a holistic understanding of runoff generation. Journal of Hydrology, 359(3-4), pp.287-302.

Tetzlaff, D., Soulsby, C., Buttle, J., Capell, R., Carey, S.K., Laudon, H., McDonnell, J., McGuire, K., Seibert, J. and Shanley, J., 2013. Catchments on the cusp? Structural and functional change in northern ecohydrology. Hydrological Processes, 27(5).

Theron, C., Lorentz, S.A. and Xu, Y., 2022. Rainfall-induced groundwater ridging and the Lisse effect on tailings storage facilities: A literature review. Journal of the Southern African Institute of Mining and Metallurgy, 122(2), pp.37-44.

Thiros, N.E., Siirila-Woodburn, E.R., Dennedy-Frank, P.J., Williams, K.H. and Gardner, W.P., 2023. Constraining Bedrock Groundwater Residence Times in a Mountain System With Environmental Tracer Observations and Bayesian Uncertainty Quantification. Water Resources Research, 59(2), p. e2022WR033282.

Toth, J., 1963. A theoretical analysis of groundwater flow in small drainage basins. Journal of geophysical research, 68(16), pp.4795-4812.

Toucher ML, Clulow A, van Rensburg SJ, Morris F, Bray B, Majozi S, Everson C, Jewitt GPW, Taylor MA, Mfeka S and Lawrence K. 2016. Establishment of and Demonstration of the Potential of the Cathedral Peak Research Catchments as a Living Laboratory. Report No. 2236/1/16. Water Research Commission, Pretoria, RSA.

Triska, F.J., Kennedy, V.C., Avanzino, R.J., Zellweger, G.W. and Bencala, K.E., 1989. Retention and transport of nutrients in a third-order stream in northwestern California: Hyporheic processes. Ecology, 70(6), pp.1893-1905.

Tromp-van Meerveld, H.J. and McDonnell, J.J., 2006. Threshold relations in subsurface stormflow: 2. The fill and spill hypothesis. Water resources research, 42(2).

Tweed, S., Leblanc, M. and Cartwright, I., 2009. Groundwater–surface water interaction and the impact of a multi-year drought on lakes conditions in South-East Australia. Journal of Hydrology, 379(1-2), pp.41-53.

Uhlenbrook, S., Wenninger, J. and Lorentz, S., 2005. What happens after the catchment caught the storm? Hydrological processes at the small, semi-arid Weatherley catchment, South-Africa. Advances in Geosciences, 2, pp.237-241.

Van Der Velde, Y., Torfs, P.J.J.F., Van Der Zee, S.E.A.T.M. and Uijlenhoet, R., 2012. Quantifying catchment-scale mixing and its effect on time-varying travel time distributions. Water Resources Research, 48(6).

van Tol, J.J. and Le Roux, P.A., 2019. Hydropedological grouping of South African soil forms. South African Journal of Plant and Soil, 36(3), pp.233-235.

Vervier, P., Gibert, J., Marmonier, P. and Dole-Olivier, M.J., 1992. A perspective on the permeability of the surface freshwater-groundwater ecotone. Journal of the North American Benthological Society, 11(1), pp.93-102.

Vogt, T., Hoehn, E., Schneider, P., Freund, A., Schirmer, M. and Cirpka, O.A., 2010. Fluctuations of electrical conductivity as a natural tracer for bank filtration in a losing stream. Advances in Water Resources, 33(11), pp.1296-1308.

Wang, X., Yang, G., Wang, Q., Huang, P., Wang, T., Zhang, P. and Zhang, B., 2018. Investigation of occurrence characteristics and influencing factors of radon in Cambrian

limestone geothermal water. Journal of Radioanalytical and Nuclear Chemistry, 317, pp.1191-1200.

Warburton Toucher, M.L., Clulow, A , Van Rensburg, S. , Bulcock, H., Jewitt, G.P.W., Everson, C.E., Horan, M.J.C. Toward understanding the environmental change impacts on hydrological responses through long-term monitoring: Reestablishment of the cathedral peak research catchments, South Africa. Centre for Water Resources Research, University of KwaZulu-Natal.

Waswa, G.W. and Lorentz, S.A., 2015. Energy considerations in groundwater-ridging mechanism of streamflow generation. Hydrological Processes, 29(23), pp.4932-4946.

Water Resources of South Africa, 2012 Study: Resource Centre. Water Research Commission Report K5/2143/1. http://waterresourceswr2012.co.za/resource-centre/

Weathers, K.C. and Likens, G.E., 1996. Clouds in southern Chile: an important source of nitrogen to nitrogen-limited ecosystems?. Environmental Science and Technology, 31(1), pp.210-213.

Weiler, M. and McDonnell, J., 2004. Virtual experiments: a new approach for improving process conceptualization in hillslope hydrology. Journal of Hydrology, 285(1-4), pp.3-18.

Wels, C., Cornett, R.J. and Lazerte, B.D., 1991. Hydrograph separation: A comparison of geochemical and isotopic tracers. Journal of hydrology, 122(1-4), pp.253-274.

Wels, C., Taylor, C.H., Cornett, R.J. and Lazerte, B.D., 1991. Streamflow generation in a headwater basin on the Precambrian Shield. Hydrological Processes, 5(2), pp.185-199.

Welgus, M.N. and Abiye, T.A., 2022. Surface water and groundwater interaction in the Vredefort Dome, South Africa: a stable isotope and multivariate statistical approach. Environmental Monitoring and Assessment, 194(10), p.672.

Wenninger J, Uhlenbrook S, Lorentz L, Leibundgut C (2008) Identification of runoff generation processes using combined hydrometric, tracer and geophysical methods in a headwater catchment in South Africa. Hydrological Sciences Journal, 53:1, 65-80, DOI: 10.1623/hysj.53.1.65

Weyman, D.R., 1973. Measurements of the downslope flow of water in a soil. Journal of Hydrology, 20(3), pp.267-288.

Winter, T.C., Harvey, J.W., Franke, O.L. and Alley, W.M., 1998. Groundwater and surface water: A single resource: US Geological Survey Circular 1139. US Geological Survey, Denver, CO.

Wondzell, S.M., 2015. Groundwater–surface-water interactions: perspectives on the development of the science over the last 20 years. Freshwater Science, 34(1), pp.368-376.

World Bank (20123). World Bank Open Data [Database]. Available at: https://data.worldbank.org (Accessed August 30 2023).

Yang, L., Song, X., Zhang, Y., Han, D., Zhang, B. and Long, D., 2012. Characterizing interactions between surface water and groundwater in the Jialu River basin using major ion

Zhang, Y.K. and Schilling, K.E., 2006. Increasing streamflow and baseflow in Mississippi River since the 1940 s: Effect of land use change. Journal of Hydrology, 324(1-4), pp.412-422.

Zierl, B., Bugmann, H. and Tague, C.L., 2007. Water and carbon fluxes of European ecosystems: An evaluation of the ecohydrological model RHESSys. Hydrological Processes: An International Journal, 21(24), pp.3328-3339.